**Synthesis, Transport Activity and Selectivity of an Artificial Photogated Ion Channel**

by

Chengjin Shan
B.Sc., Beijing Normal University, 1985
M.Pharm., Academy of Military Medical Sciences (Beijing), 1988

A Thesis Submitted in Partial Fulfilment of the Requirements for the Degree of

MASTER OF SCIENCE

in the Department of Chemistry

We accept this thesis as conforming to the required standard

[redacted]

Dr. T.M. Fyles, Supervisor (Department of Chemistry)

[redacted]

Dr. R.H. Mitchell, Departmental Member (Department of Chemistry)

[redacted]

Dr. C. Bohne, Departmental Member (Department of Chemistry)

[redacted]

Dr. J. Owens, Outside Member (Department of Biology)

[redacted]

Dr. N.J. Livingstone, External Examiner (Department of Biology)

Supervisor: Dr. Thomas M. Fyles

## Abstract

An 18-crown-6 derived ion transporter **1** was synthesized as a potential photogated ion channel. This compound is composed of a macrocyclic core bearing four wall units to which polar head groups attach. The macrocyclic core is a tartaric acid derived 18-crown-6. The wall units are azobenzene derivatives capable of photoisomerization. The design assumed that the open and closed states of the ion channel would be controlled by configuration conversion of the azobenzene.

The azobenzene moiety was constructed by diazonium coupling reaction between phenol and 4'-(5,6-dihydroxyhexyloxy)diazonium chloride. The wall unit was completed by a Williamson ether coupling of the phenol with 6-phthalimidohexyl bromide followed by deprotection to give an aminodiolazobenzene derivative. Protection of the diol as the isopropylidene ketal followed by coupling with *R,R,R,R*-18-crown-6 tetraacid chloride and deprotection gave the target **1**. The target compound and intermediates were all characterized by $^{1}H$ and $^{13}C$ NMR spectroscopy and mass spectroscopy (CI or electrospray), and elemental analysis.

The photoisomerization of compound **1** was explored in homogeneous solution by irradiation of the compound in methanol-chloroform (v/v 1:1). The UV-visible spectra indicated that the initial form was *trans*-azobenzene ($\lambda_{max}$ = 360 nm, $\varepsilon$ = 76300 $M^{-1} \cdot cm^{-1}$) which shifted to a photostationary state that

was predominantly *cis*-azobenzene ($\lambda_{max}$ = 320 nm). It was found that the extinction coefficient of *trans*- **1** is only 3.4 times that of a compound with one azobenzene moiety. A thermal back reaction of *cis*- to *trans*- was non-first order with an approximate half life of 15 minutes. Compound **1** can also photoisomerize between *trans*- and *cis*- isomers reversibly.

The target compound was poorly soluble in polar solvents, thus it could not be added as a solution to pre-formed vesicles. The compound was directly incorporated into pre-formed vesicles from the solid state, leading to a modified pH-stat titration experiment. The transport activity of this compound is approximately 10 times lower than some previously reported ion transporters with similar structures. The transport selectivity of the compound is in the order of $K^+ > Rb^+ > Cs^+ > Na^+ > Li^+$.

The reversible photoisomerization of compound **1** in vesicle solution was detected by irradiation followed by extraction with chloroform. Conversion to a predominantly *cis*- photostationary state was achieved after 15 minutes irradiation at 360 nm. The lifetime of the *cis*- isomer was found to be approximately 15 minutes in vesicle solution. This limits the exploration of the photogating using pH-stat titration because the lifetime is too short for the pH-stat experiment. In general, the poor solubility, which is caused by the contradiction of the strong polarity of the head groups and strong nonpolarity of the wall units, is a major problem in the detection of the photogate effect and should be avoided in future photogated ion channel designs.

Examiners:

[redacted]

Dr. T.M. Fyles, Supervisor (Department of Chemistry)

[redacted]

Dr. R.H. Mitchell, Departmental Member (Department of Chemistry)

[redacted]

Dr. C. Bohne, Departmental Member (Department of Chemistry)

[redacted]

Dr. J. Owens, Outside Member (Department of Biology)

[redacted]

Dr. N.J. Livingstone, External Examiner (Department of Biology)

# Table of Contents

## List of Tables

## List of Figures

## List of Schemes

# Chapter 1

# Introduction

## 1. Ion channels: from natural to synthetic

Ion transport is a very common phenomenon in nature. Bilayer cellular membranes separate the cytoplasm from the extracellular environment while ion channels function as the routes for the entry and exit of metal ions such as $K^+$ and $Na^+$, which are essential for life. The ion channels in cellular membranes[1] closely control the metal ion flux across cellular membrane. They selectively regulate the metal ion concentration within a cell with a switch, or gate, so that the concentration ratios of all ions in the cell can be kept almost constant. The importance of ion channels can not be overemphasized.

Ion transporters may also be useful for sensor and separation technologies in the long run, thus it is necessary to synthesize ion channels in order to explore them under experimentally controllable conditions. All known natural ion channels in cellular membranes[1] are proteins with molecular weight of more than $10^5$, but simpler compounds such as the antibiotics gramicidin, amphotericin, and valinomycin were also found to be active in ion transport[2]. This activity by low molecular weight compounds hints that we can synthesize ion transporters with much simpler structures than that of naturally occurring ion channels in cellular membranes.

The simplest type of ion transporter is a carrier similar in function to

valinomycin (see **Fig. 1**). An ion carrier catches a metal ion by the formation of a complex on one side of a bilayer membrane, then carries it across to the other side and releases it. A carrier is usually a small molecule, because it must be sufficiently mobile for its motion from one side of the membrane to the other. Therefore, it is relatively easy to synthesize. Carriers have been widely explored, and reviews by Fyles[3] and Tsukube[4] summarized the development of this field.

A relay transporter is structurally more complicated than a carrier (see **Fig. 2**). It has more than one ion complexing site and transports by passing an ion from one side of the membrane via a sequence of complexing sites.

Both carriers and relays transport ions by mechanisms different from that of natural ion channels. On a kinetic level, a relay may be the best description for all kinds of transporters. A carrier and a channel are simply two limiting models of a relay. If the free energy for the transfer of an ion from one complexing site to another is very small, the transporter simulates a channel. In contrast, if the free energy is very large, so that the transfer of an ion from one complexing site to another is hardly possible, the transporter simulates a carrier[25].

The closest mimics of natural transport proteins are amphotericin and gramicidin. These compounds act by forming transmembrane aqueous pores for ion diffusion. Since amphotericin and gramicidin function similarly to natural ion channels, they hint at what a synthetic ion channel could look like

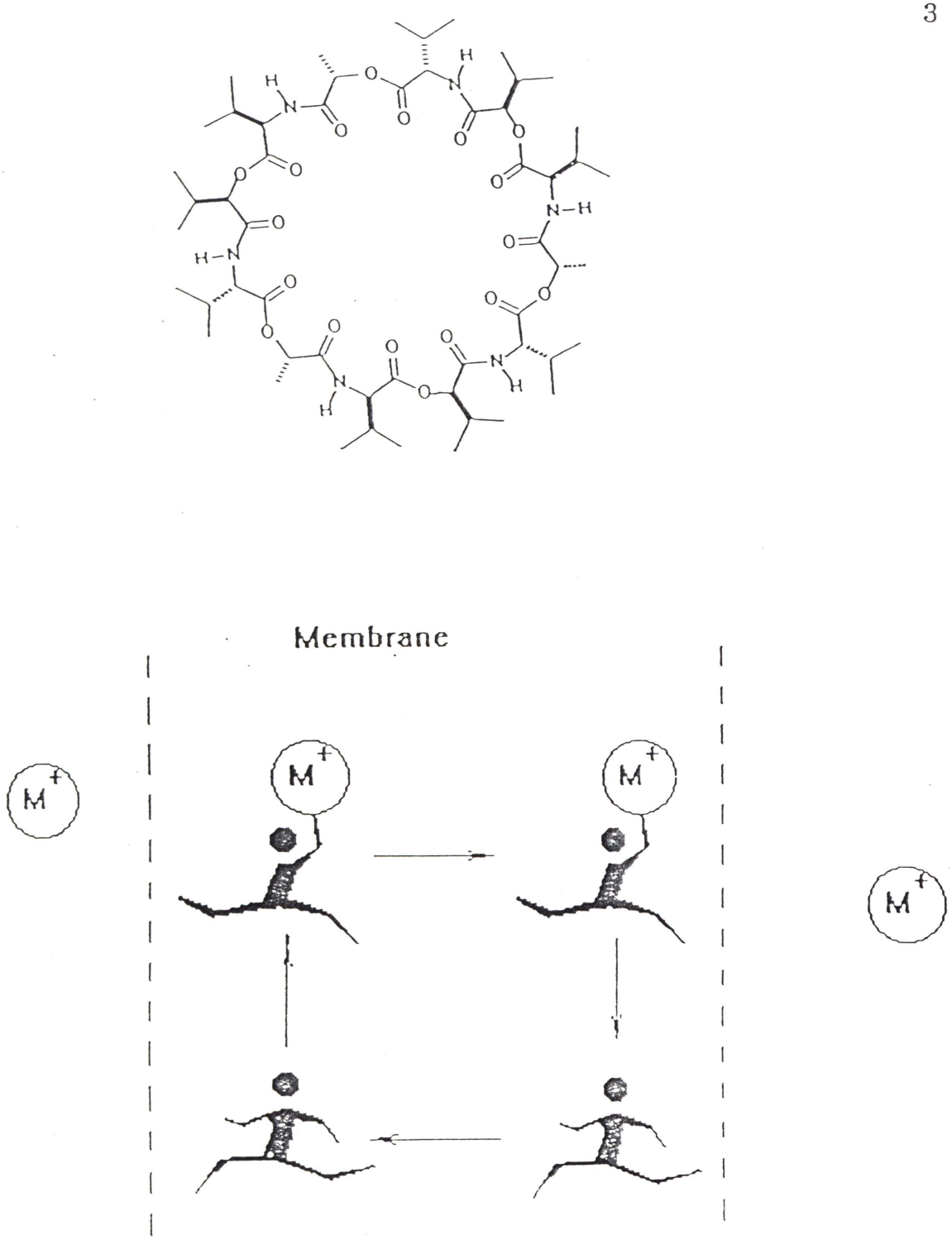


Fig. 1. Valinomycin and cartoon of carrier mechanism

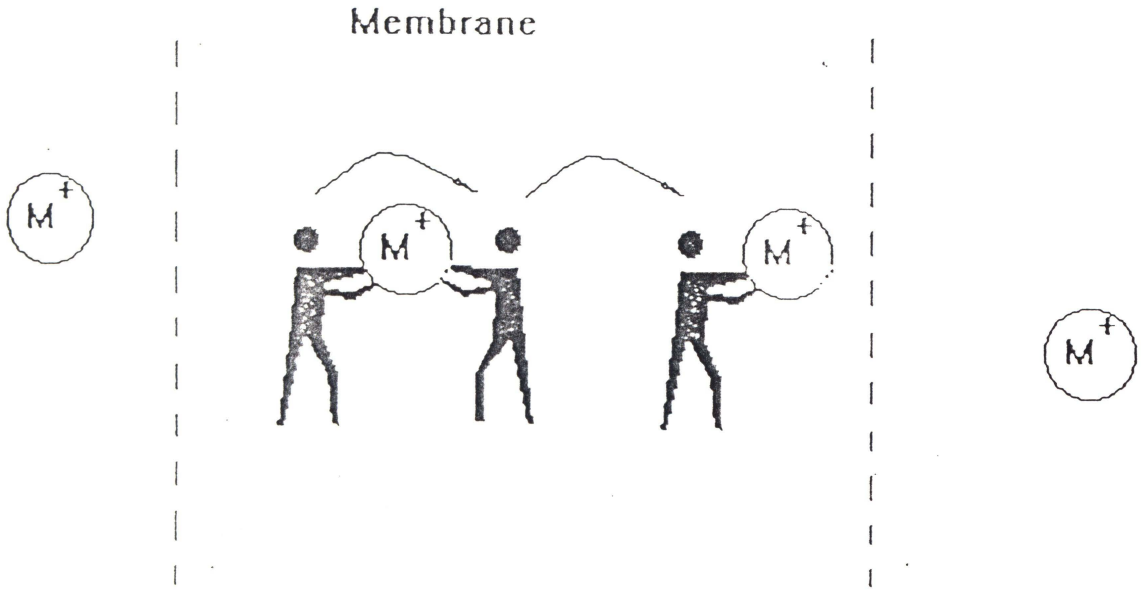


**Fig. 2**. Cartoon of relay mechanism

structurally.

The gramicidin group of antibiotics[2] are linear polypeptides composed of amino acids with alternate D and L configurations (see **Fig. 3**). The alternation of the configurations of amino acids makes the gramicidins have a helical structure. In non-polar media, two gramicidin molecules span bilayer membrane by an end-to-end dimer. The ion is assumed to pass through across the membrane within the helical structure, stabilized by the carbonyl oxygens of the gramicidin.

The amphotericins[2] are a group of macrocyclic antibiotics with a polyene sequence along one side and a hydrocarbon chain substituted with hydrophilic groups along the other side (see **Fig. 4**). Within a membrane environment, about 10 amphotericin molecules organize a cylindrical tube, and two such

Formyl-L-Val-Gly-L-Ala-D-Leu-L-Ala-D-Val-L-Val-D-Val-
1 2 3 4 5 6 7 8

L-Trp-D-Leu-L-Trp-D-Leu-L-Trp-D-Leu-L-Trp-$NHCH_2CH_2OH$
9 10 11 12 13 14 15

**Fig. 3**. Gramicidin and a channel formed thereof

tubes span bilayer membrane in an end-to-end aggregate to permit metal ions to get through.

Both the amphotericins and the gramicidins form "artificial" channels, but they are naturally occurring compounds. By the examples above, however, we can summarize that a synthetic ion channel, either a unimolecular or a multimolecular one, should have the following structural characteristics:

(1) A tubular shape in order to accept a metal ion and allow it to get through.

(2) A total length of about 40 Å in order to span a lipid bilayer membrane. Since the lipid bilayer membrane is flexible, the length can vary to some degree.

(3) A hydrophilic interior to make it capable of complexing metal ions, a hydrophobic exterior to make it capable of inserting into a lipid bilayer

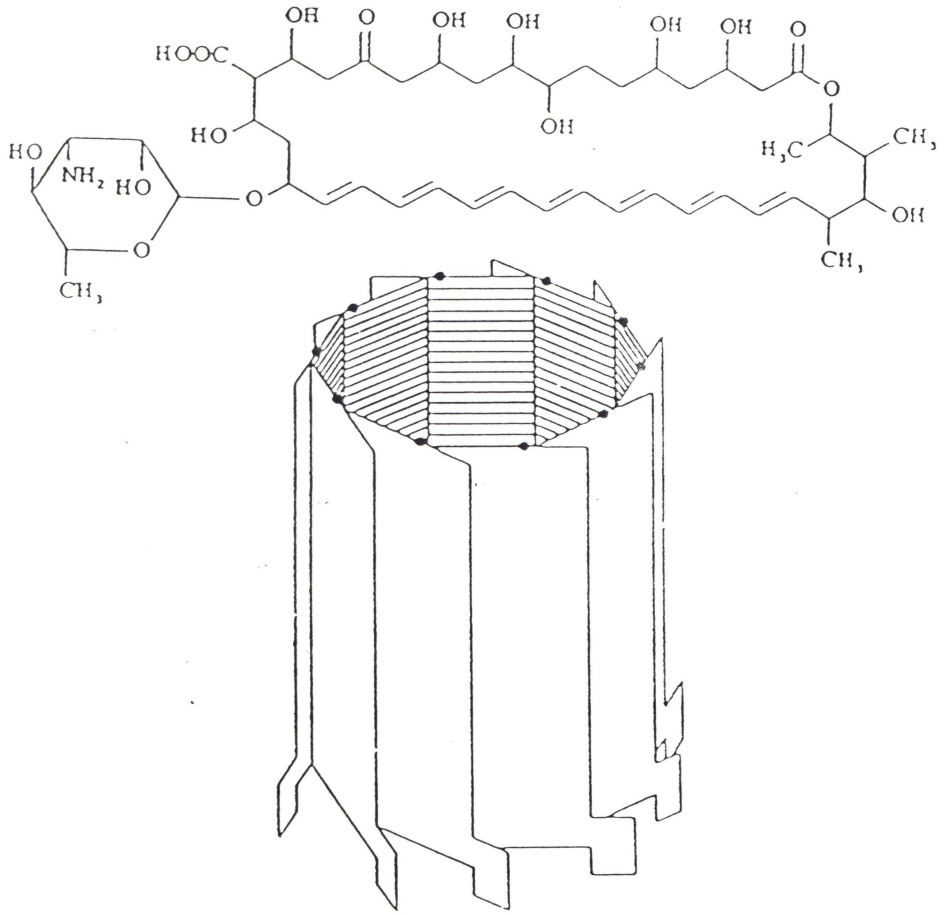


**Fig. 4**. Amphotericin and half a pore formed thereof

membrane, and hydrophilic head groups which can anchor the structure across the membrane.

In addition to the above characteristics, the compound itself should be synthesized via easy and dependable reactions because artificial ion channels usually are fairly large molecules or organized bundles of fairly large molecules which often cause difficulty in synthesis and purification.

Amphotericins are smaller molecules than gramicidins. Thus, their mimics should structurally be simpler than those of gramicidins. Kunitake[5]

reported two amphotericin mimics which acted within an artificial bilayer membrane. The two mimics were quaternary ammonium salts with a hydrophobic chain (hydrocarbon or fluorocarbon) and a hydrophilic chain (ester/polyether). It was found that the hydrocarbon chain mimic was more active than the fluorocarbon mimic in transporting hydroxide ions into vesicles.

Menger[6] reported an even simpler series of compounds which were composed of a section of hydrocarbon chain, a section of polyether chain, and a benzyl terminal group. These compounds were the intermediates from the synthesis of a series of substituted phosphatidyl cholines which were supposed to be active in ion transport. The substituted phosphatidyl cholines were found not to be active while the intermediates were dramatically shown to be even more active than gramicidin. As neither the hydrophobic chain nor the hydrophilic chain was long enough to span a bilayer membrane, the mimics were suggested to be dimer channels as are the gramicidins. It is more likely that an amphotericin-like aggregate is the active structure.

An amphotericin mimic was reported by Fuhrop[7] in 1984. The pyromellitate ester of the natural product monensin has an overall length of 20 Å with negative charges at either end. A 20-Å thick monolayer vesicle made from a bolaamphiphilic macrocyclic tetraester was employed to measure the activity of the channel. Some of the macrocycles were found to be active in transporting $Li^+$ across monolayer membrane.

Zojaji[8] reported a series of bolaamphilic pore formers of macrocyclic

tetraesters containing polyether and/or hydrocarbon chains. They are dimerized with a tartaric acid or a *m*-xylylenedithiol unit (see **Fig. 5**). The structure is capped with hydrophilic head groups. The activity of these compounds was measured and three of them were found to have activity comparable to or greater than amphotericin. The apparent kinetic orders and the alkali metal selectivity were all consistent with the proposal that the mimics are not carriers but behaved similarly to the pore forming antibiotic amphotericin B.

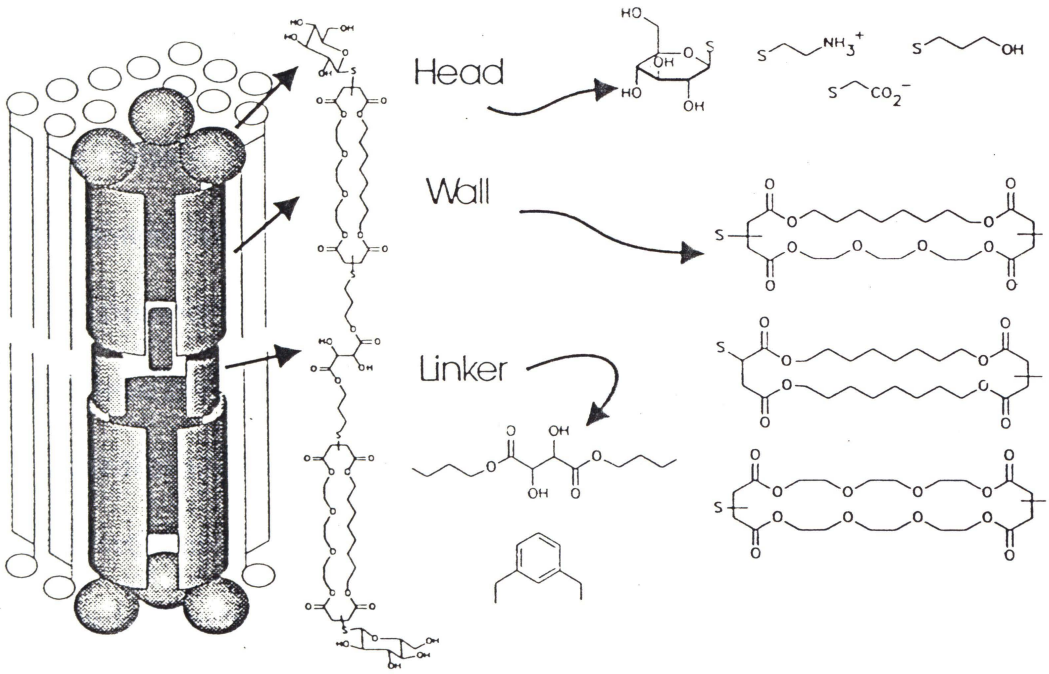


**Fig.** 5. Zojaji's synthetic pore formers

Gramicidin mimics, although a little more structurally complicated, have been reported frequently as well. Polypeptides were the first gramicidin mimics chosen by chemists[9]. However, the synthetic peptides did not form the same β-helix as their natural prototype. Therefore, they were not as active, or as

selective as the gramicidins.

Tabushi[10] reported a channel forming compound derived from cyclodextrin. With four hydrophobic tails and three metal binding sites in each molecule, the channel is formed by end-to-end organization as with the gramicidins. With hydroxyls as hydrophilic groups, the channel was found to transport $Co^{2+}$ very slowly. In spite of its low transport activity, it was the earliest active synthetic ion channel.

Later on, a polymer of isocyanide with attached benzo-18-crown-6 macrocycles was reported by Nolte[11]. The polymer forms a tight helix with four repeating units per turn. As a result, the whole molecule is a cluster of four tubes consisting of stacked benzo-18-crown-6 macrocycles. The polymer was active in transporting $Co^{2+}$. The Arrhenius activation energy of the channel transport was derived as 24 $kJ \cdot mol^{-1}$ from the relation between transport rate and temperature. The $E_a$ value is consistent with a channel mechanism for the ion transport. For example, $E_a$ for gramicidin A transport is 20.5-22.5 $kJ \cdot mol^{-1}$ while for a carrier transport is 90-120 $kJ \cdot mol^{-1}$.

Gokel[12] reported a compound composed of three azacrown ethers held together by two spacers. The channel was completed by two side arms. The compound was found to transport $Na^+$ across lipid membrane by dynamic $^{23}Na$ NMR spectroscopy. The transport rate was 40 times faster than a diazacrown carrier but 100 times slower than gramicidin. Gokel suggested that the transport was by a channel mechanism because it exhibited first order kinetics.

Lehn[13] reported a series of channel mimics based on 18-crown-6 tetraacid as well as on cyclodextrins. He called these molecules "bouquet" molecules. Taking his crown ether based molecules as examples, we can see that those compounds follow the synthetic channel design principles in overall length, hydrophilic head groups though the pendant chains are either hydrocarbon or polyether. They are about equally active whatever the pendant chains are.

Fyles[14] reported an ion channel based on a 18-crown-6 hexaacid in 1989. The whole molecule was composed of a macrocyclic core, amphiphilic wall units and hydrophilic head groups (see **Fig. 6**). The channel design was based on conformations of the tartaric acid derived arms placed in axial positions. The axial oriented arms would make the molecule a tubular shape with a total length close to the thickness of a lipid bilayer membrane (c.a. 40 Å). A number of ion channel mimics similar to this structure were subsequently reported[15] and the transport activity of the channel mimics behaved similar to gramicidin D but dissimilarly from valinomycin in activation energy and transport extent dependence on transporter's concentration. Therefore, the transporters acted as a channel, not a carrier.

## 2. Synthetic ion channels: from uncontrolled to switch controlled

An uncontrolled channel transports metal ions until the concentration on both sides of the membrane reaches equilibrium. That is, however, not the

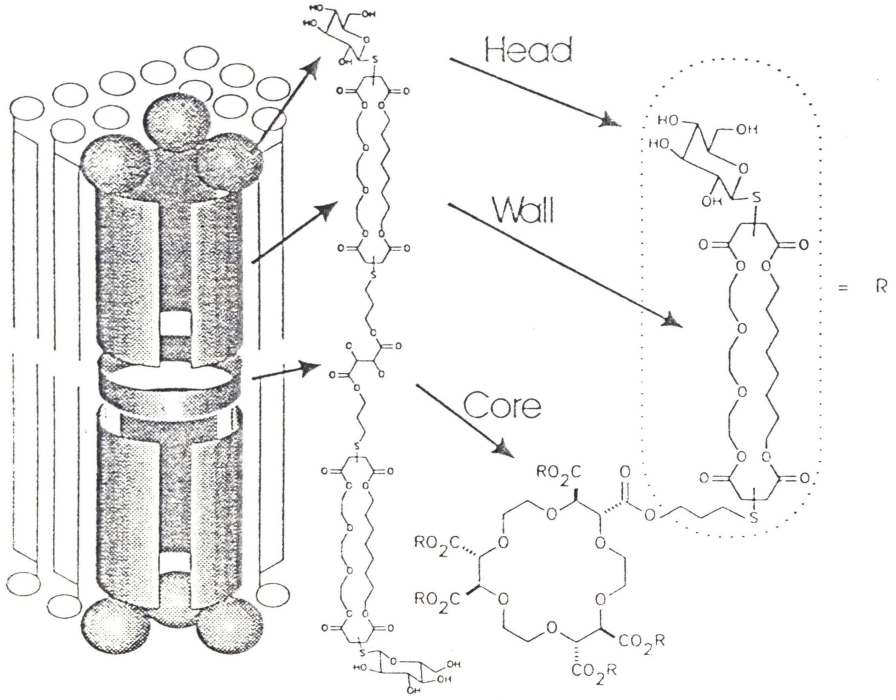


**Fig. 6**. Fyles' synthetic channel

case in cellular membranes. As is known, natural ion channels[1] transport metal ions not only selectively, but also controllably, i.e., the transport is controlled by a switch, or gate. The on-off function of a gate[18], from the view of a electrophysiologist, may appear as a variety of microscopic changes. Of the gating mechanisms described in **Fig. 7**, some seem to be easier than others to realize by conversion of chemical configurations or conformations. For example, mechanisms **F** and **C** could be realized by interconversion of configurations or conformations, and **B** could be realized by changing the binding of pore formers. In comparison, mechanisms **A**, **D**, and **E** are not easy to realize by simple chemical changes. Natural ion transport across membranes is frequently controlled by a transmembrane voltage sensor or a light sensor, i.e.,

a voltage gate or a photogate. Therefore, it is apparent that a switch controlled synthetic ion channel would be a better mimic of natural ion channels.

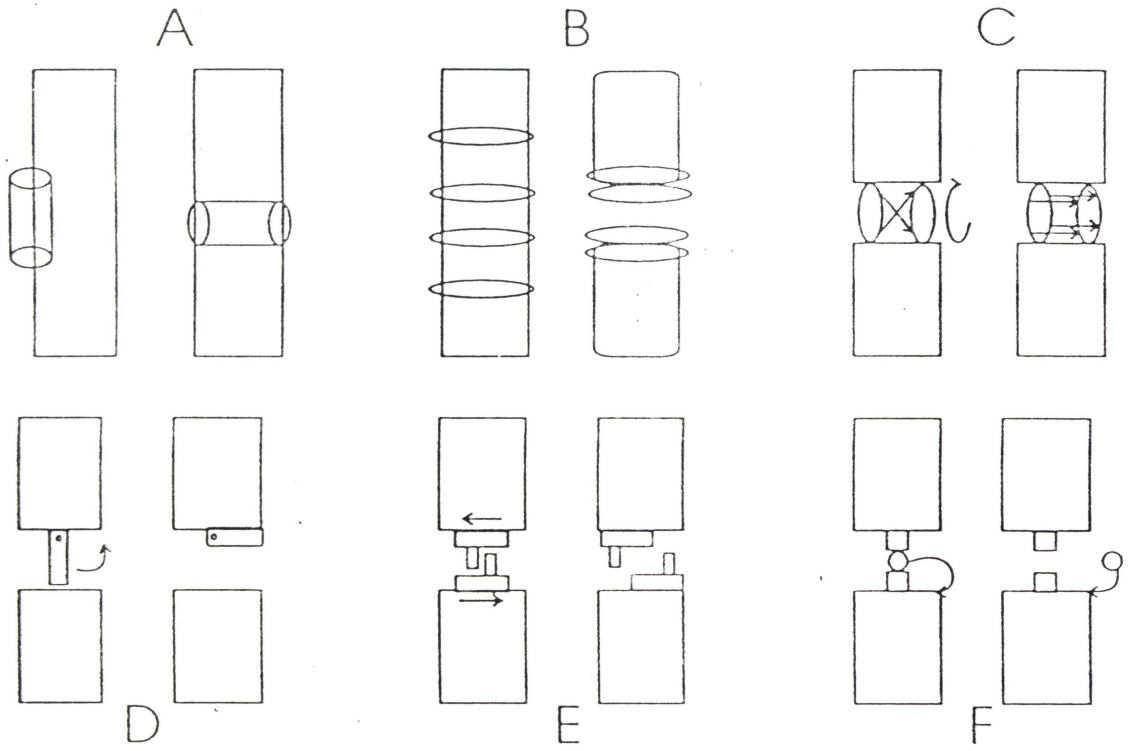


**Fig. 7.** Cartoon of gating mechanisms

A light-switch is one of the most interesting choices for transport control. A light-switch or photogate requires a reliable and high yield photoisomerization reaction. The photoisomerization doesn't have to be reversible, though a reversible reaction makes a more versatile switch. Stilbenes, azobenzenes or spiropyran/merocyanine systems are all potential candidates for a photogate[19].

Azobenzene is one of the most suitable candidates because it is easy to

prepare and it is completely reversible between *trans*- and *cis*- configurations. Shinkai, et al.[20] have reported many azobenzene-switched ion carriers, of which the series of tail-biting azobenzene-switched crown ethers[20 a-c] was most interesting for photogated ion transporter design. When the azobenzene converts from *trans*- configuration to *cis*-, an ammonium at the end of the tail can complex intramolecularly with the crown ether to form a pseudo-cyclic structure that facilitates the release of metal ions. This result suggests that if a channel is based on a crown ether, an azobenzene with a chain functionalized with an ammonium group at the end may act as a photogate by plugging or unplugging the crown ether to hinder or permit metal ions to pass through the crown ether.

Cross[21] has reported the attempt of synthesis of such a photogated ion channel, which is based on the mechanism **F** (in **Fig. 7**). Although the final target channel was not prepared, the photoswitch component was prepared and characterized. When the azobenzene was irradiated with a 360-nm UV, the expected photoisomerization occurred (see **Fig.** 8). The back thermal reaction had a half life of hours.

### 3. Proposed target compound: a new photogated ion channel

Both Shinkai's[20a-c] and Cross'[21] systems provide important suggestions for the design of a photogated ion channel. It still remains unknown, however, whether the ammonium blocking in Cross' channel is essential for a photogate

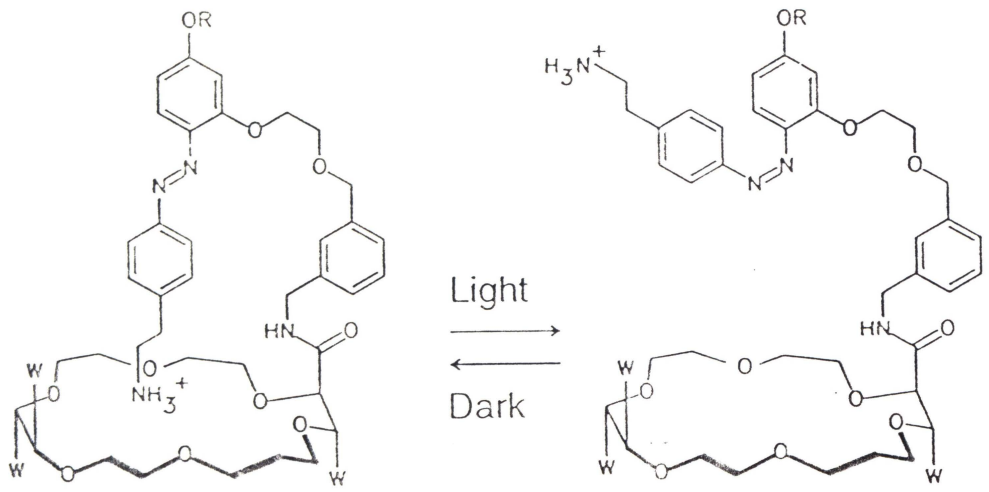


**Fig. 8.** Cartoon of Cross' photogated channel

because an ion channel doesn't have to be closed by plugging. It is possible that configuration conversion alone could close a channel by mechanism E. We can imagine that an ion channel based on a crown ether will not function normally when the configuration of one or more of its wall units convert from extended to shortened. If the tubular shape was dramatically shifted when the wall units switch configuration, then channel activity would be disrupted. This suggests that very simple azobenzene derived crown ethers might give a photoswitched channel.

The target compound can be proposed by the consideration of synthesis and functions as stated previously. The following are the features which will appear in the target channel:

(1) The target channel will be based on a tartaric acid derived crown

ether tetraacid as the core as in previous work by Fyles[14], Lehn[13] as well as Cross[21].

(2) Azobenzene derived wall units will provide the channel with photochemical reactivity. In addition, azobenzene has liquid crystal properties which could assist the approach of two wall units to one another to help in the formation of a tubular shape. It is expected that the channel's tubular shape will not be kept when one or more of the wall units convert their configuration photochemically. Azobenzene is of course a hydrophobic structure, but the hydrophilic crown ether cooperates with it to fulfil the "hydrophilic interior -- hydrophobic exterior" requirement.

(3) Any hydrophilic structure could theoretically be a candidate for the head group, but glycol is easy to prepare in the synthesis of the proposed compound. The ease and dependability of synthesis are factors that must be considered seriously because difficulties are often met in purification of compounds with large molecular weight. Glycol was selected as the head group simply because it will be easy to obtain in the process of this synthesis.

Based on the above ideas, the target compound was selected. The length of the hydrocarbon units were selected to produce an overall length of about 40 Å using readily available $(CH_2)_n$ sequence. As shown in **Fig. 9**, the compound is the active all *trans-* form of a tetraamide of 18-crown-6. As pointed out previously, this compound was expected to act as a photogated ion channel by reorganization or disruption during isomerization to the *cis-* isomer.

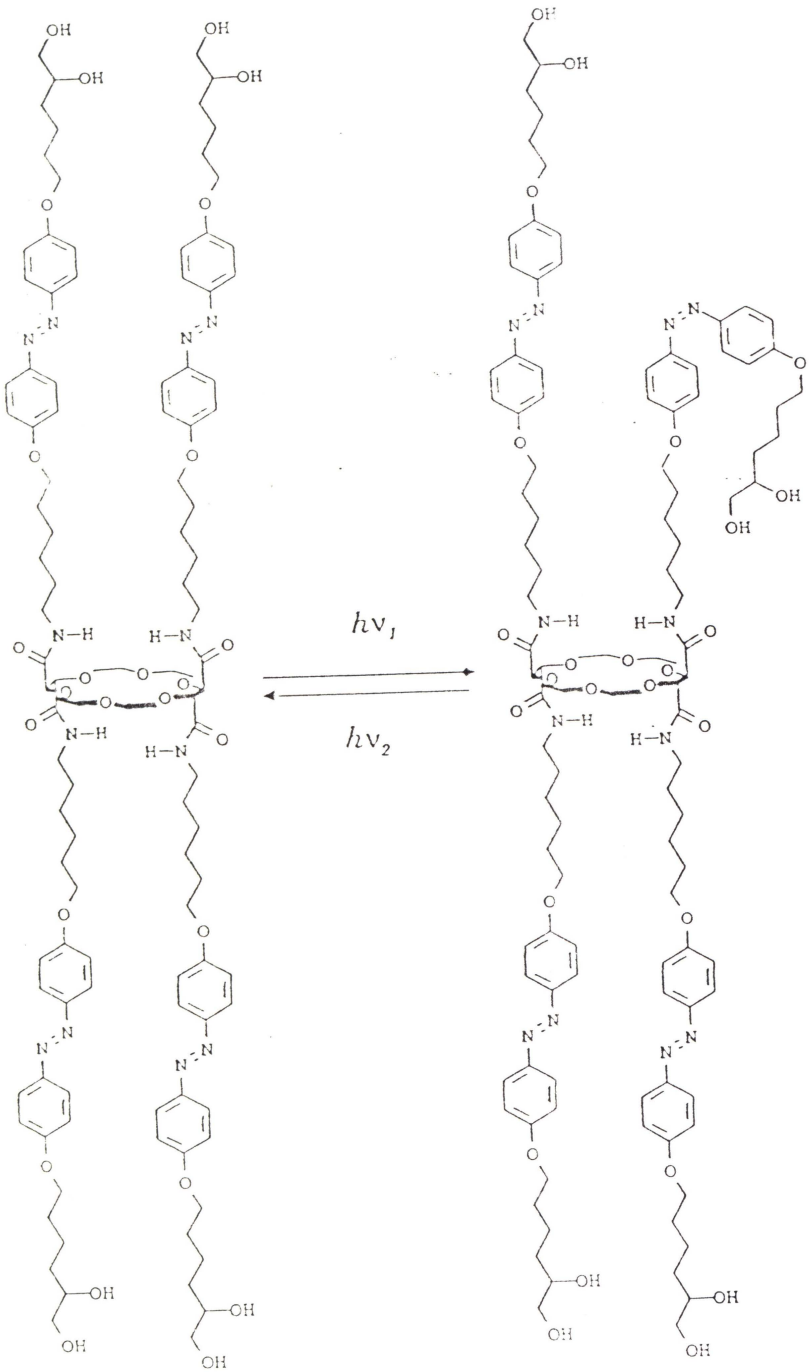


Fig. 9. Proposed target photogated channel

The ion transport activity of the ion channel, as well as the photogate activity, would be measured by pH-stat titration[16, 17] of large unilamellar vesicle (LUV) solution. The synthesis, developed in the next chapter, was expected to be straightforward.

# Chapter 2

# Synthesis

## 1. Retrosynthesis

The amide structure of the target compound (1) could be formed by the reaction of a crown ether acyl chloride and a suitable amine. The synthesis of the 18-crown-6 tetracarboxyl chloride (2)[22] was reported earlier and improved by Fyles, et al[23]. Therefore, the key problem was the synthesis of the amine (see **Scheme 1**). Cross' thesis outlines a variety of limitations for preparation of amide derivatives of 18-crown-6 tetracarboxylic acid, but the required reaction of four equivalents of a primary amine simultaneously is not expected to cause difficulties.

It is obvious that the amine (3) can be dissected into three parts: a 6-aminohexyl unit at one end, and azobenzene moiety in the middle, and a 5,6-dihydroxyhexyl at the other end. In principle, the formation of the long chain could start from either end. However, the diazonium coupling reaction is an aqueous phase reaction. This means that the more water soluble the aniline is, the better for the reaction. Also, a primary amine does not resist the diazonium forming reaction and therefore must be protected before the coupling reaction. Any protection certainly decreases the water solubility of the amino terminated unit, hence, of the whole molecule. The dihydroxyhexyl unit is expected more hydrophilic than the aminohexyl unit and would not need to

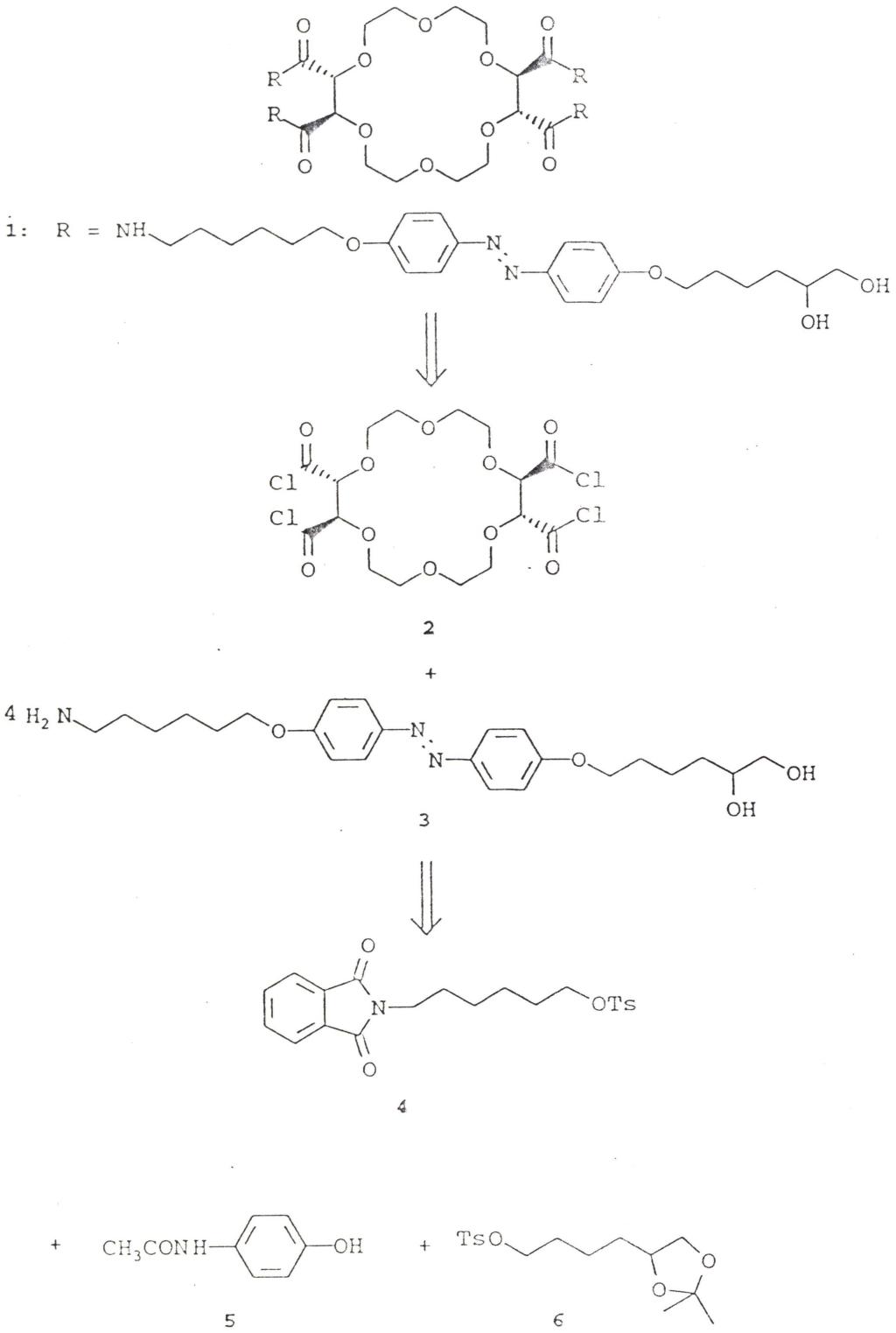


**Scheme 1.** Retrosynthesis of target compound **1**

be protected. That is why we began the synthesis from the preparation of compound **14** (see **Scheme 2**), on which a 4-hydroxyazobenzene would be formed by diazonium coupling. The resultant phenolic compound would react with an amino-protected alkyl halide to give a compound which could be converted to compound **3**.

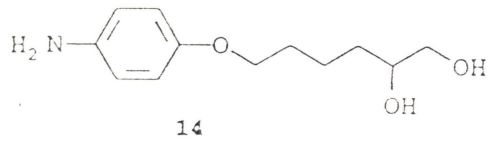


14

Scheme 2. Structure of compound **14**

**2. The 5,6-dihydroxyhexyl unit**

Cross[21] prepared the ketal **10**, a protected intermediate, from 6-bromo-1-hexene (**9**) via epoxidation, hydrolysis and ketalization, as shown in **Scheme 3**.

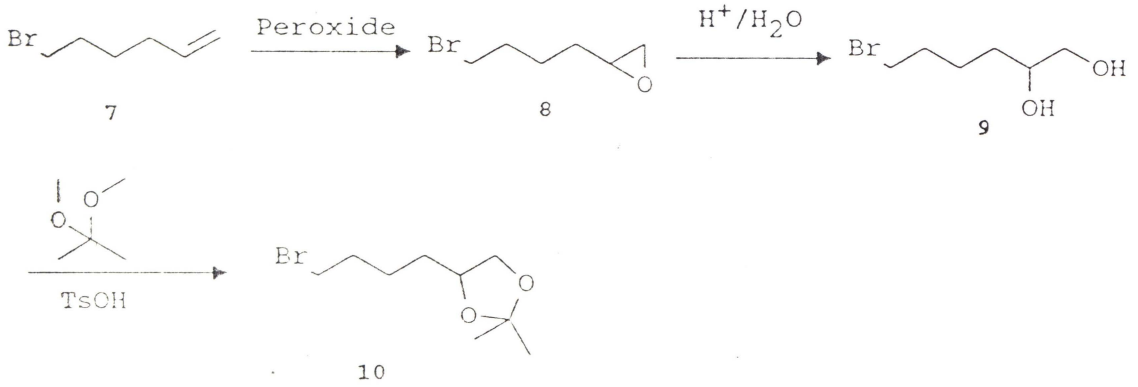


Scheme 3. Cross' preparation of compound **10**

1,2,6-Hexanetriol (**11**), however, might be a better starting reagent. It is much cheaper than **7** and could be converted to the bromide via only two reactions: protection of the glycol with acetone and substitution of the remaining hydroxyl. It would be a shorter, cheaper, and more convenient synthetic route. We also considered the substitution of the equivalent tosylate (**6**) for the bromide (**10**) (see **Scheme 4**) since tosyl chloride is cheaper than

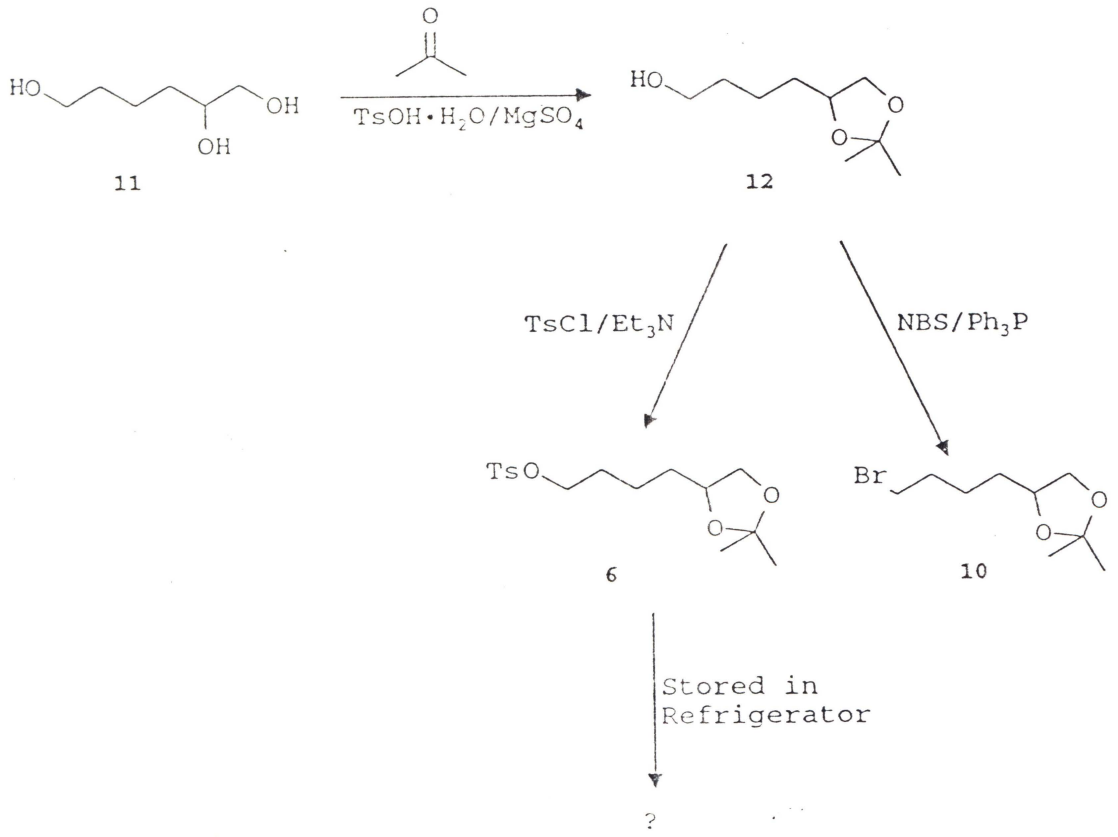


**Scheme 4**. Preparation of **13** and **12** from 1,2,6-hexanetriol

bromination reagents. The preparation started with ketalization of 1,2,6-hexanetriol. The ketalization was done by a modified method[24] with acetone under the catalysis of *p*-toluenesulfonic acid. The $^1$H NMR spectrum of the

product **12** was consistent with that previously reported[24], and the molecular weight (174) by MS (CI) was consistent with expectation, so we concluded that the protection of the glycol moiety was successful. The tosylate **6** was obtained by the reaction of **12** with tosyl chloride in the presence of triethylamine. However, the tosylate **6** obtained was difficult to purify, and the impure tosylate apparently decomposed overnight even when stored in a refrigerator. This phenomenon had not been mentioned previously[24]. It is possible that the crude product was contaminated with unreacted tosyl chloride which would decompose to release hydrogen chloride and the latter destroyed the acid-sensitive ketal structure. No further research was performed on this problem.

Then we considered the bromide **10**. Obviously, acidic reagents such as phosphorus tribromide could not be used because they would simply decompose the ketal moiety. Therefore, a mild bromination reagent had to be used. Triphenylphosphine and NBS[26] was chosen as the bromination reagent. Compound **12** reacted with triphenylphosphine and NBS to give the expected bromide **10** without damage to the ketal moiety. The product was characterized with MS (CI) and $^{1}H$ and $^{13}C$ NMR. The two singlets at 1.34 ppm and 1.28 ppm, which represent the existence of the two methyl groups in the ketal moiety, clearly showed that the ketal moiety survived the bromination. The M+1 (237) and M+3 (239) peaks in MS (CI) confirmed that the product molecule contains one bromine atom. This product, identified as the correct compound, was used without extensive purification.

**3. The azobenzene moiety**

The azobenzene was prepared as shown in **Scheme 5**. The reaction of the bromide **10** with both 4-acetamidophenol (**5**) and KOH in absolute ethanol gave the acetanilide **13**. Acidic hydrolysis deprotected the amino group as well as the glycol. The deprotection was confirmed by the disappearance of characteristic peaks in $^{1}H$ and $^{13}C$ NMR spectra. For example, the singlets at 2.1 ppm, 1.4 ppm and 1.3 ppm representing the acetyl methyl and the two methyl groups in the ketal moiety in $^{1}H$ NMR of **13** disappeared in $^{1}H$ NMR of the product **14**. Similarly, in the $^{13}C$ NMR, the peaks at 168 ppm and 24 ppm representing the acetyl and at 27 and 26 representing the two methyl groups in the ketal moiety in also disappeared in the $^{13}C$ NMR. The molecular weight of the product was 307 by MS (CI).

The diazonium salt was prepared in $NaNO_2$/HCl solution at 5 °C. Although the solubility of the anilinium chloride was not very high, the diazonium salt was completely soluble in water and coupled with sodium phenolate to give the azobenzene derivative **15** in an overall yield of greater than 50%. The expected product was obtained with satisfactory elemental analysis results as well as clean MS (CI) and $^{1}H$ and $^{13}C$ NMR spectra. The two AA'XX' systems (J = 9.0 Hz and 8.9 Hz respectively) between 7.9-6.9 ppm in $^{1}H$ NMR spectrum showed that the product contained two *para*- substituted benzene rings. Similarly, the eight peaks between 162 and 115 ppm in $^{13}C$ NMR spectrum confirmed the two *para*- substituted phenyl groups. The

molecular weight from the MS (CI) was 330. The absorption peak at 360 nm in the UV-visible spectrum confirmed that the product was the *trans*- form[28].

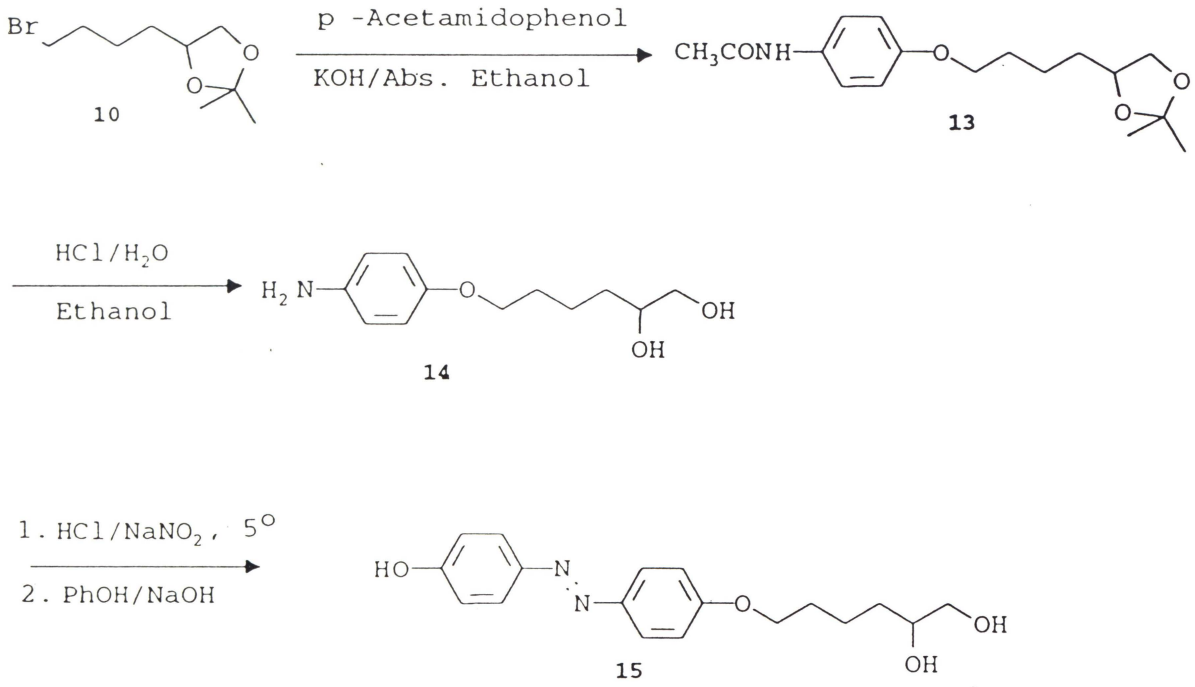


**Scheme 5**. Preparation of azobenzene moiety

## 4. The 6-aminohexyl unit

The aminohexyl section was derived from 1-chloro-6-phthalimidohexane. This intermediate was prepared via a Gabriel reaction of 6-chloro-1-hexanol and potassium phthalimide. It was found that the reaction of 6-chloro-1-hexanol and potassium phthalimide in DMF under reflux temperature gave the required 6-phthalimido-1-hexanol, which could be converted into the bromide **18** or the tosylate **4** respectively (see **Scheme 6**).

Bromide **18** proved to be superior to tosylate **4** because the former was easy to purify by recrystallization to give satisfactory elemental analysis data

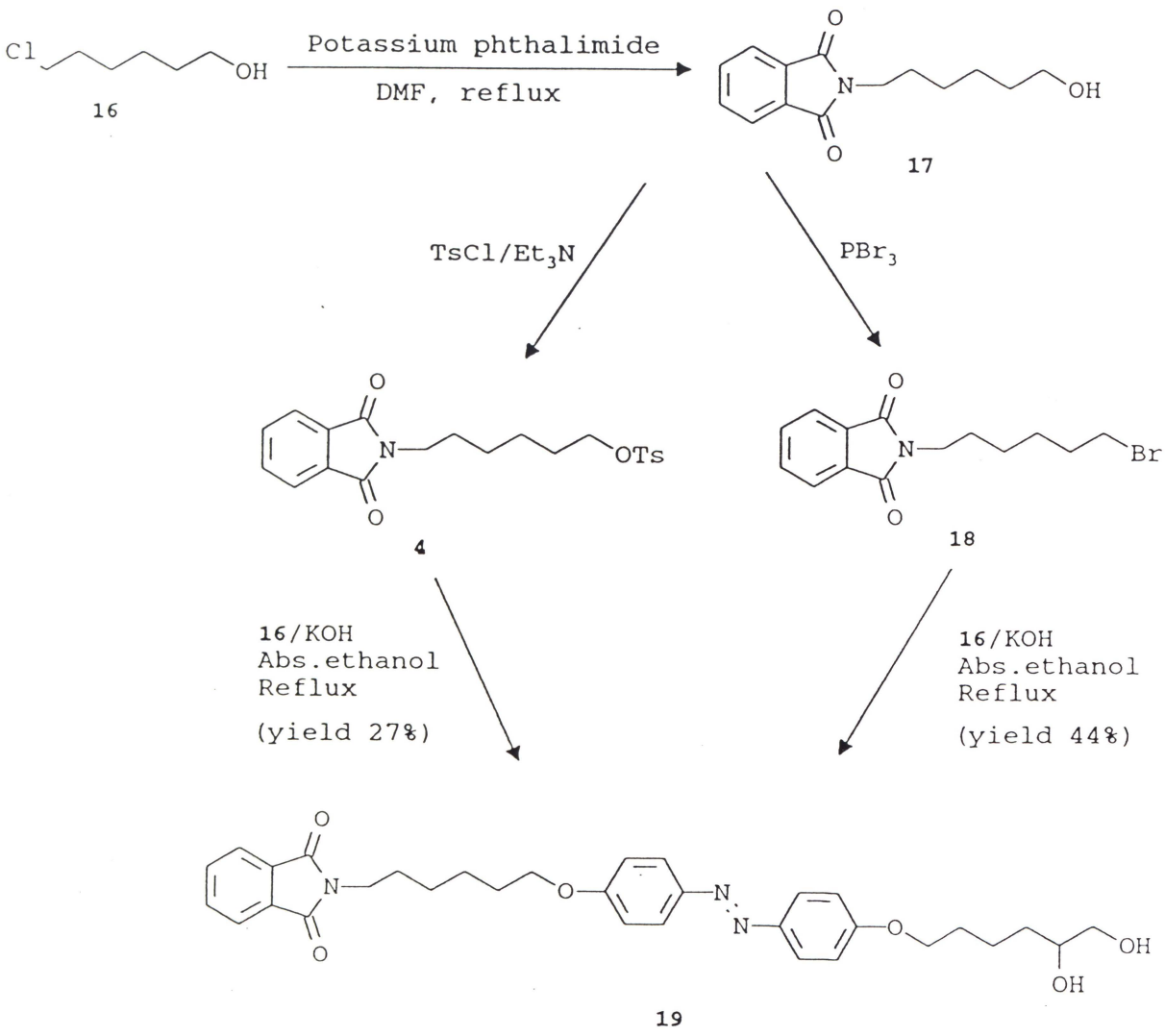


**Scheme 6**. Formation of 6-aminohexyl unit

while the latter was a glassy solid which was hard to purify. We subsequently showed that the following reaction with purified bromide **18** gave significantly higher yield than did the tosylate **4**. The total yield of the two steps from 6-chloro-1-hexanol to 6-phthalimidohexyl bromide was more than 70%.

**5. Formation of the wall unit**

Our original plan was to form the wall unit by the reaction of the hydroxyazobenzene **15** and 6-phthalimidohexyl bromide **18**, followed by deprotection of the phthalimide (see **Scheme 7**). Both reactions worked as expected, and the products **19** and **3** were identified by $^{1}H$ and $^{13}C$ NMR and MS (CI). Compound **3**, however, is not a suitable intermediate since it is insoluble in all solvents usually used for amide forming reactions with acid chlorides. Only solvents such as DMF or DMSO dissolve it to any extent. One possible reason for the insolubility of **3** could be the contradiction of the strong hydrophilicity of the two ends coupled with the strong hydrophobicity of the long carbon chain including the azobenzene moiety. We reasoned that if the polarity was decreased, the solubility of the compound would be improved.

Consequently, the glycol moiety was converted back to a ketal with 2,2-dimethoxypropane under the catalysis of *p*-toluenesulfonic acid to give compound **20** in a yield of 97% (see **Scheme 8**). The product was characterized by $^{1}H$ and $^{13}C$ NMR as well as MS (CI), and gave satisfactory elemental analysis data. Boron trifluoride in diethyl ether was considered as an alternative catalyst, but no **20** was recovered from an attempted synthesis using this catalyst. Compound **20** was converted to the glycol-protected amine **21** with hydrazine hydrate. Molecular weights of **20** and **21**, from the results of MS (CI), were respectively 599 and 469, which were consistent with expected values.

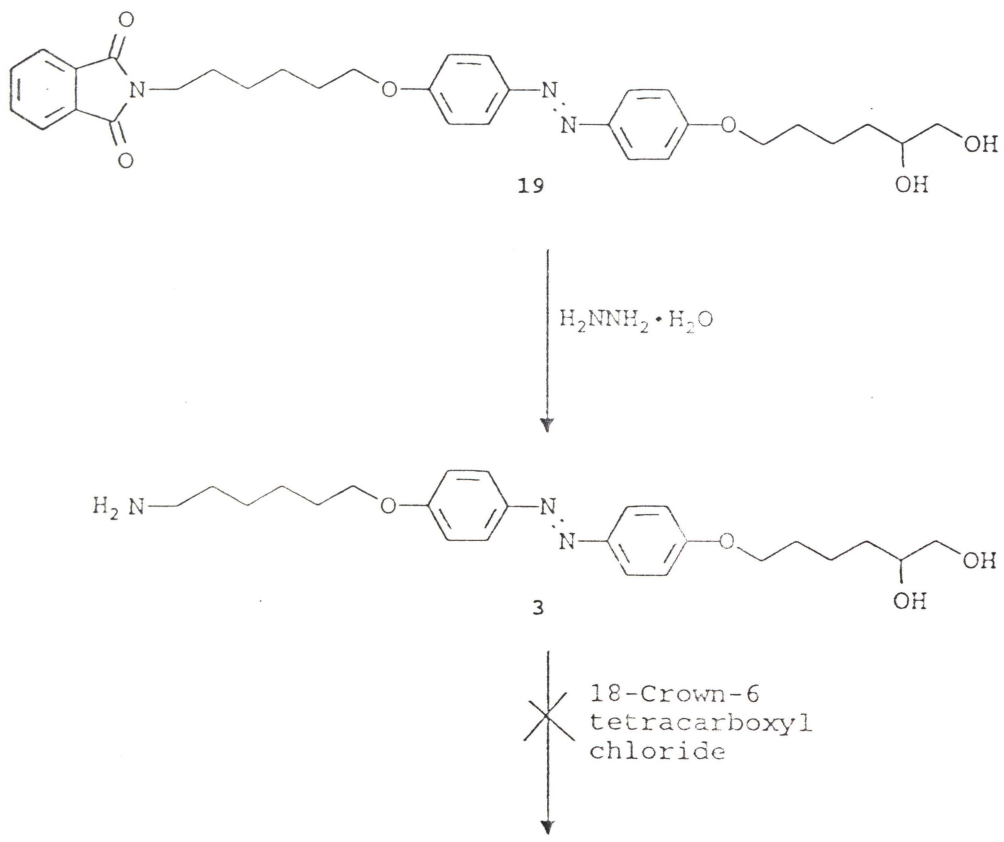


**Scheme 7**. Unsuccessful attempt in the formation of target compound **1**

By comparison of $^{1}H$ and $^{13}C$ NMR spectra, it was seen that the peaks representing the phthalimide group disappeared, while the peaks representing the ketal moiety still remained. Compound **21**, fairly soluble in solvents such as chloroform, dichloromethane and THF, was expected to be a good intermediate for the amide forming reaction.

## 6. Formation of the target compound

The amine **21** reacted with 18-crown-6 tetraacid chloride[17] in

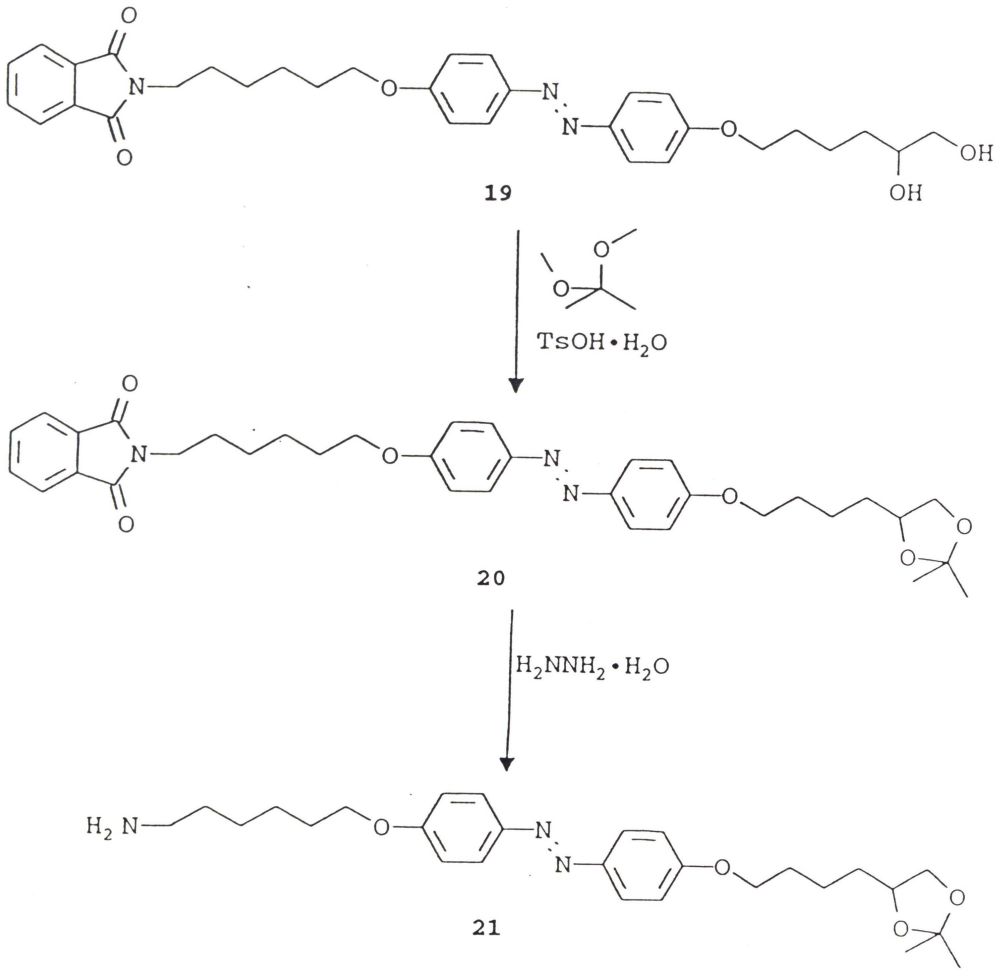


**Scheme 8**. Preparation of **21** instead of **3**

dichloromethane in a 4:1 ratio in the presence of excess triethylamine to give the glycol protected compound **22** which was separated by column chromatography (alumina). Compound **22** was then hydrolyzed with acid catalysis to produce the target compound **1** (see **Scheme 9**), which was purified by gel permeation column chromatography (Sephadex LH 20). As $Na^+$ and $Cl^-$ were introduced in the purification process by the use of sodium hydroxide and hydrochloric acid, it is expected that the target product would

be obtained in the form of a sodium complex of the crown ether.

Due to the large molecular weights, neither **22** nor **1** can be identified with chemical ionization MS. Fast Atom Bombardment (FAB) MS gave only some suggestive fragment peaks, but no molecular ion peak was seen in the spectra. Electrospray MS has been successful in the characterization of other high molecular weight crown ethers[27]. The electrospray MS were eventually obtained in methanol-chloroform (1:1) containing excess potassium iodide. The electrospray MS spectra clearly show the expected $M{\cdot}K^+$ (2025.0) and $M{\cdot}2K^+$ (1081.8) peaks together with $M{\cdot}K^+{\cdot}Na^+$ (1073.3) peaks. Elemental analysis data of C, H, and N were consistent with a formula of $C_{112}H_{156}N_{12}O_{26}{\cdot}NaCl$. $^1H$ and $^{13}C$ NMR verified the structure of the tartaric acid derived crown ether (singlet at 4.7 ppm and multiplet at 4.0 ppm in $^1H$ NMR and the peak at 82 ppm in $^{13}C$ NMR) and the *para*- substituted benzene rings (doublets at 7.8 and 6.9, J = 9 Hz in $^1H$ NMR and 8 peaks between 162 ppm and 115 ppm in $^{13}C$ NMR) as well as the formation of the amide structure (singlet at 4.7 ppm in the $^1H$ NMR and the peak at 171 in the $^{13}C$ NMR).

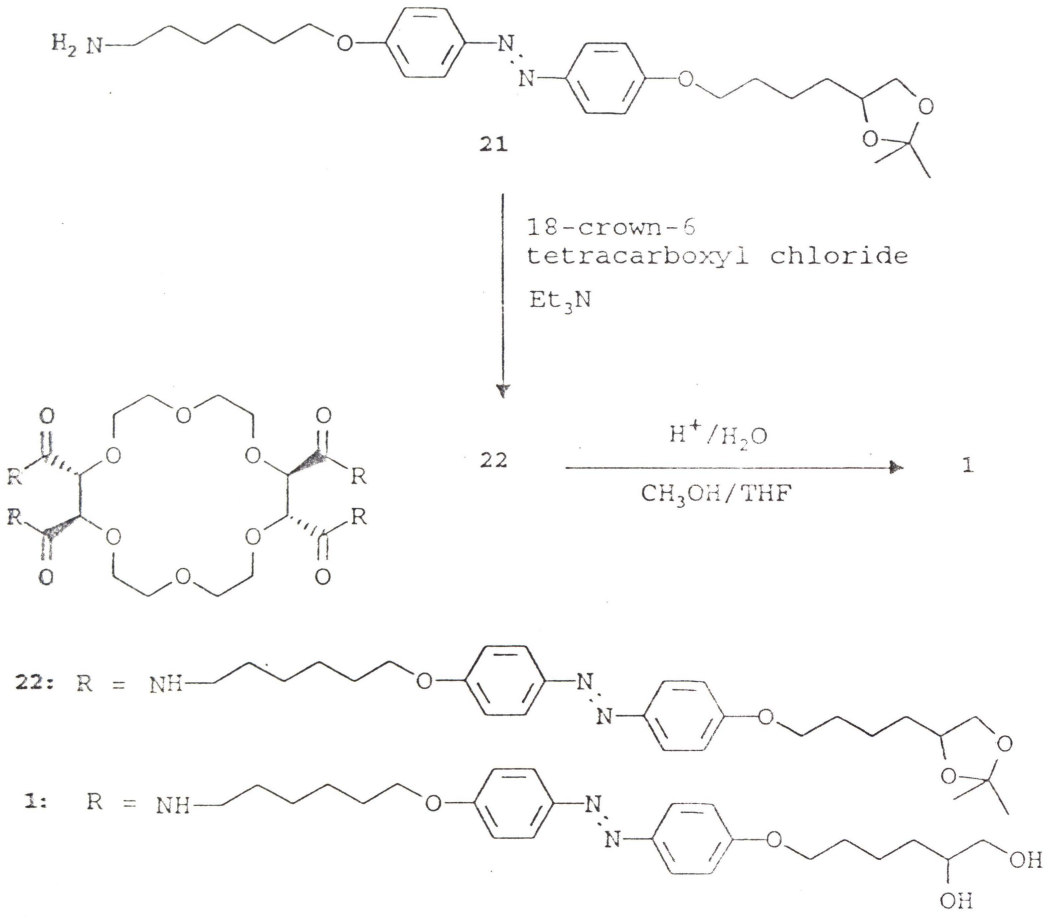


**Scheme 9.** Formation of target compound **1**

# Chapter 3

## Photogated ion transport

### 1. Photochemistry of the azobenzene moiety

Photoisomerization of **1** is the key factor for the photogate. As mentioned in Chapter 1, the photoisomerization is expected to determine the open and closed state of the channel.

The photochemistry of compound **1** was explored by following the UV-visible spectra of a solution of **1** (16.4 μM) in methanol-chloroform. As shown in **Fig. 10**, compound **1** has a major absorption peak at 360 nm, which is due to $\pi$-$\pi^*$ transition of the *trans*-azobenzene[28].

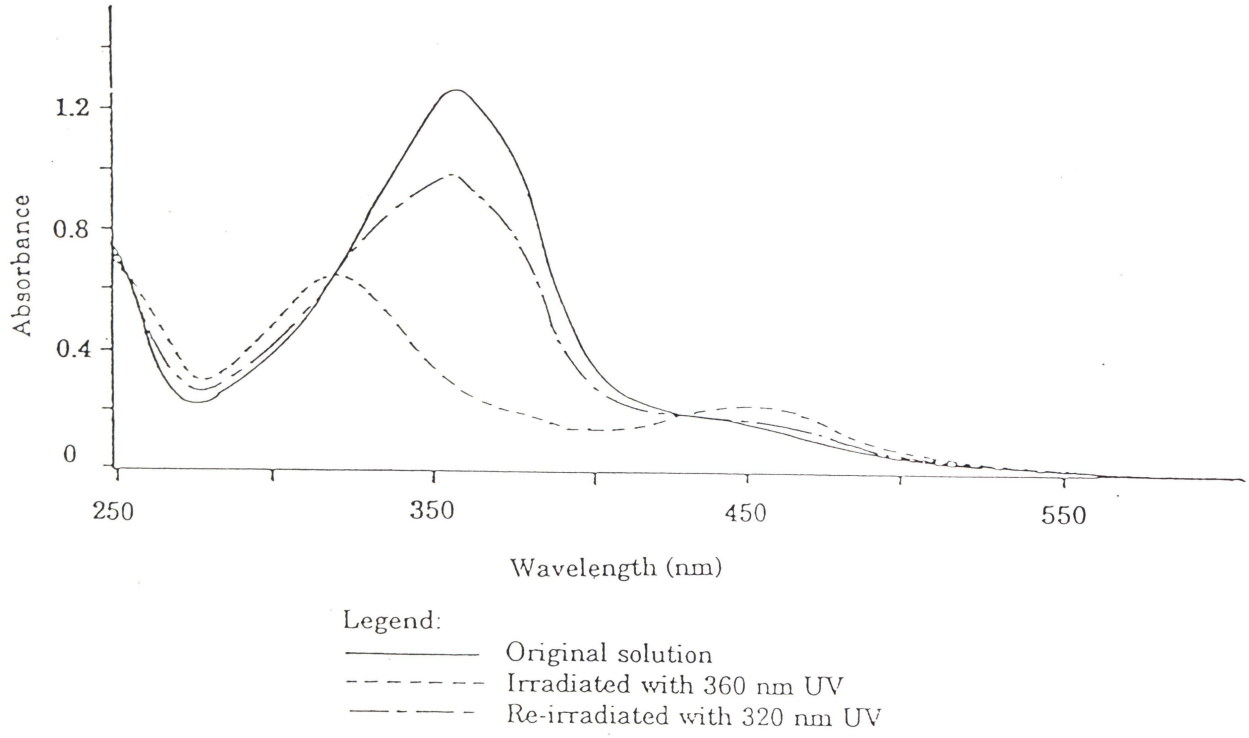


**Fig. 10**. UV-visible spectrum of photoisomerization of **1** (Concentration 16.4 μM in methanol-chloroform)

When the solution of **1** was irradiated with 360 nm UV for 5 minutes, the 360-nm band was reduced and the most intense absorption moved to 320 nm, which is due to the $\pi$-$\pi^*$ transition of the *cis*-azobenzene. Assuming the non-irradiated sample was pure *trans*- isomer, the residual absorption at 360 nm in the irradiated sample spectrum can be used to calculate a photostationary state ratio of *cis*- vs. *trans*-azobenzene. The ratio of *cis*- vs. *trans*- in the irradiated solution of **1** was approximately 75:25. When this sample was re-irradiated with 320 nm UV, the highest absorption moved back to 360 nm. From the absorbance of 360 nm peak, the ratio of *cis*- vs. *trans*- at this time was 25:75. The results presented are consistent with those found with other azobenzene derivatives that undergo reversible photoisomerization.

When the *trans*- azobenzene form of **1** (18.0 mM) in methanol-chloroform (v/v 1:1) was irradiated with 360 nm UV for 5 min and the irradiated sample was held at room temperature in the dark, a thermal isomerization of the photostationary state back to the *trans*- isomer happened. This reaction could be followed by the momentary increase in the 360-nm peak. **Fig. 11** shows the time course for growth of the 360-nm peak. The isomerization of *cis*-azobenzene to *trans*-azobenzene in compound **1** is not a first order reaction since any logarithmic transformation of the data retained the sigmoidal curve shape. Therefore, the lifetime of *cis*-azobenzene could not be calculated by any simple analytical method. However, by estimation from the plot, the half life of the *cis*-azobenzene form in **1** is approximately 15 min.

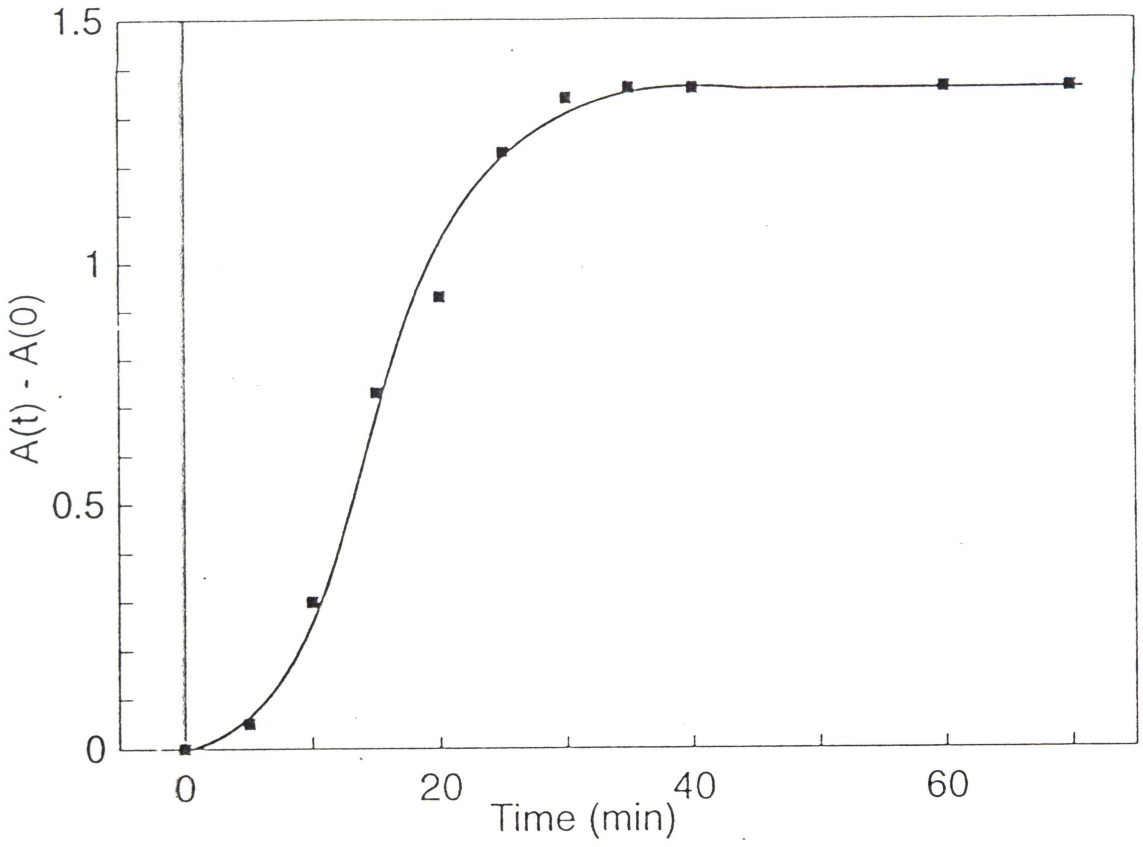


**Fig. 11**. Thermal isomerization of *cis*-azobenzene moiety (Concentration 18 μM in methanol-chloroform)

In principle, the molar absorptivity of a compound containing multiple chromophore is in proportion to the number of chromophores in a single molecule. As there are 4 azobenzene moieties in **1**, its molar absorptivity should be 4 times that of precursor **19**, in which there is only one azobenzene moiety. The molar absorptivities of **1** and **19** at 360 nm were obtained from the absorbances of a series of samples with different concentrations (see **Table 1** and **2**). Both compounds gave excellent linear plots of absorbances vs.

concentration ($r^2$ = 0.999 for **19** and 0.996 for **1**). The slopes of the straight lines in the plots are the molar absorptivities. The molar absorptivity of **1** at 360 nm (76300 ± 3000) is approximately 3.4 times higher than that of **19** (22400 ± 400). As shown in Chapter 2, the final product was verified as a tetramide of 18-crown-6 and no tri-substituted product was found by MS (Electrospray) or NMR spectra, so the deficiency of the absorbance of **1** is not the result of non-tetra- substituted by-product(s). The lower molar absorptivity could be caused by the intramolecular interaction between adjacent azobenzene units. This finding is consistent with the non-first order return to the all *trans*-form which could also be influenced by interactions between adjacent azobenzene units.

**Table 1**. Absorbance of **19** at 360 nm vs. concentration

(Methanol-chloroform, v/v 1:1)

| Concentration (M) | Absorbance |
|---|---|
| 0 | 0 |
| $3.0 \times 10^{-6}$ | 0.060 |
| $6.0 \times 10^{-6}$ | 0.129 |
| $9.0 \times 10^{-6}$ | 0.197 |
| $1.2 \times 10^{-5}$ | 0.268 |

**Table 2**. Absorbance of **1** at 360 nm vs. concentration

(Methanol-chloroform, v/v 1:1)

| Concentration (M) | Absorbance |
|---|---|
| 0 | 0 |
| $7.0 \times 10^{-7}$ | 0.052 |
| $1.4 \times 10^{-6}$ | 0.100 |
| $2.1 \times 10^{-6}$ | 0.167 |
| $2.8 \times 10^{-6}$ | 0.209 |

**2. Preparation of transporter set-in vesicle (TSV) solution**

The measurement of ion transport activity of transporters structurally similar to **1** has typically been performed by pH-stat titration of large unilamellar vesicle (LUV) solution[17]. Bilayer vesicles are spherical structures composed of bilayer phospholipid membrane containing internal solution[29]. In a typical experiment[17], the pH value of internal solution is 6.6. The pH of external solution is adjusted to 7.6 right before the titration experiment begins. The transporter and FCCP, which is a proton carrier, are dissolved in methanol and added to the vesicle solution during the experiment. Before the addition of transporter and salt to the vesicle solution, there is no material exchange between internal and external solutions. When the transporter and

salt are added into the vesicle solution with FCCP, protons are carried from the internal solution by the driving force of the pH gradient. Metal ions are transported into the vesicles to keep the internal and external solutions electroneutral. The protons flowing out are neutralized by the addition of choline hydroxide from an automated titrimeter to keep the pH of external solution at 7.6. By recording the amount of choline hydroxide added, the amount of cation transported can be calculated. Near the end of the titration, Triton X-100 is added to disrupt all vesicles. The amount of internal solution entrapped by the vesicles can be calculated from the lyse volume.

For compound **1**, however, this method is impractical because this compound is insoluble in methanol or any other usable solvent such as acetone. It is soluble in DMF, but this solvent causes apparent leaking of vesicles under the conditions of the pH-stat experiment.

After several attempts, the transport activity of compound **1** was successfully measured by pH-stat titration of a transporter set-in vesicle (TSV) solution. The transporter set-in vesicle solution was prepared by the following method. Compound **1** was dissolved in a chloroform-methanol mixed solvent to a concentration of 24.2 mg/ml. This solution (0.4 ml) was transferred into a flask and evaporated to form a thin layer of solid at the bottom of the flask. A vesicle solution (2 ml) prepared by the reverse evaporation method[17] was added to the flask with glass beads (diameter = 3 mm, 2.5 g). The flask was slowly rotated until all the solid disappeared (ca. 20 minutes), then the flask was

sonicated in a small bath for 10 minutes. Control experiments established that some vesicle damage occurred during the process. The total entrapped volume decreased by 20-30% due to the mixing and sonication. A prolonged sonication degraded more vesicles. The pale yellow transporter set-in vesicle solution was used directly. When the transporter set-in vesicle solution was run through a Sephadex GM-25 PD-10 gel permeation column, only one pale yellow band was obtained at the void volume. This confirms that **1** was incorporated with the vesicles fraction.

**3. Irradiation of target compound in vesicle solution**

Because of the light scattering effect of vesicles, the photoisomerization of the azobenzene moieties in **1** could not be measured directly by using UV-visible spectra of compound **1** in the TSV solution. The photoisomerization was estimated by UV-visible spectra of a series of extracts of the vesicle solution using chloroform.

The extraction was achieved as following: A portion of TSV solution (0.2 ml) was diluted with an isomolal solution of choline sulfate (4 ml). The diluted TSV solution was shaken with 0.5 ml of chloroform on a vortex for 1 minute. The chloroform was transferred to a small flask and shaken with a small amount of anhydrous sodium sulfate until the solution became clear. The clear solution was decanted and diluted to 1 ml with chloroform. The UV-visible spectrum of the extract is shown in **Fig. 12a**. The absorption at 360 nm

indicates that the extraction was successful. However, calculation of the concentration from the absorbance data and the extract volumes indicates the concentration of **1** in TSV solution was 0.26 μM. By calculation from the amount of compound **1** added in the preparation of the TSV solution, the maximum concentration of **1** in the TSV solution should be 116 μM. If the chloroform extraction was assumed to be complete, the amount of transporter incorporated with vesicles was only 0.2% of the total amount of transporter added in the experiment. Although this is very low, it is not too surprising considering that the transporter is transferred to the vesicles directly from the solid state. As noted below, the batch-to-batch variation is a problem with vesicle solutions and is largely due to the low efficiency of the solid-liquid transporter incorporation step.

Having established that the extraction process is feasible, the time to achieve complete photoisomerization was investigated. A TSV solution (0.2 ml) was diluted with an isomolal solution of choline sulfate (4 ml). Four portions of such diluted TSV solution were irradiated with 360 nm UV under argon bubbling for 5, 10, 15, and 20 minutes, respectively. Then each irradiated sample was extracted with chloroform immediately after the irradiation, and the extract was dried, diluted with chloroform to 1 ml, and the UV-visible spectrum of the sample was recorded. The spectra are weak, but clear bands at 360 nm were observed for insufficient irradiation times. It was found that the photoisomerization apparently reached saturation after 15 minutes

irradiation by giving a UV-visible spectrum as shown in **Fig. 12b.** All samples eventually showed regenerated *trans*-azobenzene spectra due to thermal back reaction as discussed previously.

a.

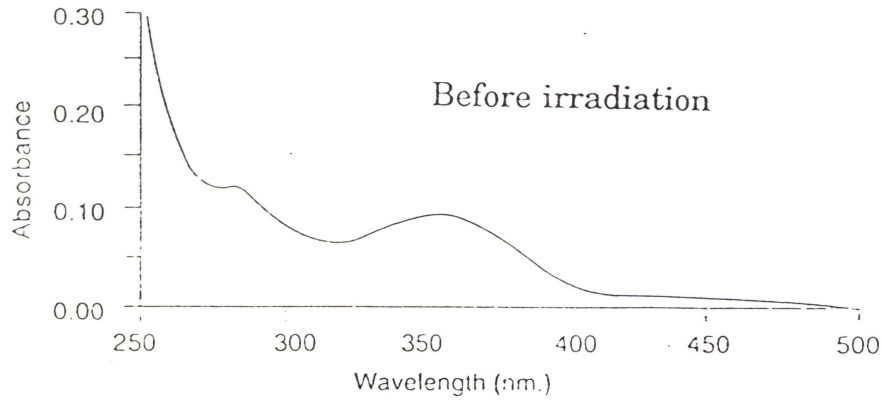


b.

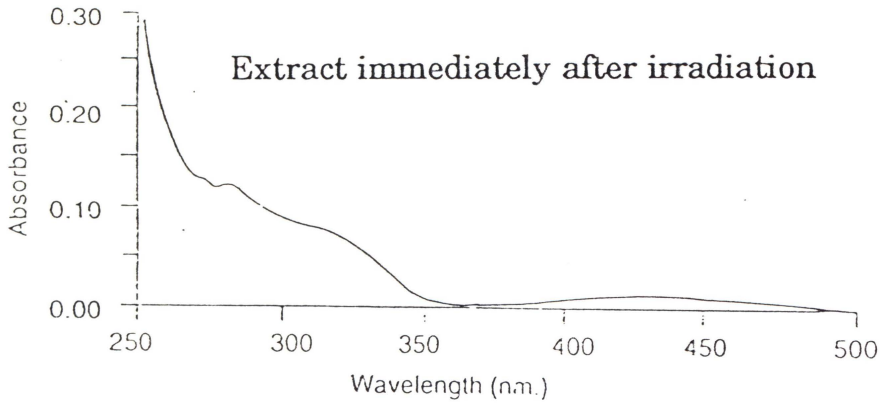


c.

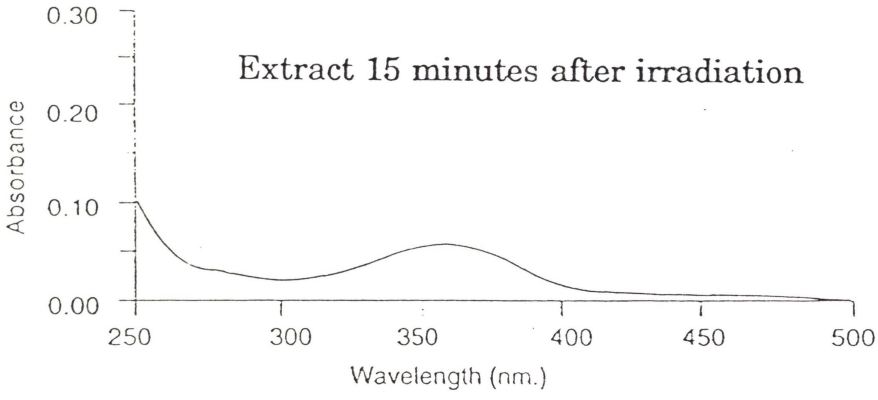


**Fig. 12.** UV-visible spectra of extracts from TSV solution

To determine the lifetime of the *cis*-azobenzene in vesicle solution, the irradiated TSV solution was held in the dark for variable times before extraction. Specifically, each portion of TSV solution (0.2 ml) was diluted with isomolal solution (4 ml) and irradiated with 360-nm UV for 15 minutes under argon bubbling. The irradiated samples were held at room temperature in the dark for 0, 15, 30, and 60 minutes, respectively, and extracted, dried, and diluted to 1 ml with chloroform. The UV-visible spectra of these extracts were taken and absorbance data at 360 nm were recorded. As discussed above, **Fig. 12b** is the spectrum of the extract immediately after irradiation, where the absorption at 360 nm is much lower than in **Fig. 12a**. The spectrum of the extract from a TSV solution 15 minutes after irradiation is shown in **Fig. 12c**. The absorption at 360 nm is apparently higher than that in **Fig. 12b**. All these extracts of the solutions gave almost the same absorbance at 360 nm when held at room temperature in the dark overnight.

The absorbance data were collected and plotted (**Fig. 13**). The data are sparse, but a sigmoidal curve like **Fig. 11** is consistent with the results. Absorbance data varied even within the same batch of TSV solution because the time for the extraction and drying of the extract was difficult to control. Any delay might result in an absorbance difference. As the precision of the experiment was not very good, the half life of the *cis*-azobenzene in TSV solution can only be estimated to be approximately 12 minutes, which is consistent with that in chloroform-methanol solution.

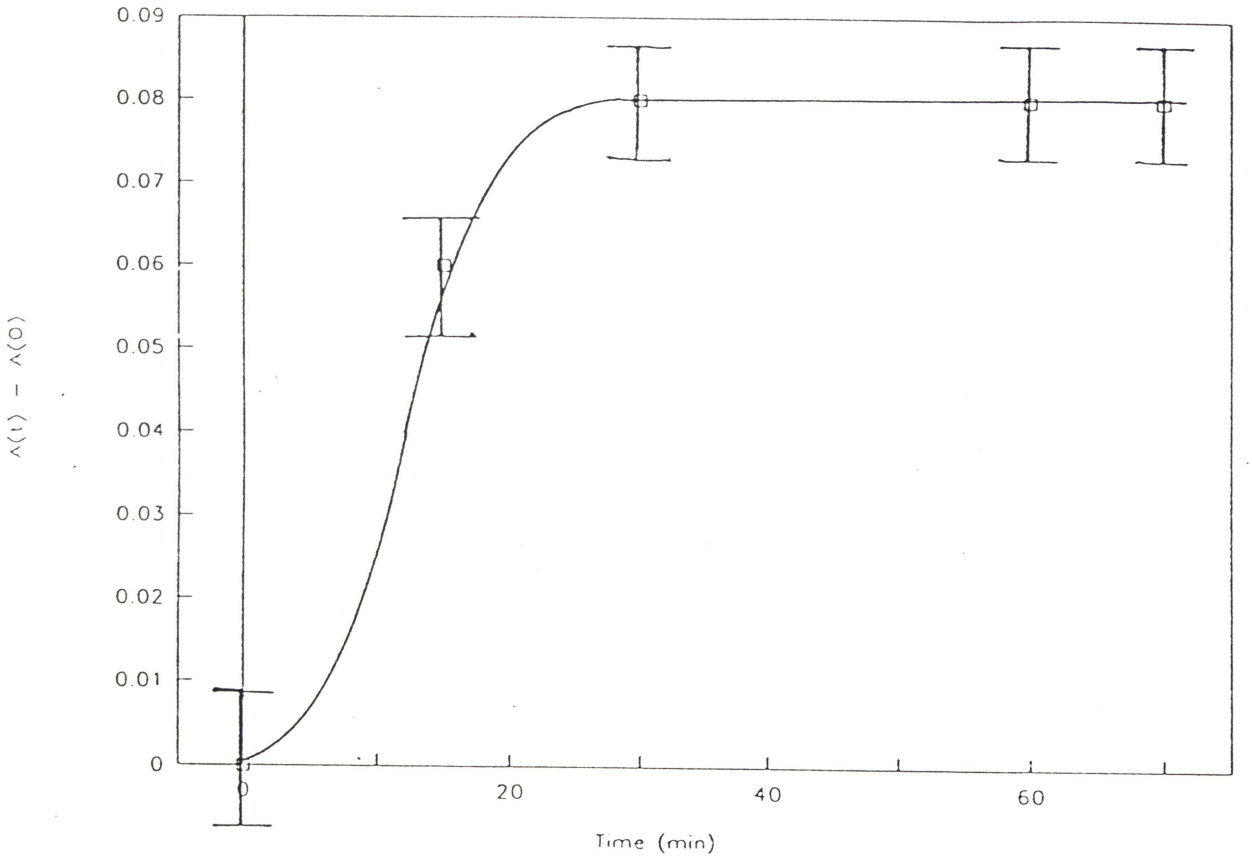


**Fig. 13**. Thermal reversal of irradiated compound **1** in TSV solution

## 4. Transport activity and selectivity

The pH-stat titration of the transporter set-in vesicle solution was basically the same as that of a vesicle solution as described previously (see **Fig. 14**). The TSV solution was set to pH = 7.6 by addition of choline hydroxide. This is time zero of **Fig. 14**. Addition of salt and subsequent addition of FCCP each caused a small amount of immediate lysis due to osmotic shock. A steady transport process began when the system was fully constituted. At a later point of the titration, Triton X-100 was added to disrupt

all the vesicles in the solution, and the lysis volume ($V_{lysis}$) was obtained.

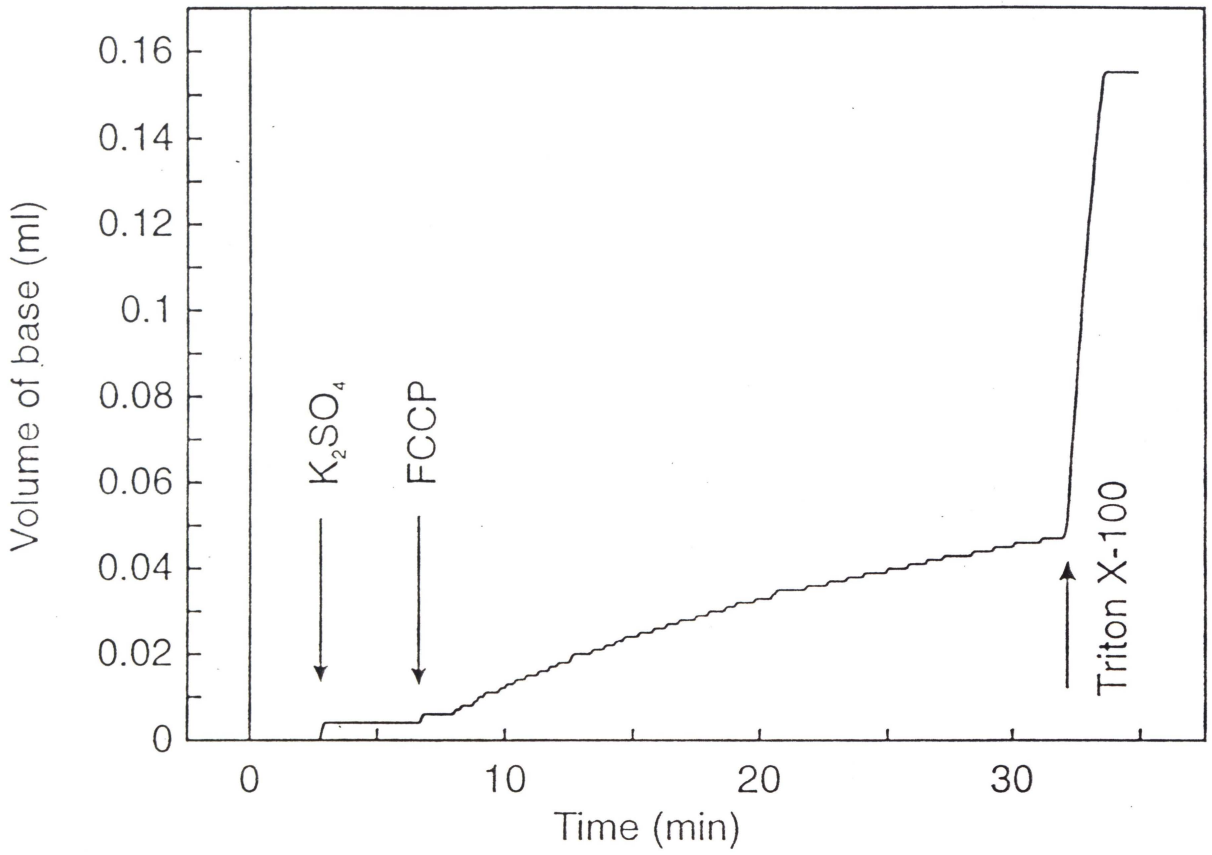


**Fig. 14.** A pH-stat titration of TSV solution for transport activity of **1**

The data were transferred to a PC and the apparent first order rate constant was obtained for the portion of the record following FCCP addition (t = 0). Linear regression of the logarithm of the base volume added as a function of time gives good correlation ($r^2 > 0.997$) except for $Na^+$ ($r^2 = 0.580$), for which only a limited volume of base was added. An initial proton efflux was calculated as previously[17] using the equation:

$$r_0 = k \cdot (V_{inf} - V_0) \cdot c_{base}$$

Where $r_0$ = initial rate of proton efflux, k is the first order rate constant, $V_{inf}$ is the "infinity" volume of base added, $V_0$ is the volume of base at time zero, and $c_{base}$ is the concentration of choline hydroxide solution.

The extent of transport is expressed as percent of the total amount of entrapped protons assessed by Triton lysis ($V_{inf}/V_{lysis}$).

In order to compare the activity of this compound with previously reported synthetic transporters with similar structures, the initial efflux rate was normalized to a concentration of $2 \times 10^{-6}$ M (see **Table 3**). The normalized rate for $K^+$ is approximately 10 times lower than some previously reported channel-like synthetic transporters with similar structures[17]. From the rate data it is obvious that $K^+$ is the most favored ion, then $Rb^+$, $Cs^+$, and $Na^+$, and there is no transport for $Li^+$. The transporter **1** is not very active in transport of alkali metal ions. But despite the low transport activity, the transport properties are very similar to some previously reported compounds with similar structures[17]. **Table 3** shows that the larger the extent of transport, the larger the initial rate. This phenomenon was previously taken as a gramicidin-like indicator of a channel.

The transport selectivity of **1** for alkali metal ions, by initial rates, is in the order of $K^+$, $Rb^+$, $Cs^+$, $Na^+$, and $Li^+$. The effect is more clearly seen in **Fig. 15**. If the rate for $K^+$ is assumed to be 100, then the selectivity is 70 for $Rb^+$, 40 for $Cs^+$, 12 for $Na^+$, and 0 for $Li^+$. The selectivity order is the same as some previously reported 18-crown-6 derived ion channels[17], but does not directly

indicate a mechanism.

**Table 3**. Transport activity and selectivity of compound 1

| $M^+$ | Rate constant x $10^4$ ($s^{-1}$) | Initial rate x $10^{12}$ (mol $H^+ \cdot s^{-1}$) | Normalized Initial rate* x $10^{12}$ (mol $H^+ \cdot s^{-1}$) | Extent of transport (%) |
|---|---|---|---|---|
| $Li^+$ | 0 | 0 | 0 | ----- |
| $Na^+$ | 21 | 3.4 | 26 | 9 |
| $K^+$ | 7.9 | 25 | 192 | 31 |
| $Rb^+$ | 9.5 | 18 | 138 | 26 |
| $Cs^+$ | 9.5 | 10 | 77 | 13 |

* Normalized to [Tr] = 2 x $10^{-6}$. $r_n$ = (2 x $10^{-6}$ / [Tr]) x r

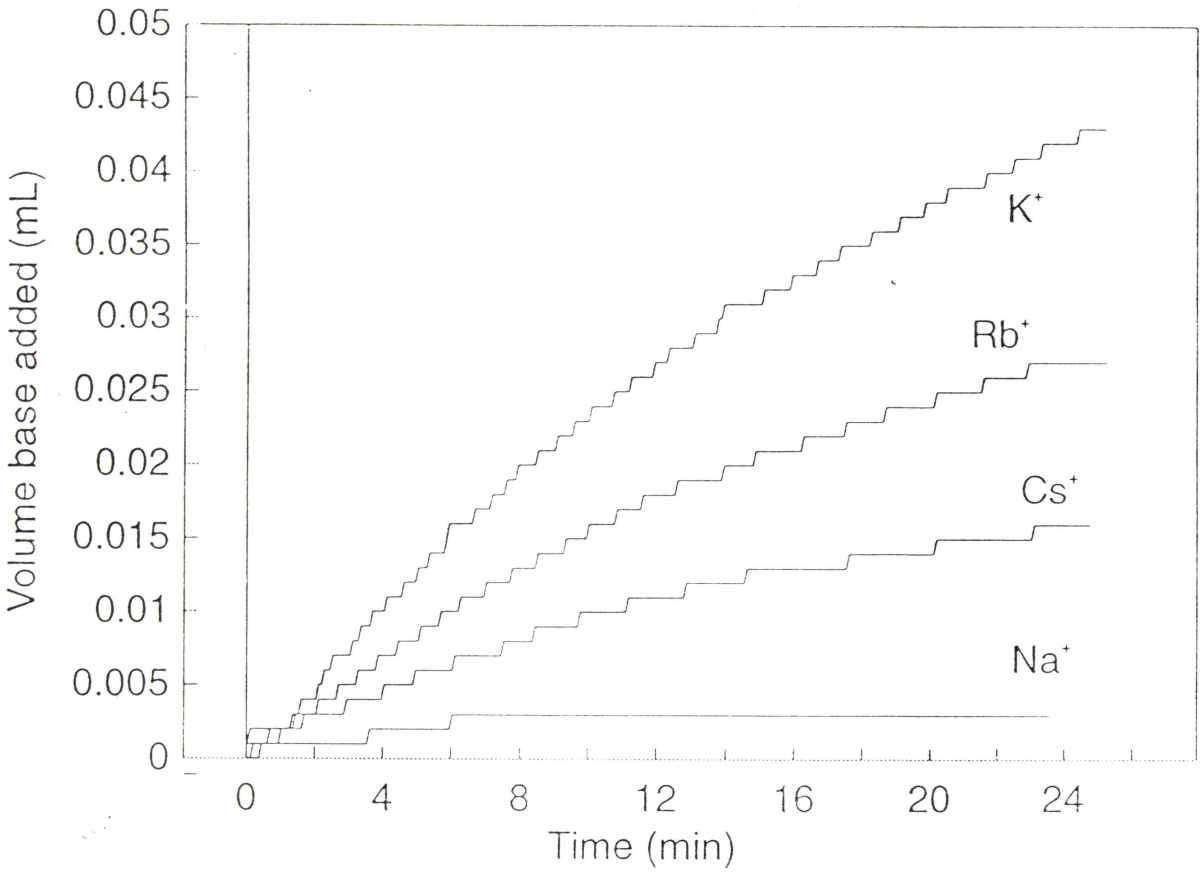


**Fig. 15**. Transport selectivity of alkali metal cations

**5. Photogate effect**

The effect of photoisomerization on transport was explored by doing the pH-stat experiment immediately following 15-minute irradiation of the TSV solution at 360 nm. As shown above, the photostationary state is established under these conditions, but the *cis*- isomer will persist for only a short period (half life is ca. 15 minutes). The results are shown in **Fig. 15**. In this experiment, the transport rate for the non-irradiated vesicle solution was very slow, and the irradiated vesicle solution showed a substantial increase in transport rate. The actual rate was very similar to that in the selectivity experiment. This difference is typical of the variation between different TSV solution preparations. There might be two explanations for the phenomenon. The first could be that the incorporation of **1** with vesicles was not efficiently achieved during the sonication, and the photoisomerization of **1** might improve the incorporation by reorganization. Alternatively, the photoisomerization might destroy the packing of the bilayer membrane adjacent to the transporter and thus cause a leaking of the vesicles.

It is obvious that a photogate effect was not detected by the titration of the TSV solution, but this does not mean that a photogate effect does not exist. The lifetime of the *cis*-azobenzene form of **1** in vesicle solution is too short for a successful pH-stat titration experiment, and the amount of **1** in the vesicle solution is too low. Both are problems related to the target selected, and could be solved using alternative photoswitching elements. The close proximity of

several chromaphores is a persistent problem which should be avoided in future designs.

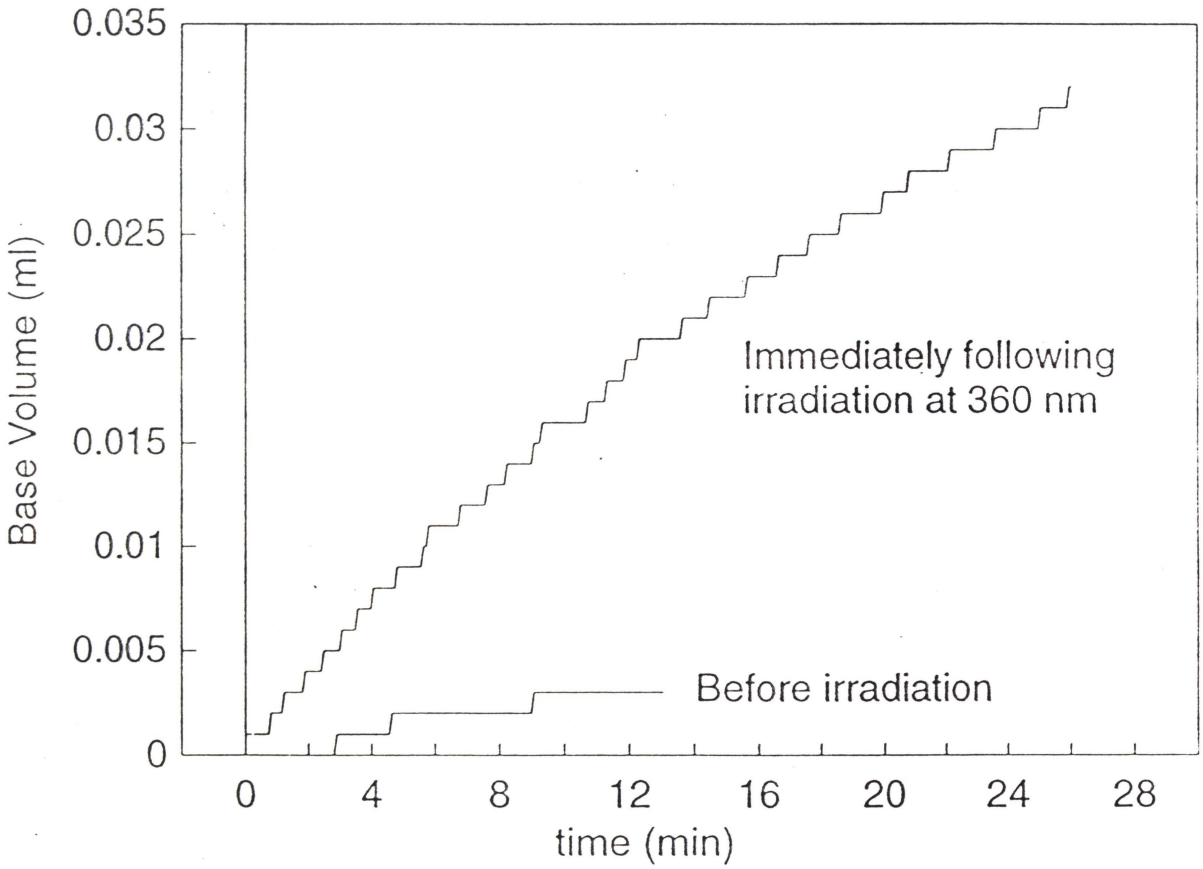


**Fig. 16.** Photogate effect on $K^+$ transport by pH-stat titration of TSV

## Conclusions

1. Target compound **1**, as an artificial ion transporter, was successfully synthesized. The compound, as well as its intermediates, were identified by NMR, MS, and elemental analysis.

2. Photoisomerization of compound **1** was achieved, but the lifetime of the *cis-* isomer is short (half life c.a. 15 minutes). The molar absorptivity of this compound at 360 nm is apparently smaller than 4 times of that a single azobenzene precursor because of intramolecular interaction between adjacent azobenzene moieties.

3. Compound **1** has a low transport activity for alkali metal ions. Compound **1**'s transport selectivity is in the order of $K^+ > Rb^+ > Cs^+ > Na^+ > Li^+$. Despite its low activity, its transport properties are similar to the artificial ion channels of similar structures previous reported[17].

4. The photoswitching of compound **1** was supposed to be controlled by the photochemical conversion of azobenzene moieties. This effect cannot be measured by pH-stat titration of a vesicle solution or TSV solution because the lifetime of the predominantly *cis-* form of **1** is too short, and the amount of **1** incorporated is small. The solubility properties of the transporter inhibit a more rapid experiment.

# Experimental

## 1. Synthesis

Melting points were taken in capillaries. NMR spectra, scaled in ppm, were taken on a Bruker WM 250 (250 MHz, FT. 62.89 MHz for $^{13}C$) instrument or a Bruker AMX 360 (360.14 MHz, FT) instrument with the solvents as standards ($^{1}H$: chloroform-d 7.24, DMSO-$d_6$ 2.49, methanol-$d_4$ 4.78. $^{13}C$: chloroform-d 77.0, DMSO-$d_6$ 39.5, methanol-$d_4$ 49.0). MS were taken on a Finnigan 3300 GC.MS instrument or a Kratos Concept-IH instrument. UV-visible spectra were taken on a Varian Cary-5 UV-VIS spectrometer. Temperature and pressure data are all uncorrected. Elemental analysis was done by Canadian Microanalytical Services, Ltd., New Westminster, B.C.

**4-(4-Hydroxybutyl)-2,2-dimethyl-1,3-dioxolane (12)**

To a 500-ml round bottomed flask fitted with a drying tube was added 1,2,6-hexanetriol (10 g, 74.6 mmol), anhydrous magnesium sulfate (3 g), 4-toluenesulfonic acid monohydrate (0.3 g) and dry acetone (75 ml). The mixture was stirred at room temperature for 18 hours. Sodium carbonate monohydrate (0.3 g) was then added to the reaction mixture and the mixture was stirred for one more hour. Solids were filtered and the filtrate was evaporated on a rotary evaporator. The residue was distilled under reduced pressure to give 10.9 g of

colorless liquid, b.p. 92-94°/1 mm, yield 82%. Second reaction gave 11.6 g of the same product, yield 89%. $^1$H NMR ($CDCl_3$): 4.01-3.91 (m, 2H, $CH_2O$), 3.51 (t, J = 6.3 Hz, 2H, $C\underline{H}_2OH$), 3.48-3.38 (m, 1H, CHO), 2.79 (br, 1H, OH), 1.57-1.17 (m, 6H, $CH_2$), 1.30, 1.25 (2 x s, 6H, $CH_3$). $^{13}$C NMR ($CDCl_3$): 108.5 (OCO), 75.9, 69.2 (CHO and $CH_2O$), 62.1 ($CH_2OH$), 33.1, 32.4, 21.9 ($CH_2$), 26.8, 25.5 ($CH_3$). MS (CI): M+1 175, M+29 203, M+41 215.

Elemental analysis: $C_9H_{18}O_3$ = 174.24

| | | |
|---|---|---|
| Calculated: | C 62.04 | H 10.41 |
| Found: | C 58.91 | H 9.85 |

**4-(4-Bromobutyl)-2,2-dimethyl-1,3-dioxolane (10)**

A 500-ml 3-necked round-bottomed flask fitted with a mechanical stirrer and a thermometer was charged with **12** (69.7 g, 0.400 mol) and triphenylphosphine (115.4 g, 0.440 mol). Under stirring, NBS (67.6 g, 0.380 mol) was added in portions at such a rate that the temperature was kept below 90°. A cold water bath was applied whenever necessary. When the addition of NBS was complete, the mixture was filtered with suction and the filter cake was washed as thoroughly as possible with 750 ml of petroleum ether (30-60). The solution of the crude product in petroleum ether was washed with two 250-ml portions of water and dried over anhydrous magnesium sulfate. The solvent was evaporated on a rotary evaporator and distillation of the residue under reduced pressure gave 60.2 g of colorless liquid, b.p. 75-80°/1 mm, yield

67%. $^1$H NMR ($CDCl_3$): 4.00-3.94 (m, 2H, $CH_2O$), 3.47-3.42 (m, 1H, CHO), 3.35 (t, J = 6.8 Hz, 2H, $CH_2Br$), 1.86-1.47 (m, 6H, $CH_2$), 1.34, 1.28 (2 x s, 6H, $CH_3$). $^{13}$C NMR ($CDCl_3$): 108.6 (OCO), 75.6 (CHO), 69.2 ($CH_2O$), 32.6 ($CH_2Br$), 33.3, 32.5, 24.3 ($CH_2$), 26.8, 25.6 ($CH_3$). MS (CI): M+1 237 (100), M+3 239 (94), M+29 265.

Elemental analysis: $C_9H_{17}BrO_2$ = 237.14

| | | | |
|---|---|---|---|
| Calculated: | C 45.59 | H 7.23 | Br 33.70 |
| Found: | C 42.92 | H 6.67 | Br 33.35 |

**_N_-(6-Hydroxyhexyl)phthalimide (17)** and **_N_-(6-bromohexyl)phthalimide (18)**

A mixture of 6-chloro-1-hexanol (54.6 g, 0.40 mol), potassium phthalimide (88.8 g, 0.48 mol) and DMF (200 ml) was heated at reflux temperature for 24 hours. After cooling to room temperature, chloroform (400 ml) was added to the reaction mixture and the mixture was then washed with a 400-ml portion and two 200-ml portions of water and dried over anhydrous magnesium sulfate. The solvent was removed on a rotary evaporator and residual DMF was removed under high vacuum on an oil pump. The residue formed a waxy solid which was used without further purification. $^1$H NMR ($CDCl_3$): 7.80-7.54 (2 x m, 4H, aromatic), 3.65-3.52 (2 x t, J = 7.2 Hz, 6.5 Hz, 4H, $OCH_2$ and $NCH_2$), 2.22 (br, 1H, OH), 1.66-1.29 (m, 8H, $CH_2$). $^{13}$C NMR ($CDCl_3$): 168.3 (CO), 133.8, 131.9, 123.0 (aromatic), 62.4 ($OCH_2$), 37.7 ($NCH_2$),

32.4, 28.4, 26.4, 25.1 ($CH_2$). MS (CI): M+1 250, M+29 278, M+41 290.

To the waxy solid **17** obtained above was added phosphorus tribromide (54.2 g, 0.20 mol) with shaking. When all the solid dissolved, the mixture was stirred until it solidified. The solid was heated with water (500 ml) until it melted and the mixture was poured onto crushed ice (700 g) with stirring. The solid was collected by suction filtration and dried in the air. Recrystallization from 95% ethanol gave 90.7 g of white leaflets, m.p. 53-55°, yield 73.1% from 6-chloro-1-hexanol. $^1H$ NMR ($CDCl_3$): 7.81-7.24 (2 x m, 4H, aromatic), 3.64 (t, J = 7.2 Hz, 2H, $NCH_2$), 3.35 (t, J = 6.8 Hz, 2H, $CH_2Br$), 1.86-1.28 (4 x m, 8H, $CH_2$). $^{13}C$ NMR ($CDCl_3$): 168.3 (CO), 133.8, 132.0, 123.1 (aromatic), 37.7 ($NCH_2$), 33.6 ($CH_2Br$), 32.5, 28.3, 27.6, 25.9 ($CH_2$). MS (CI): M+1 310 (100), M+3 312 (100), M+29 338, M+41 350.

Elemental analysis: $C_{14}H_{16}BrNO_2$ = 310.19

| | | | | |
|---|---|---|---|---|
| Calculated: | C 54.21 | H 5.20 | Br 25.76 | N 4.52 |
| Found: | C 54.74 | H 5.19 | Br 26.12 | N 4.59 |

A little more product with a lower m.p. 50-53° was recovered by concentration of the mother liquor.

**4-(4-Acetamidophenoxybutyl)-2,2-dimethyl-1,3-dioxolane (13)**

A 250-ml round-bottomed flask was charge with a solution of potassium hydroxide (85%, 7.92 g, 0.120 mol) in absolute ethanol (80 ml). 4-Acetamidophenol (18.14 g, 0.120 mol) was added into the flask to form a pale

purple solution. To the solution of the phenoxide, **10** (23.71 g, 0.100 mol) was added with absolute ethanol (20 ml) for complete transfer. The reaction mixture was heated to reflux for 2 hours. After cooling, the reaction mixture was poured into water (300 ml). The combined dichloromethane extract was washed with 150 ml of 1% sodium hydroxide and then 150 ml of water, and dried over anhydrous magnesium sulfate. The solvent was evaporated on a rotary evaporator and the residue solidified on standing at room temperature overnight. Recrystallization from acetone-water gave 25.2 g of colorless needles, yield 82%. $^{1}$H NMR ($CDCl_3$): 8.03 (br, 1H, CONH), 7.33, 6.76 (2 x d, J = 9.0 Hz, 9.0 Hz, aromatic), 4.09-3.92, 3.50-3.44 (2 x m, 3H, $OCH_2$, OCH), 3.87 (t, J = 7.1 Hz, 2H, $ArOCH_2$), 2.06 (s, 3H, $COCH_3$), 1.80-1.27 (m, 6H, $CH_2$), 1.36, 1.30 (2 x s, $CH_3$). $^{13}$C NMR ($CDCl_3$): 168.7 (CO), 155.7, 130.9, 127.8, 122.1 (aromatic), 108.6 (OCO), 75.8 ($ArOCH_2$), 69.3 (OCH), 67.8 ($OCH_2$), 33.2, 29.1, 22.3 ($CH_2$), 26.8, 25.6 ($CH_3$), 24.0 ($\underline{C}H_3CO$). MS (CI): M+1 308, M+29 336, M+41 348.

Elemental analysis: $C_{17}H_{24}NO_4$ = 307.39

| | | | |
|---|---|---|---|
| Calculated: | C 66.42 | H 8.20 | N 6.22 |
| Found: | C 64.68 | H 8.10 | N 6.02 |

**6-(4-Aminophenoxy)-1,2-hexanediol (14)**

A mixture of **13** (15.4 g, 0.050 mol), concentrated hydrochloric acid (17 ml), water (17 ml) and 95% ethanol (35 ml) was heated at reflux temperature for 4 hours. The ethanol was removed on a rotary evaporator, and the residual

aqueous solution was made basic with 10% sodium hydroxide to pH > 10 and chilled in a refrigerator to give pale yellow plates. The crystals were collected by filtration and washed with ice-chilled water to neutral (pH < 8). The product weighed 9.16 g after drying in air, yield 81%. $^{1}H$ NMR (DMSO-$d_6$): 6.65-6.45 (2 x d, J = 8.8 Hz, 8.8 Hz, 4H, aromatic), 4.55 (br, 2H, $NH_2$), 4.46 (t, J = 5.7 Hz, 1H, $CH_2O\underline{H}$), 4.40 (d, J = 4.9 Hz, 1H, CHO$\underline{H}$), 3.78 (t, J = 6.3 Hz, 2H, $ArOCH_2$), 3.40-3.20 (2 x m, 3H, C$\underline{H}$OH and C$\underline{H_2}$OH), 1.64-1.18 (2 x m, 6H, $CH_2$). $^{13}C$ NMR (DMSO-$d_6$): 150.1, 142.2, 115.3, 115.0 (aromatic), 71.1 ($ArOCH_2$), 68.0 (OCH), 66.0 ($OCH_2$), 33.2, 29.2, 21.9 ($CH_2$). MS (CI): M+1 226, M+29 254, M+41 266.

Elemental analysis: $C_{12}H_{19}NO_3$ = 225.29

| | | | |
|---|---|---|---|
| Calculated: | C 63.98 | H 8.50 | N 6.22 |
| Found: | C 61.81 | H 8.63 | N 6.02 |

**4-Hydroxy-4'-(5,6-dihydroxyhexyl)-*E*-azobenzene (15)**

Compound **14** (9.0 g, 0.040 mol) was dissolved in 1:3 (v:v) hydrochloric acid (48 ml) with mild heating. The solution was chilled in an ice bath with stirring to form a slurry. A solution of sodium nitrite (3.04 g, 0.44 mol) in 16 ml of water was added dropwise to the slurry with vigorous stirring and ice-salt chilling at such a rate that the temperature was controlled below 5°. With the addition of the nitrite solution, the slurry became thinner and thinner and changed into an orange solution. Cadmium iodide-starch test papers were used

to monitor the end of the reaction. When the reaction was complete, the newly formed diazonium solution was added dropwise to a solution of phenol (3.76 g, 0.040 mol) in 10% sodium hydroxide (33.2 ml) with chilling in an ice a=bath. The deep yellow precipitate was collected by filtration, and washed with water until pH > 6. The crude product was dried *in vacuo* overnight and recrystallized from methanol to give 8.6 g of deep yellow plates, yield 65%, m.p. 146-148°. $^{1}$H NMR (DMSO-$d_6$): 10.21 (br, 1H, ArOH), 7.77, 7.74, 7.04, 6.92 (4 x d, J = 9.0 Hz, 8.8 Hz, 9.0 Hz, 8.8 Hz, 8H, aromatic), 4.50 (t, J = 5.6 Hz, 1H, $CH_2O\underline{H}$), 4.46 (d, J = 4.9 Hz, 1H, CHO$\underline{H}$), 3.43 (m, 1H, C$\underline{H}$OH), 3.29-3.24 (m, 2H, C$\underline{H_2}$OH), 1.74-1.24 (m, 6H, $CH_2$). $^{13}$C NMR (DMSO-$d_6$): 160.8, 160.3, 146.2, 124.4, 124.0, 115.9, 114.9 (aromatic), 71.1, 68.0, 66.1 ($OCH_2$ and OCH), 33.2, 28.9, 21.9 ($CH_2$). MS (CI): M+1 331, M+29 359, M+41 371.

Elemental analysis: $C_{18}H_{22}N_2O_4$ = 330.39

| | | | |
|---|---|---|---|
| Calculated: | C 65.44 | H 6.71 | N 8.48 |
| Found: | C 65.13 | H 6.68 | N 8.45 |

**4-(6-Phthalimidohexyloxy)-4'-(5,6-dihydroxyhexyloxy)-*E*-azobenzene (19)**

A mixture of **15** (6.60 g, 0.020 mol), potassium hydroxide (85%, 1.32 g, 0.020 mol), and absolute ethanol (40 ml) was heated until all the solid dissolved. Then a suspension of **18** (6.20 g, 0.020 mol) in absolute ethanol (40 ml) was added and the mixture was heated at reflux temperature for 24 hours.

After cooling to room temperature, an orange precipitate, which was mainly composed of potassium bromide and the expected product, was formed from the solution. The solid was collected by suction filtration, and extracted on a Soxhlet extractor with dichloromethane. A small amount of solid suspended in the extract was filtered, and the solvent was evaporated on a rotary evaporator. The residue was recrystallized from 95% ethanol to give 4.96 g of orange plates, yield 44%, m.p. 132.5-134°. $^{1}$H NMR (DMSO-$d_6$): 7.80-7.75 (m, 8H, phthalimide aromatic and azobenzene aromatic), 7.06-6.99 (2 x d, J = 8.9 Hz, 8.9 Hz, 4H, azobenzene aromatic), 4.46 (t, J = 5.6 Hz, 1H, $CH_2O\underline{H}$), 4.41 (d, J = 5.0 Hz, 1H, $CHO\underline{H}$), 4.01, 3.97 (2 x d, J = 7.0 Hz, 5.3 Hz, 4H, $ArOCH_2$), 3.54 (t, J = 6.8 Hz, 2H, $NCH_2$), 3.36-3.26 (m, 3H, $C\underline{H}OH$ and $C\underline{H_2}OH$), 1.68-1.29 (m, 14H, $CH_2$). $^{13}$C NMR (DMSO-$d_6$): 167.9 (CO), 160.9, 160.8, 146.0 (2C), 124.0 (4C), 114.8 (4C) (azobenzene aromatic), 134.3, 131.5, 122.9 (phthalimide aromatic), 71.0 (CHO), 68.0, 67.8 ($ArOCH_2$), 66.0 ($OCH_2$), 37.3 ($NCH_2$), 33.1, 28.8, 28.4, 27.8, 26.0, 25.1, 21.8 ($CH_2$). MS (CI): M+1 560, M+29 588, M+41 600.

Elemental analysis: $C_{32}H_{37}N_3O_4$ = 559.67

| | | | |
|---|---|---|---|
| Calculated: | C 68.68 | H 6.66 | N 7.51 |
| Found: | C 68.29 | H 6.82 | N 7.67 |

**4-(6-Phthalimidohexyloxy)-4'-[4-(3,3-dimethyl-2,4-dioxolyl)butoxy]-*E*-azobenzene (20)**

A mixture of **19** (4.20 g, 7.5 mmol), 2,2-dimethoxypropane (10.0 g, 96 mmol), 4-toluenesulfonic acid monohydrate (0.20 g, 1 mmol) and dichloromethane (50 ml) was stirred at room temperature for 18 hours. The mixture was washed with 60 ml of saturated sodium bicarbonate solution and 60 ml of water successively, and dried over anhydrous sodium sulfate. After evaporation of the solvent on a rotary evaporator, the residue was recrystallized from 95% ethanol to give 4.25 g of orange plates, yield 95%, m.p. 104-106°. $^{1}$H NMR ($CDCl_3$): 7.86-7.65 (2 x m, 8H, phthalimide aromatic and azobenzene aromatic), 6.96-6.93 (2 x d, J = 9.0 Hz, 9.0 Hz, 4H, azobenzene aromatic), 4.13-4.03, 3.53-3.49 (2 x m, 3H, $CH_2O$, CHO), 4.05-3.97 (2 x t, J = 6.3 Hz, 8.0 Hz, 4H, $ArOCH_2$), 3.68 (t, J = 7.2 Hz, 2H, $NCH_2$), 1.87-1.36 (m, 14H, $CH_2$), 1.40, 1.34 (2 x s, 6H, $CH_3$). $^{13}$C NMR ($CDCl_3$): 168.4 (CO), 161.1, 161.0, 146.8, 146.7, 124.3 (4C), 114.6 (2C) (azobenzene aromatic), 133.8, 132.1, 123.1 (phthalimide aromatic), 108.7 (OCO), 75.9 ($OCH_2$), 69.4 (OCH), 67.9, 67.8 ($ArOCH_2$), 37.8 ($NCH_2$), 29.2, 29.0, 28.5, 26.5, 25.7, 22.4 ($CH_2$), 26.9, 25.6 ($CH_3$). MS (CI): M+1 600, M+29 628.

Elemental analysis: $C_{35}H_{41}N_3O_6$ = 599.73

| | | | |
|---|---|---|---|
| Calculated: | C 70.10 | H 6.89 | N 7.01 |
| Found: | C 69.98 | H 6.88 | N 6.92 |

**4-(6-Aminohexyloxy)-4'-[4-(3,3-dimethyl-2,4-dioxolyl)butoxy]-*E*-azobenzene (21)**

A mixture of **20** (5.0 g, 8.3 mmol), 100% hydrazine hydrate (8.4 g, 168 mmol) and absolute ethanol (160 ml) was heated at reflux temperature for 18 hours. Dichloromethane (350 ml) and acetic acid (350 ml) were added to the reaction mixture and the mixture was washed successively with 300 ml of water and then two 200-ml portions of 10% sodium hydroxide. The organic extract was shaken with anhydrous potassium carbonate for ten minutes. After evaporation of solvent on a rotary evaporator, a small amount of petroleum ether (35-60) was added in order to solidify the residue. Recrystallization from 95% ethanol gave 2.3 of a loose powder, yield 59%. $^{1}H$ NMR ($CDCl_3$): 7.83, 6.95, 6.94 (3 x d, J = 9.0 Hz, 8.9 Hz, 9.0 Hz, 8H, aromatic), 4.11-4.01, 3.50-3.43 (2 x m, 3H, $CH_2O$, CHO), 4.05-3.98 (2 x t, J = 6.1 Hz, 8.0 Hz, 4H, $ArOCH_2$), 2.69 (t, 2H, $NCH_2$), 1.85-1.36 (m, 16H, $NH_2$ and $CH_2$), 1.40, 1.34 (2 x d, 6H, $CH_3$). $^{13}C$ NMR ($CDCl_3$): 161.1, 160.9, 146.9, 246.8, 124.2, 124.6 (aromatic), 108.7 (OCO), 75.9, 69.4 ($OCH_2$), 68.1, 67.9 ($ArOCH_2$), 50.5 ($NCH_2$), 33.4, 33.2, 29.1, 26.5, 25.9, 22.3 ($CH_2$), 26.9, 25.7 ($CH_3$). MS (CI): M+1 470, M+29 498.

Elemental analysis: $C_{27}H_{39}N_3O_4$ = 469.63

| | | | |
|---|---|---|---|
| Calculated: | C 69.05 | H 8.37 | N 8.95 |
| Found: | C 67.92 | H 8.28 | N 8.57 |

**_N,N',N",N"'_-Tetrakis[4-(3,3-dimethyl-2,4-dioxolylbutoxy-_E-p_-phenylazo-_p_-phenoxy)]hexyl-1,4,7,10,13,16-hexoxacyclooctadecane-_R,R,R,R_-2,3,11,12-tetracarboxamide (22)**

A mixture of 1,4,7,10,13,16-hexoxacyclooctadecane-*R,R,R,R*-2,3,11,12-tetracarboxyl chloride (0.26 g, 0.50 mmol), **20** (1.0 g, 2.1 mmol), triethylamine (1 ml) and dichloromethane (25 ml) was stirred at room temperature for 48 hours. The solvent was evaporated on a rotary evaporator, and the residue was chromatographed on an alumina column with dichloromethane-methanol (95:5). The first yellow band gave 0.2 g of a yellow solid on evaporation of solvent. The crude product was collected and solvent was evaporated to give 0.18 g of **21** as a yellow powder, yield 16%. $^{1}$H NMR ($CDCl_3$): 7.84, 7.83 (2 x d, J = 9.0 Hz, 8.9 Hz, 16H, aromatic), 6.94, 6.91 (2 x d, J = 9.0 Hz, 8.9 Hz, 16H, aromatic), 4.13-3.95, 3.67-3.06 (2 x m, 52H, $OCH_2$, OCH, $NCH_2$), 1.96 (br, 4H, CONH), 1.87-1.34 (m, 56H, $CH_2$), 1.44, 1.36 (2 x s, 24H, $CH_3$). $^{13}$C NMR ($CDCl_3$): 170.0 (CO), 161.0, 146.8, 124.3, 114.6 (aromatic), 108.7 (OCO), 81.6 (OCHC=O), 77.2, 756.9, 71.3, 69.9, 68.4, 67.9 ($OCH_2$, OCH), 53.4 ($NCH_2$), 39.3, 33.2, 29.7, 29.4, 29.1, 26.8, 22.4 ($CH_2$). MS (Electrospray, KI, chloroform:methanol, 1:1): 2284.9 (100, $M{\cdot}K^+$), 1142.8 (45, $M{\cdot}K^+{\cdot}H^+$).

Elemental analysis: $C_{124}H_{172}N_{12}O_{26}{\cdot}NaCl$ = 2246.82 + 58.44 = 2305.26

| | | | |
|---|---|---|---|
| Calculated: | C 64.60 | H 7.52 | N 7.29 |
| Found: | C 63.63 | H 7.56 | N 6.97 |

**_N,N',N'',N'''_-Tetrakis[6-(5,6-dihydroxyhexyloxy-_E_-_p_-phenylazo-_p_-phenoxy)]hexyl-1,4,7,10,13,16-hexoxacyclooctadecane-_R,R,R,R_-2,3,11,12-tetracarboxamide (1)**

A mixture of **22** (100 mg), concentrated hydrochloric acid (1 ml), water (1 ml), methanol (2 ml), and THF (16 ml) was kept at room temperature for 3 days. The solvent was evaporated as completely as possible and the 10 ml of benzene and 10 ml of absolute ethanol were added and the solvent was evaporated again. The residue was dissolved in a minimum amount of mixed solvent of chloroform-methanol (4:3) and chromatographed through a Sephadex LH 20 gel permeation column. The orange band was collected and the solvent was evaporated on a rotary evaporator. Compound **1** (80 mg) was isolated as an orange powder. $^{1}H$ NMR ($CDCl_3$-$CD_3OD$): 7.77, 7.76 (2 x d, J = 9.0 Hz, 8.9 Hz, 16H, aromatic), 6.93, 6.91 (2 x d, J = 9.0 Hz, 8.9 Hz, 16H, aromatic), 4.70 (s, 4H, OCHC=O), 4.01-3.93 (m, 16H, crown ether $OCH_2CH_2O$), 3.63-3.15 (m, 36H, $OCH_2$, OCH, $NCH_2$), 1.81, 1.37 (m, 56H, $CH_2$). $^{13}C$ NMR ($CDCl_3$-$CD_3OD$): 171.0 (CO), 161.6, 161.5, 147.3, 147.2, 124.7, 115.1 (aromatic), 81.9 (O<u>C</u>HC=O), 78.0, 72.1, 68.5, 68.4, 66.8 ($CH_2O$ and $CH_2OH$), 72.3 (CHOH), 39.8 ($NCH_2$), 33.2, 30.0, 29.6, 29.5, 27.2, 26.3, 22.5 ($CH_2$). MS (Electrospray, KI, chloroform:methanol:acetic acid, 49.5:49.5:1): 2125.0 (100, $M{\cdot}K^+$), 1081.8 (65, $M{\cdot}2K^+$).

Elemental analysis: $C_{112}H_{156}N_{12}O_{26}{\cdot}NaCl$ = 2086.56 + 58.44 = 2144.00

| | | | |
|---|---|---|---|
| Calculated: | C 62.72 | H 7.33 | N 7.84 |
| Found: | C 62.66 | H 7.42 | N 7.51 |

## 2. Ion transport

### Instruments and reagents

The titration system was a Metrohm 655 Dosimat buret and titration cell, 614 Impulsomat automatic titrator, and 632 pH-meter. The buret was linked to an HP-85 microcomputer for data acquisition. Vesicle preparation required use of a Heat Systems W385 Ultrasonic sonicator, located in the University of Victoria's Biochemistry and Microbiology Departments. Cole-Parmer Model 8845-2 ultrasonic cleaner was used for the sonication bath. UV-visible spectra were taken on a Cary-5 UV-VIS spectrometer or a Perkin-Elmer Model Lambda 4B UV-VIS Spectrophotometer. The UV light source for irradiation was Oriel Model 66002 arc lamp, filtered with a monochromator.

Egg phosphatidylcholine and egg phosphatidic acid (egg PC and PA) were purchased from Avanti Polar Lipids, Inc., Pelham, Alabama. Cholesterol was purchased from Sigma/Aldrich. Anhydrous diethyl ether and HPLC grade chloroform were purchased from BDH; methanol, choline hydroxide (20% in water), D-mannitol, and Bis-Tris (2,2-bis(hydroxymethyl)-2,2',2"-nitrilotriethanol) from Sigma/Aldrich; sulfuric acid (ultrapure) from Fluka; and PD-10 Sephadex G-25M columns from Pharmacia. Only $D^3$ (deionized, double distilled) water was used.

Unilamellar vesicle solutions were prepared by Kaye's method[16].

**Stock solutions**

Choline sulfate, internal buffer solution and external solution, choline hydroxide titrant were all prepared by Kaye's method[16].

**Photoisomerization of compound 1 in organic solvent**

Compound **1** was dissolved in chloroform-methanol (1:1) (concentration). A UV-visible spectrum (250-550 nm) was performed before the solution was irradiated. Then the solution was irradiated with 360-nm UV for 5 minutes, and a UV-visible spectrum (250-550 nm) was performed right after the irradiation. The solution was irradiated once more with 320-nm UV for 5 minutes, and one more UV-visible spectrum (250-550 nm) was performed right after the irradiation. The data of absorbance at 360 nm for each spectrum was collected for evaluation of the photoisomerization. The three spectra were plotted in one co-ordinate for comparison of before and after irradiation.

**Thermal isomerization of azobenzene configuration from *cis-* to *trans-***

The solution of compound **1** was prepared as described above. The solution was irradiated and the UV-visible spectrum was performed immediately after the irradiation. Then UV-visible spectrum of the irradiated solution was performed every 5 minutes after the irradiation. The data of absorbance at 360 nm for each spectrum were collected for the measurement of the lifetime of *cis*-azobenzene at room temperature.

**Preparation of transporters set-in vesicle (TSV) solution**

Large unilamellar vesicle (LUV) solution was prepared by the method reported by Kaye[16]. Compound **1** was dissolved in methanol-chloroform (1:1) mixed solvent to a concentration of 2.42 mg/ml. The transporter solution (0.4 ml) was transferred into a 50 ml flask and evaporation of the solvent to form a thin layer of yellow solid. LUV solution (2 ml) was added into the flask with 2.5 g of glass beads, and the flask was rotated on a rotary evaporator without pumping until all solid dissolved (c.a. 20 minutes). Then the flask was put in a sonication bath for 10 min minutes, and the TSV solution is ready.

When the TSV solution was chromatographed through a Sephadex G-25 M PD-10 gel permeation column, only one pale yellow band was eluted. This verified that compound **1** was incorporated with LUV's.

**Photoisomerization of compound 1 in TSV solution**

TSV solution (0.2 ml) was diluted with external solution (4 ml) in a quartz cell. This solution was irradiated with 360-nm UV under argon bubbling for 15 minutes. The irradiated solution was transferred into a test tube immediately after the irradiation and shaken with 0.5 ml of chloroform on a vortex for 1 minute. The organic layer was transferred into a 10-ml flask with a pipette and shaken with a small amount of anhydrous sodium sulfate until the solution became clear. The clear solution was transferred into a UV cell and diluted with chloroform to 1 ml. UV-visible spectrum of the organic

solution was performed and the absorbance at 360 nm was recorded.

A series of TSV solution was diluted and irradiated as described above, and extraction with chloroform was performed 15 minutes, 30 minutes, 60 minutes, and overnight respectively, after the irradiation. The UV-visible spectra were performed immediately after the extraction, and the absorbance data at 360 nm were recorded for estimation of lifetime of *cis*-azobenzene in TSV solution.

**Ion transport activity and selectivity**

TSV solution (0.2 ml) was diluted with external solution (4 ml) and pH of the solution was adjusted to 7.6 with choline hydroxide from an automated titrometer. The automated titrometer was zeroed, and the pH stat titration experiment began. $M_2SO_4$ (0.5 M, 200 µl) and FCCP ($7.9 \times 10^{-4}$ M, 5 µl) were added. Triton X-100, a surfactant, was added at the end of the titration, and the lyse volume showed the amount of internal solution entrapped in vesicles. The experimental data were transferred to a microcomputer for processing.

**Photogate effect**

TSV solution (0.2 ml) was diluted with external solution (4 ml) and was irradiated with 360-nm UV under argon bubbling for 15 minutes. A pH-stat titration of the irradiated solution was performed as described above immediately after the irradiation. A pH-stat titration of a non-irradiated TSV

solution was performed. The two titration curves were plotted in one co-ordinate for comparison to observe the photogate effect.

## References


1. (a) Catterall, William A. *Ann. N.Y. Acad. Sci.* **1993**, *707*, 1.

   (b) Brown, A.M.; Drewe, J.A.; Hartman, H.A.; Taglialatela, M.; De Biasi, M.; Soman, K. and Kirsch, G.E. *Ann. N.Y. Acad. Sci.* **1993**, *707*, 74.

2. (a) Houslay, M.D.; Stanley, K.A. *Dynamics of Biological Membranes.* John Wiley & Sons, Inc., New York, **1983**, 281.

   (b) Hladky, S.B.; Haydon, D.A. *Current Topics in Membranes and Transport, Vol. 21.* Academic Press, **1984**, 327.

3. Fyles, T.M. *Frontiers in Bioorganic Chemistry*, **1990**, *1*, 71.

4. Tsukube, H. *Liquid Membranes: Chemical Applications*, T. Araki and H. Tsukube eds., CRC Press Inc., Boca Raton, Florida, **1990**, 51.

5. Kunitake, T. *Ann. N.Y. Acad. Sci.*, **1986**, *471*, 70.

6. (a) Menger, F.M. *Angew. Chem. Int'l. Ed'n. Engl.*, **1991**, *30*, 1086.

   (b) Menger, F.M.; Davis, D.S.; Persichetti, R.A.; Lee, J-J. *J. Am. Chem. Soc.*, **1990**, *112*, 2451.

7. (a) Fuhrop, J-H.; David, H-H.; Mathieu, J.; Liman, U.; Winter, H-J.; Boeckema, E. *J. Am. Chem. Soc.*, **1986**, *108*, 1795.

   (b) Fuhrop, J-H.; Mathieu, J. *Angew. Chem., Int. Ed. Engl.*, **1984**, *23*, 100.

   (c) Fuhrop, J-H.; Liman, U. *J. Am. Chem. Soc.*, **1984**, *106*, 4643.

   (d) Fuhrop, J-H.; Fritsch, D. *Acc. Chem. Res.*, **1986**, *19*, 130.

8. Zojaji, M. *Doctoral Thesis*, University of Victoria, B.C., Canada, **1991**.

9. (a) Spach, G.; Merle, Y.; Molle, G. *J. Chim. Phys. -Chim. Biol.*, **1985**, *82*, 719.

(b) de Santis, P.; Palleschi, A.; Sauino, M.; Scipioni, A.; Sesta, B.; Verdini, A. *Biophys. Chem.*, **1985**, *21*, 211.

10. Tabushi, I.; Kuroda, Y.; Yokota, K. *Tetrahedron Lett.*, **1982**, *23*, 4601.

11. (a) Neevel, J.G.; Nolte, R.J.M. *Tetrahedron Lett.*, **1984**, *25*, 2263.

(b) Kragten, U.F.; Roks, M.F.M; Nolte, R.J.M. *J. Chem. Soc., Chem. Commun.*, **1985**, 1287.

12. Nakano, A.; Xie, Q.; Mallen, J.V.; Echegoyen, L.; Gokel, G.W. *J. Am. Chem. Soc.*, **1990**, *112*, 1287.

13. (a) Jullien, L.; Lehn, J-M. *Tetrahedron Lett.*, **1988**, *29*, 3803.

(b) Jullien, L.; Lehn, J-M. *J. Incl. Phen. Mol. Recogn. Chem.*, **1992**, *12*, 55.

(c) Pregel, M.J.; Jullien, L.; Lehn, J-M. *Angew. Chem. Int'l. Ed'n. Engl.*, **1992**, *31*, 1637.

(d) Canceill, J.; Jullien, L.; Lacombe, L.; Lehn, J-M. *Helv. Chem. Acta*, **1992**, *75*, 791.

(e) Jullien, L.; Lazrak, T.; Canceill, J.; Lacombe, L., Lehn, J-M. *J. Chem. Soc., Perkin Trans.* **1993**, *2*, 3110.

14. (a) James, T. *Doctoral Thesis*, University of Victoria, B.C., Canada, **1991**.

(b) Carmichael, V.E.; Dutton, P.J.; Fyles, T.M.; James, T.D.; Swan, J.A.;

Zojaji, M. *J. Am. Chem. Soc.*, **1989**, *111*, 767.

15. Carmichael, V.E.; Dutton, P.J.; Fyles, T.M.; James, T.D.; McKim, C.; Swan, J.A.; Zojaji, M. *Inclusion Phenomena and Molecular Recognition*, J. Stwood (Ed.), Plenum Press, New York, **1990**, p.145.

16. Kaye, K.C. *Master's Thesis*, University of Victoria, B.C., Canada, **1991**.

17. Fyles, T.M.; James, T.D.; Kaye, K.C. *J. Am. Chem. Soc.*, **1993**, *115*, 12315.

18. Hille, B. *Ionic Channels of Excitable Membranes*, Sinauer Associates, Inc., Sunderland, Massachussetts, **1984**.

19. (a) Rau, H.; Lüddecke, E. *J. Am. Chem. Soc.*, **1982**, *104*, 1616.

(b) Bertelson, *Photochromism*, G.H. Brown ed., Wiley Interscience, New York, **1971**, 45.

20. For example,

(a) Shinkai, S.; Ishihara, M.; Ueda, K.; Manabe, O. *J. Chem. Soc., Perkin Trans. II*, **1985**, 511.

(b) Shinkai, S.; Ishihara, M.; Ueda, K.; Manabe, O. *J. Chem. Soc., Chem. Commun.*, **1984**, 727.

(c) Shinkai, S.; Ishihara, M.; Ueda, K.; Manabe, O. *J. Incl. Phen.*, **1984**, *2*, 111.

(d) Shinkai, S.; Nakaji, T.; Nishida, Y.; Ogawa, T.; Manabe, O. *J. Am. Chem. Soc.*, **1980**, *102*, 5860.

(e) Shinkai, S.; Minami, T.; Kusano, Y.; Manabe, O. *J. Am. Chem. Soc.*,

**1982**, *104*, 1967.

21. Cross, G.G. *Doctoral Thesis*, University of Victoria, B.C., Canada, **1994**.

22. Behr, J.-P.; Girodeau, J.-M.; Hayward, R.C.; Lehn, J.-M.; Suavage, J.-P. *Helv. Chim. Acta*, **1980**, *63 (7)*, 2096.

23. Anantanarayan, A.; Carmicheal, V.A.; Dutton, P.J.; Fyles, T.M. *Synth. Commun.*, **1986**, *16 (14)*, 1771.

24. (a) Zelinski, R.; Eichel, H.J. *J. Org. Chem.*, **1958**, *23*, 462.

(b) Landini, D.; Montanari, F.; Rolla, F. *Synthesis*, **1979**, *(2)*, 134.

25. Läuger, P., *J. Memb. Biol.*, **1980**, *57*, 163.

26. Harrison, I.T.; Harrison, S. *Compendium of Organic Synthetic Methods*, Wiley Interscience, New York, **1971**, **1**, pp. 329-356.

27. (a) Smith, R.D.; Loo, J.A.; Edmonds, C.G.; Barinaga, C.J.; Udseth, H.R. *Anal. Chem.*, **1990**, *62*, 882-899.

(b) Ashton, P.R.; Brown, C.L.; Chapman, J.R.; Gallagher, R.T.; Stoddart, J.F. *Tetrahedron Lett.*, **1992**, *33 (50)*, 7771-7774.

(c) Hopfgartner, G.; Piguet, C.; Henion, J.; William, A.F. *Helv. Chim. Acta*, **1993**, *76*, 1759-1766.

(d) Leize, E.; Van Dorsselaer, A.; Krämer, R.; Lehn, J-M. *J. Chem. Soc., Chem. Commun.*, **1993**, 990-993.

28. Wallace, R.B.; Seldin, R.L.; Spoerri, P.E.; Wyman, G.M. *J. Am. Chem. Soc.*, **1955**, *77*, 2762-2765.

29. Rickwood, D.; Hames, B.D. *Liposomes*, IRL Press, New York, **1990**, 33.

# Appendix 1

## $^{1}H$ and $^{13}C$ NMR spectra of compounds in the thesis

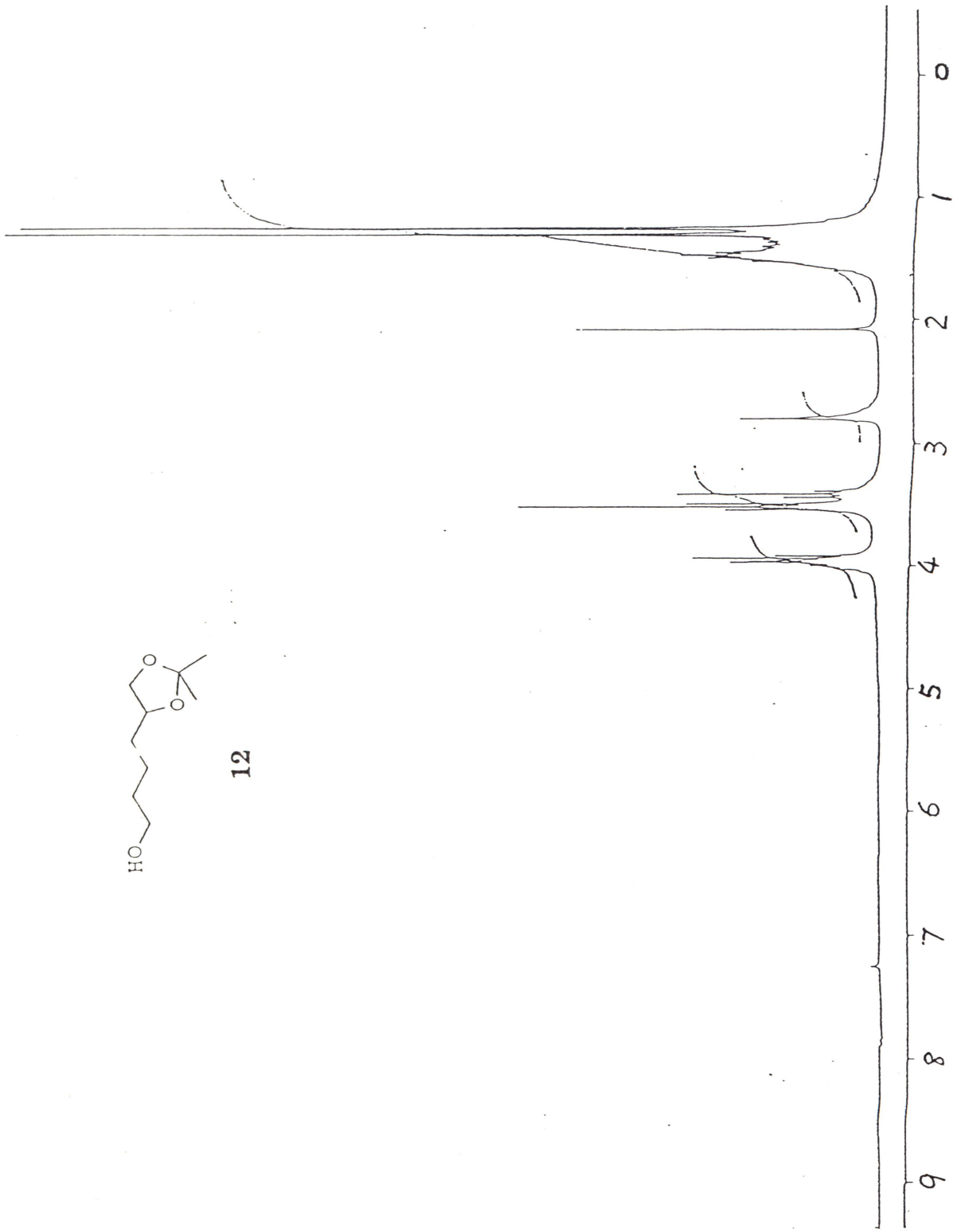


12

**Fig. A-1**. $^{1}H$ NMR spectrum of compound **12**

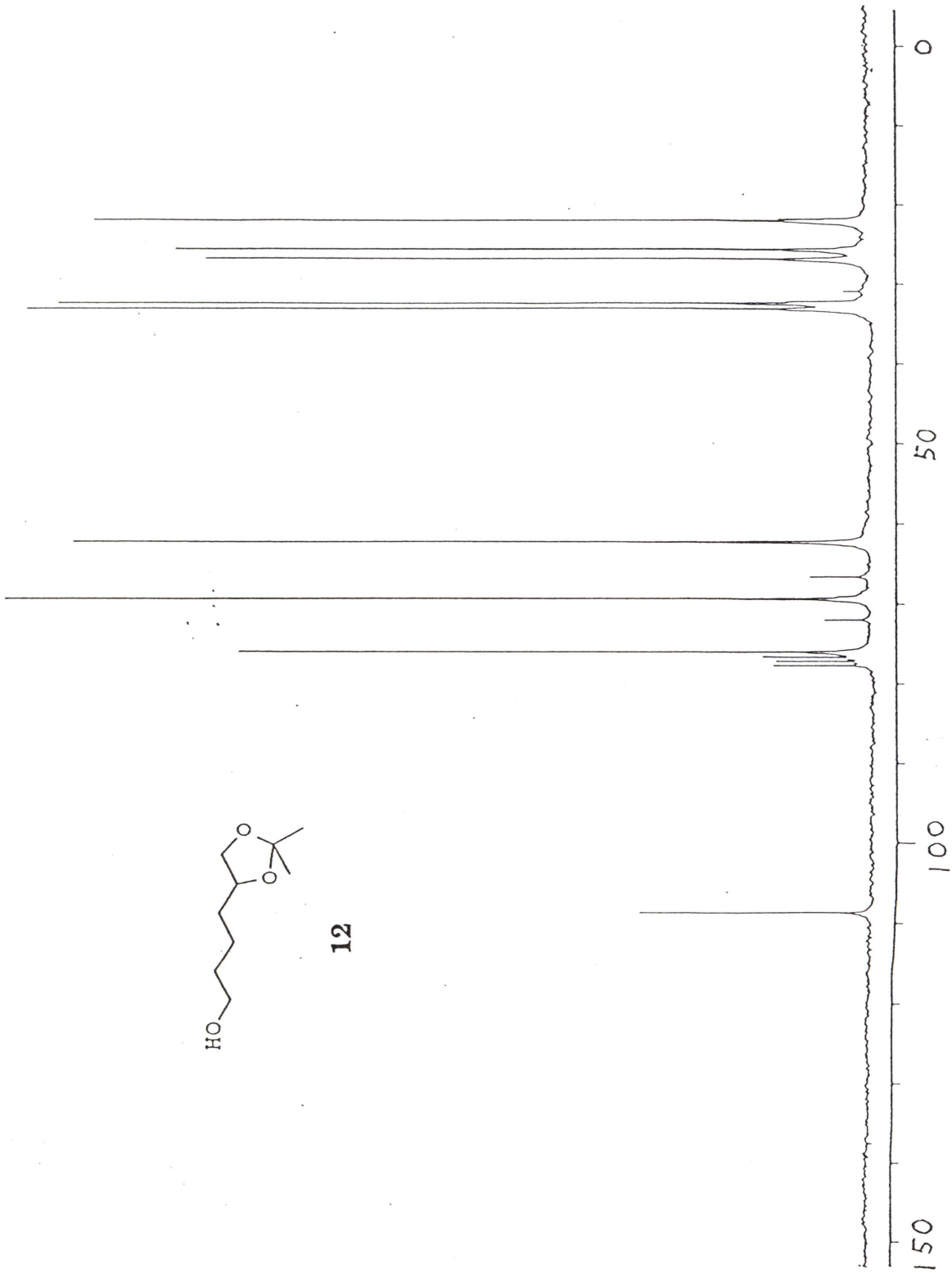


***Fig. A-2.*** *$^{13}C$ NMR spectrum of compound* ***12***

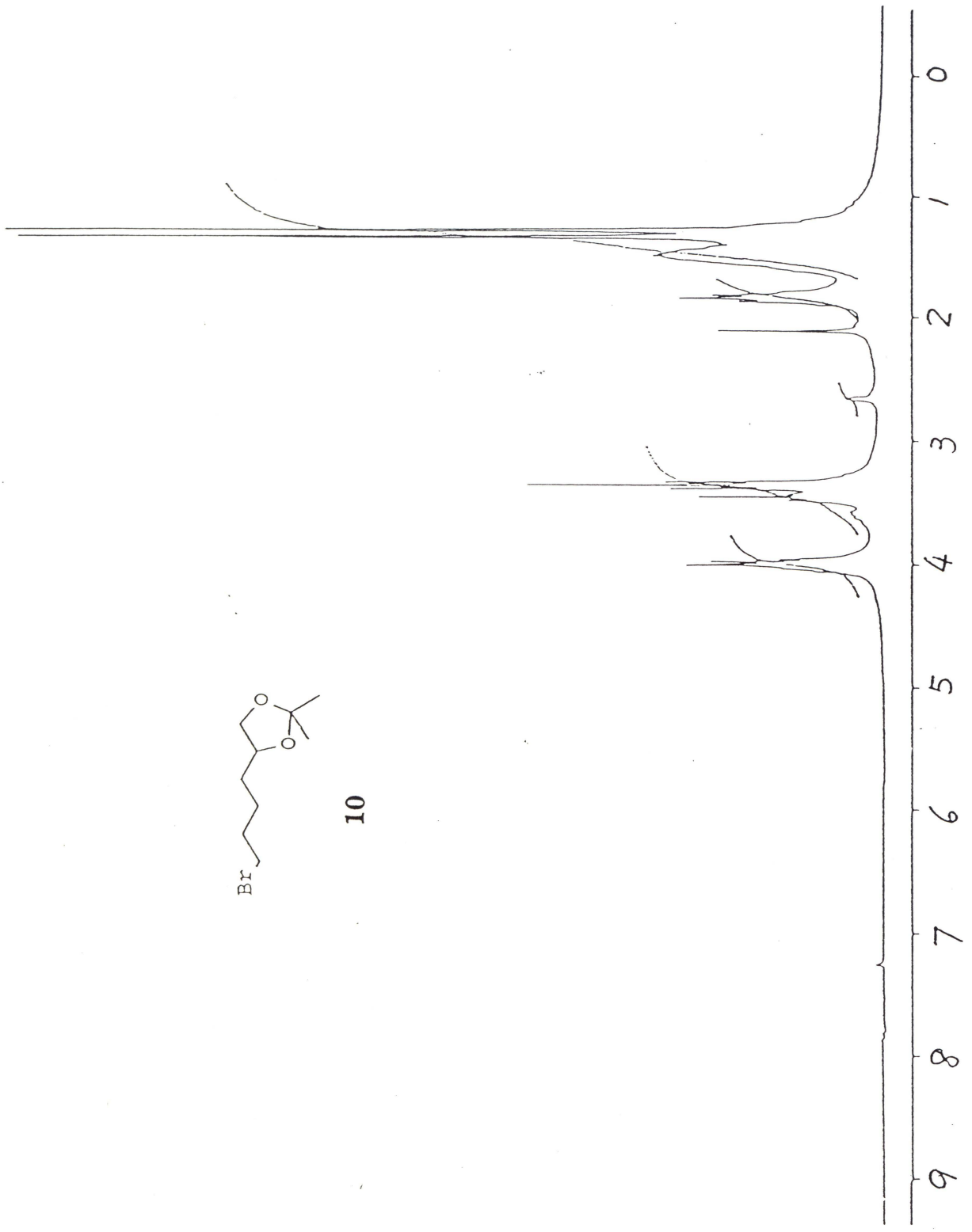


**Fig. A-3**. $^{1}H$ NMR spectrum of compound **10**

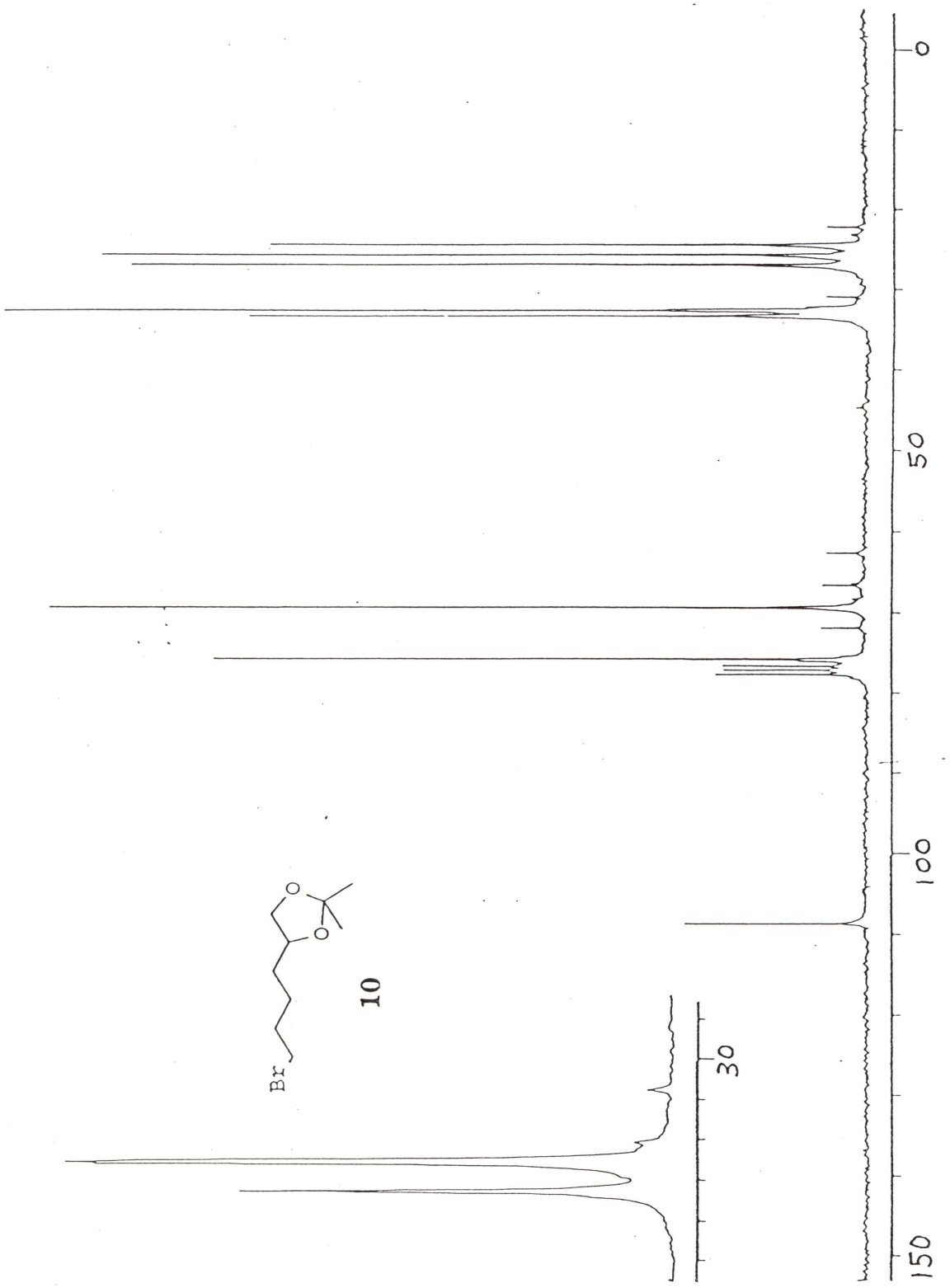


**Fig. A-4.** $^{13}C$ NMR spectrum of compound **10**

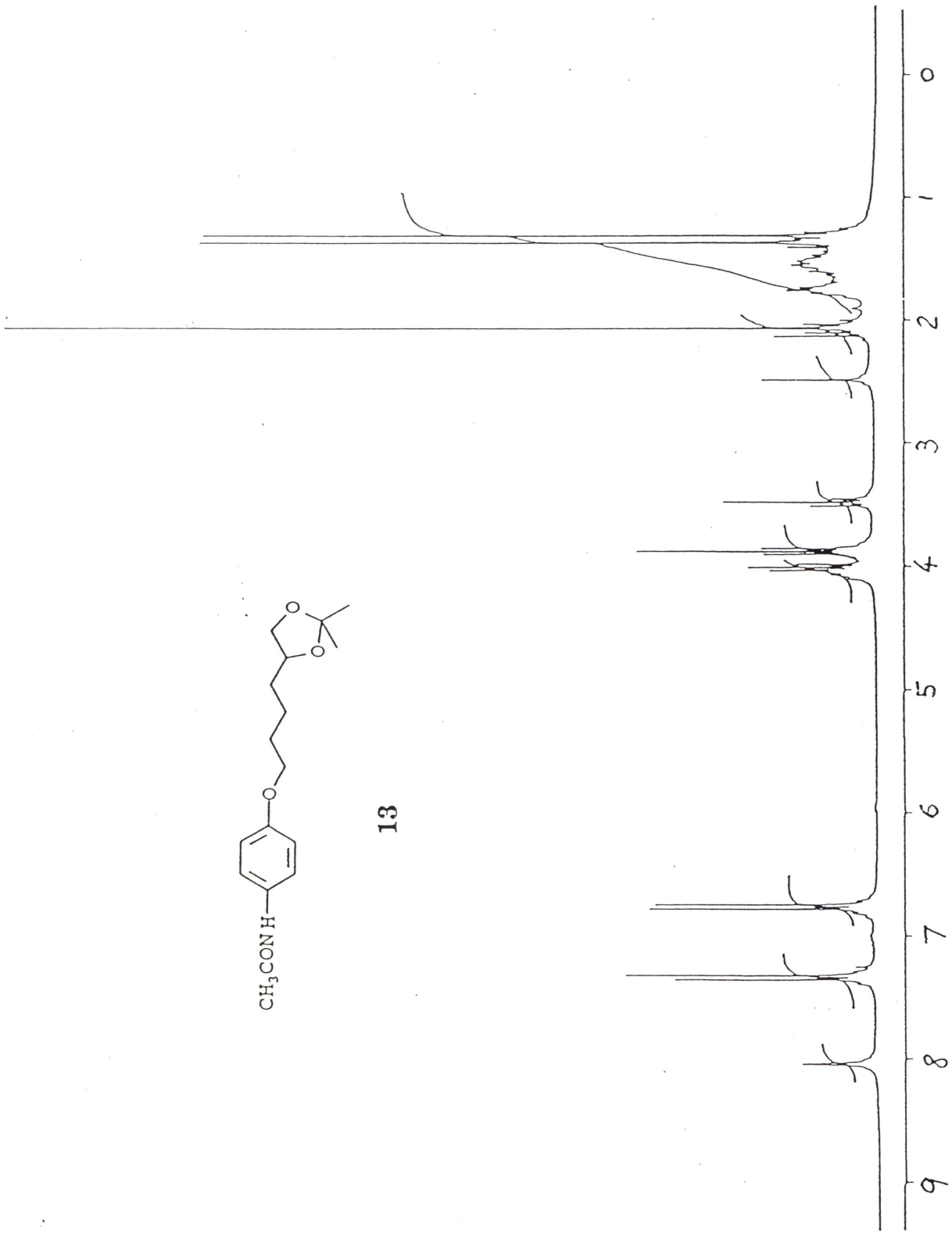


**Fig. A-5**. $^{1}H$ NMR spectrum of compound **13**

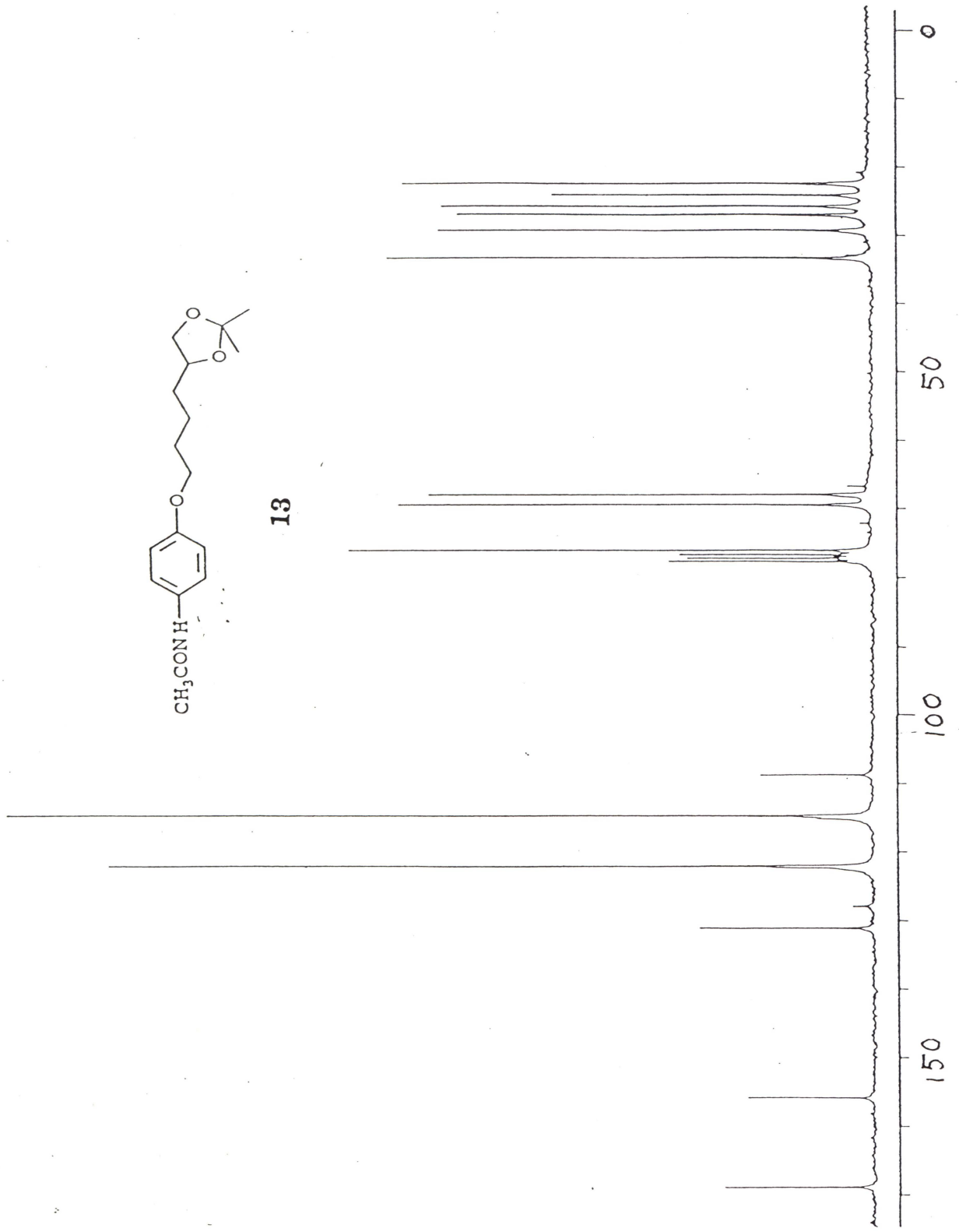


**Fig. A-6.** $^{13}C$ NMR of compound **13**

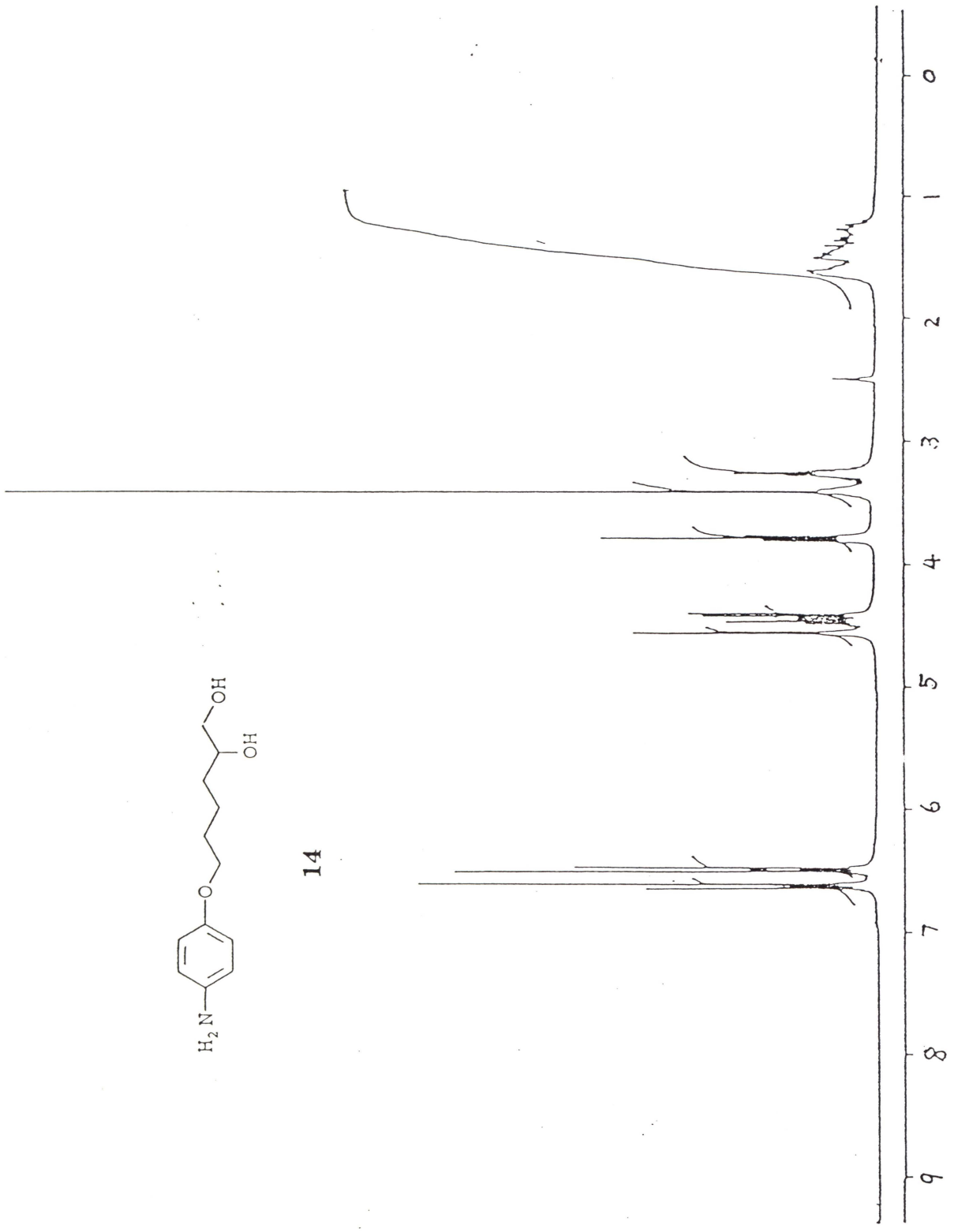


**Fig. A-7**. $^1$H NMR spectrum of compound **14**

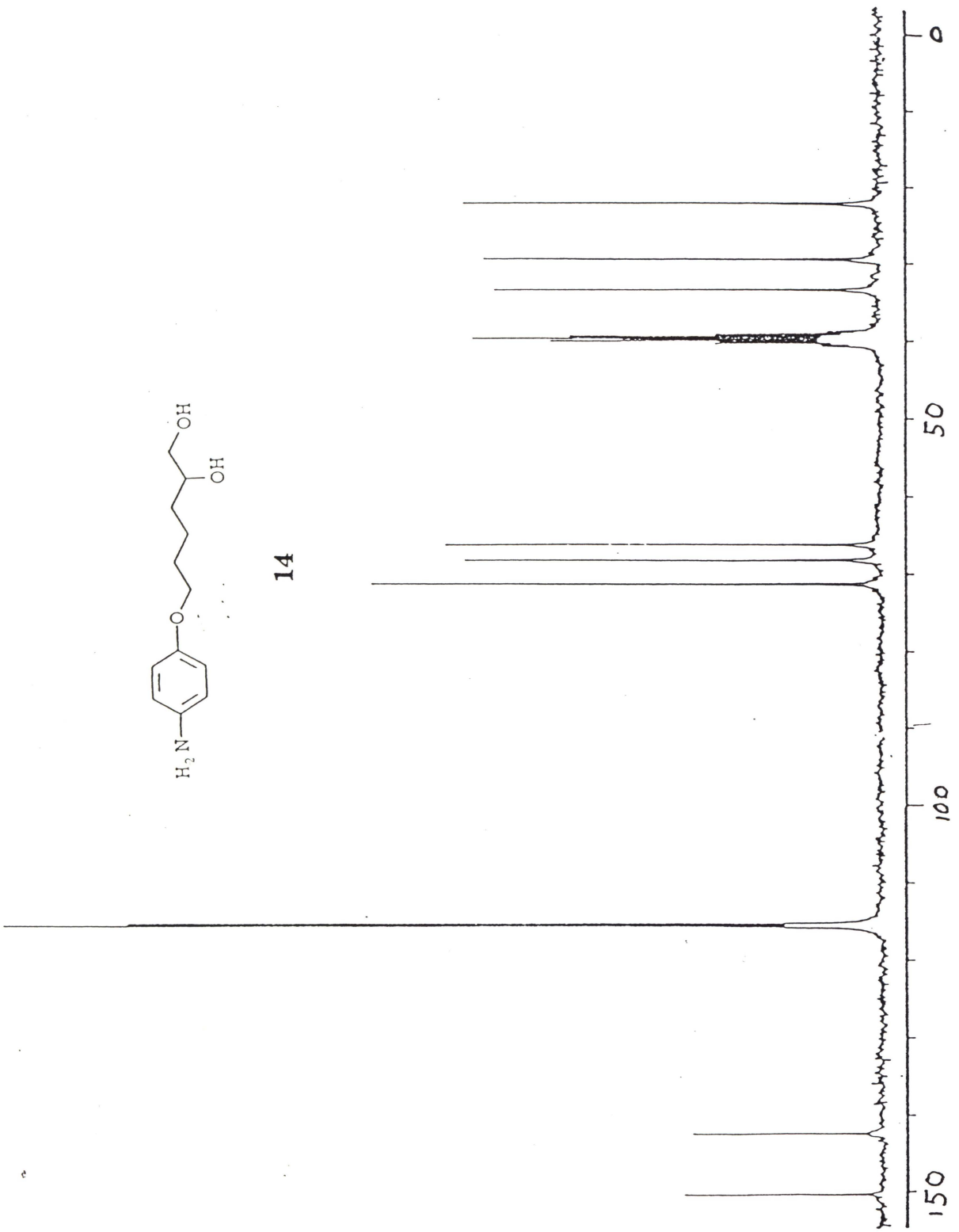


**Fig. A-8.** $^{13}C$ NMR spectrum of compound **14**

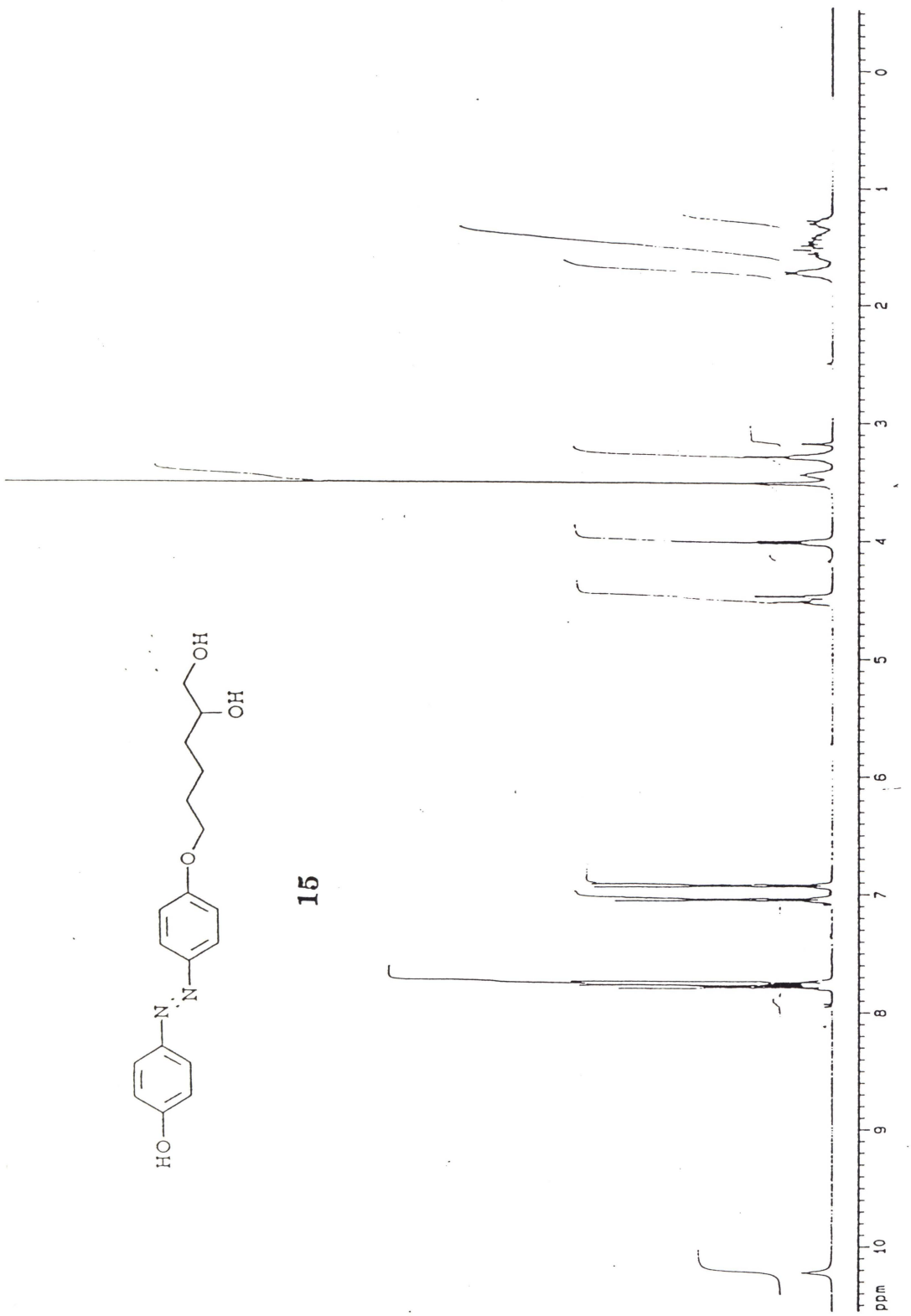


**Fig. A-9**. $^{1}H$ NMR spectrum of compound **15**

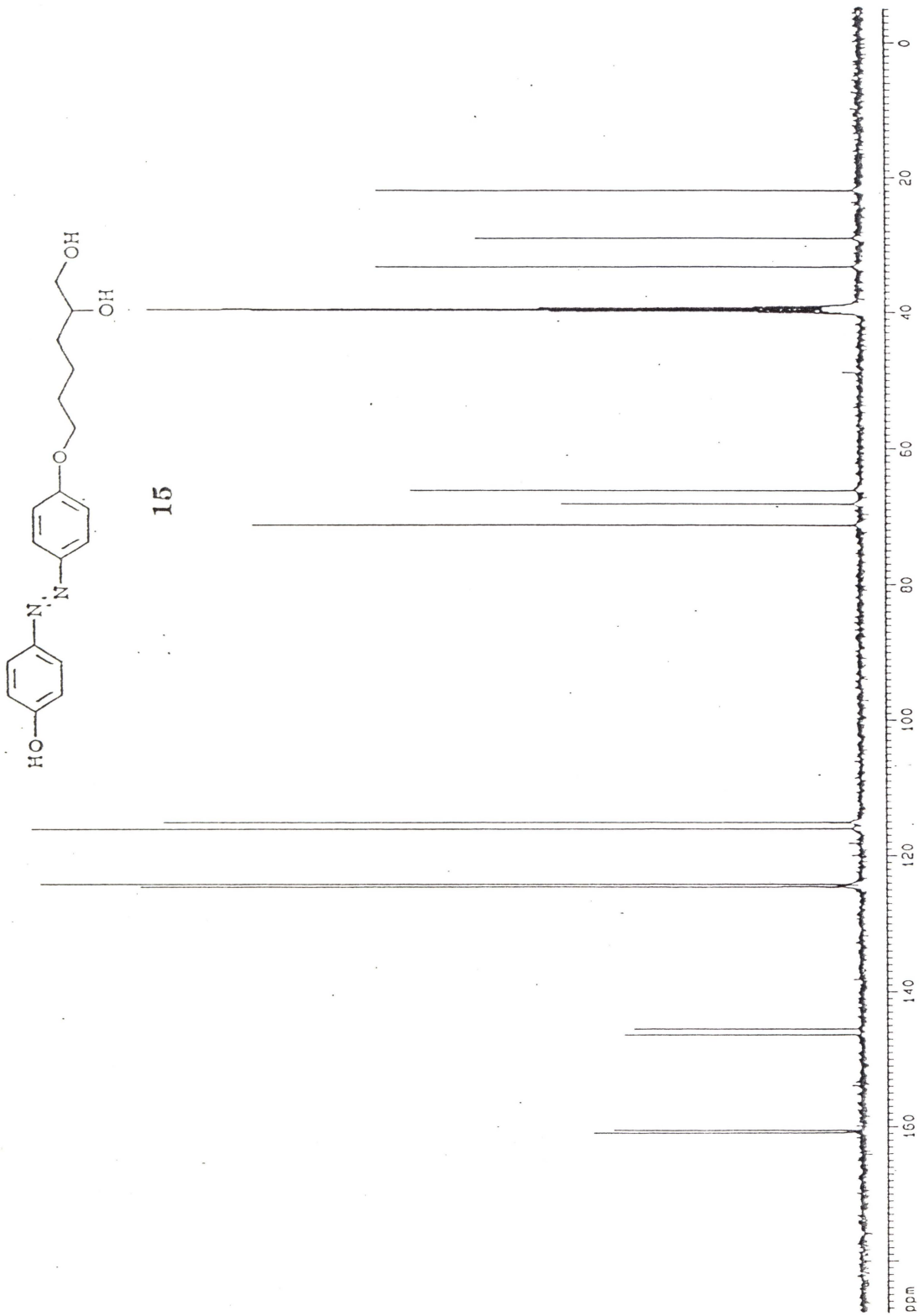


**Fig. A-10.** $^{13}C$ NMR spectrum of compound **15**

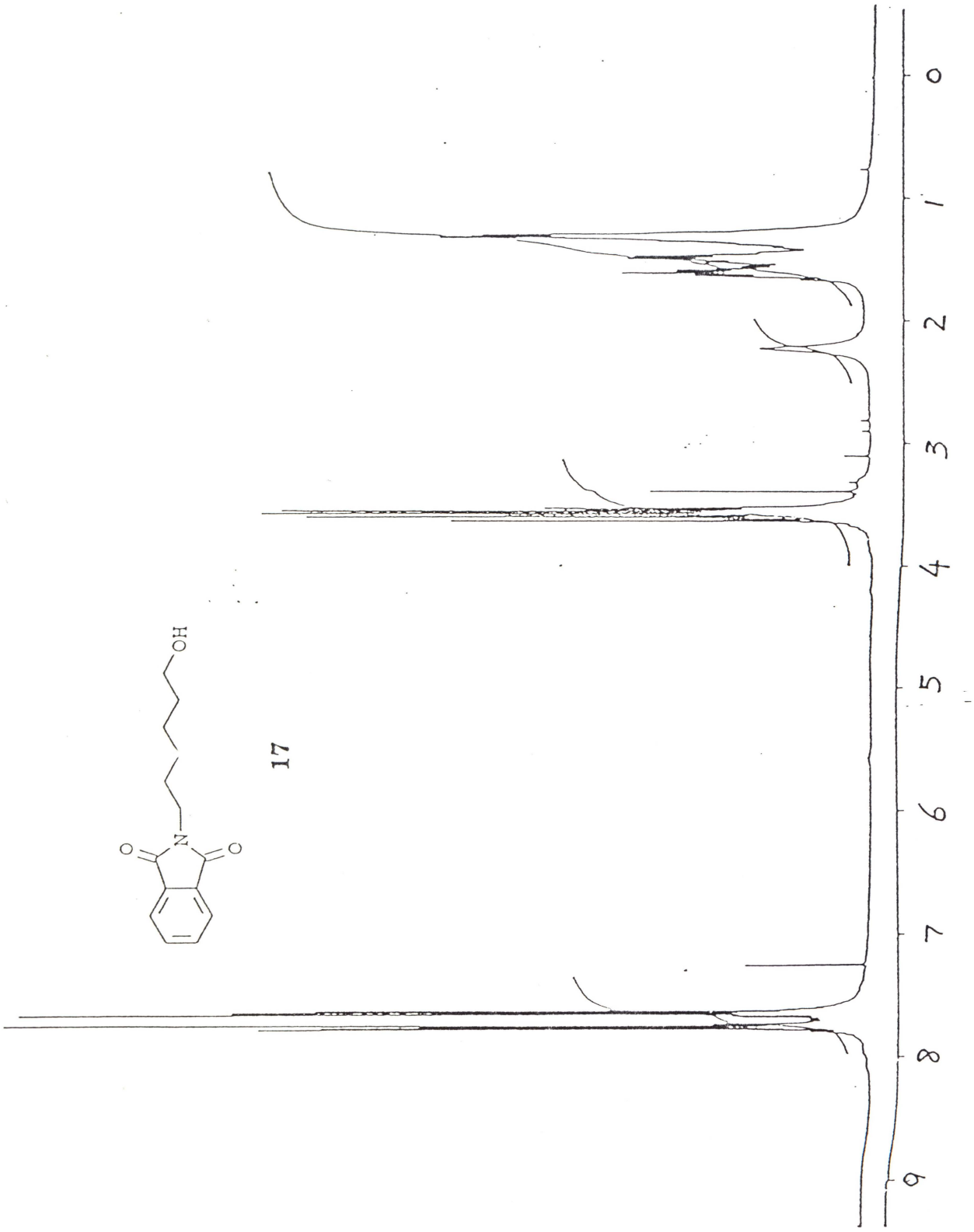


**Fig. A-11.** $^{1}H$ NMR spectrum of compound **17**

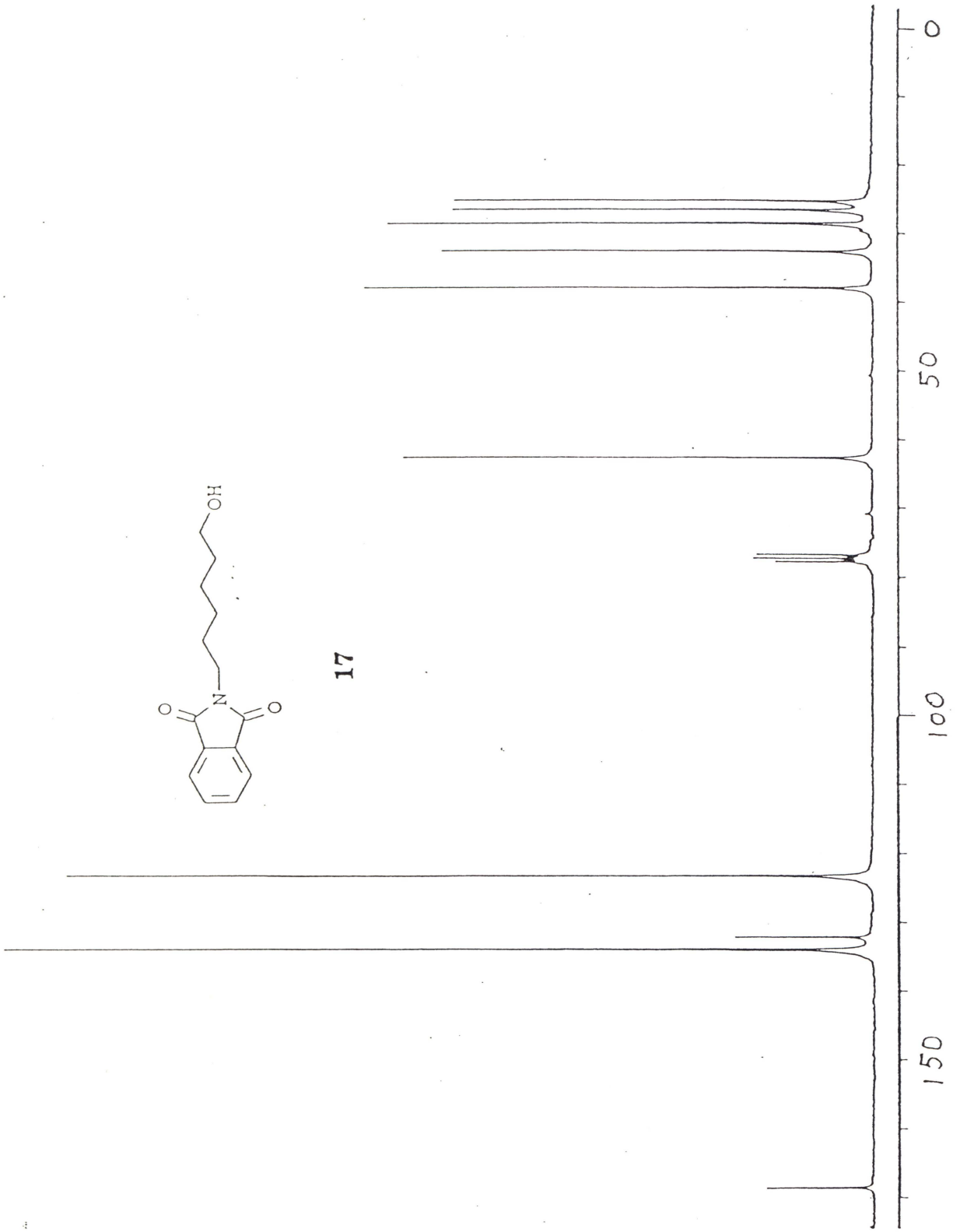


**Fig. A-12.** $^{13}C$ NMR spectrum of compound **17**

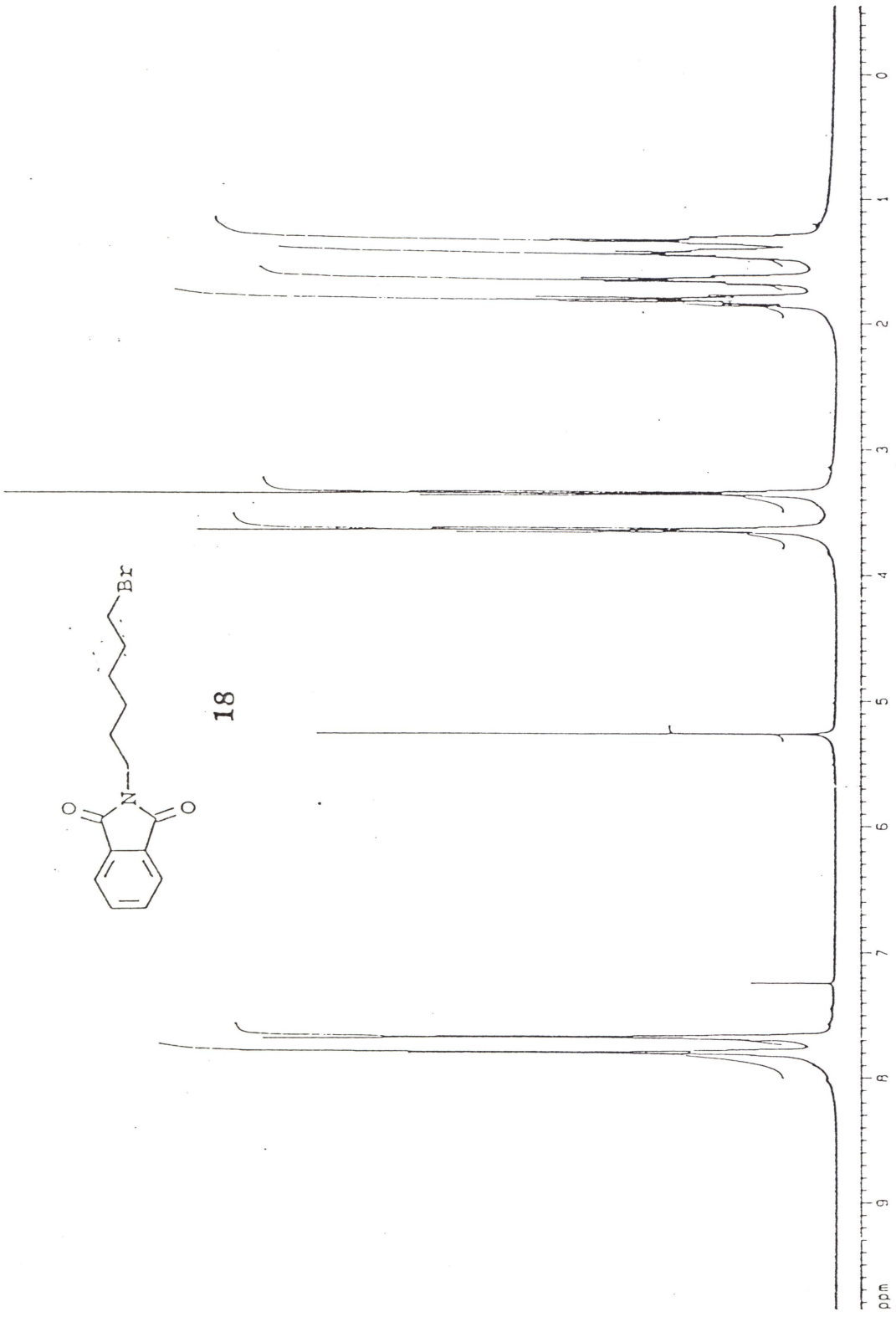


**Fig. A13**. $^{1}H$ NMR spectrum of compound **18**

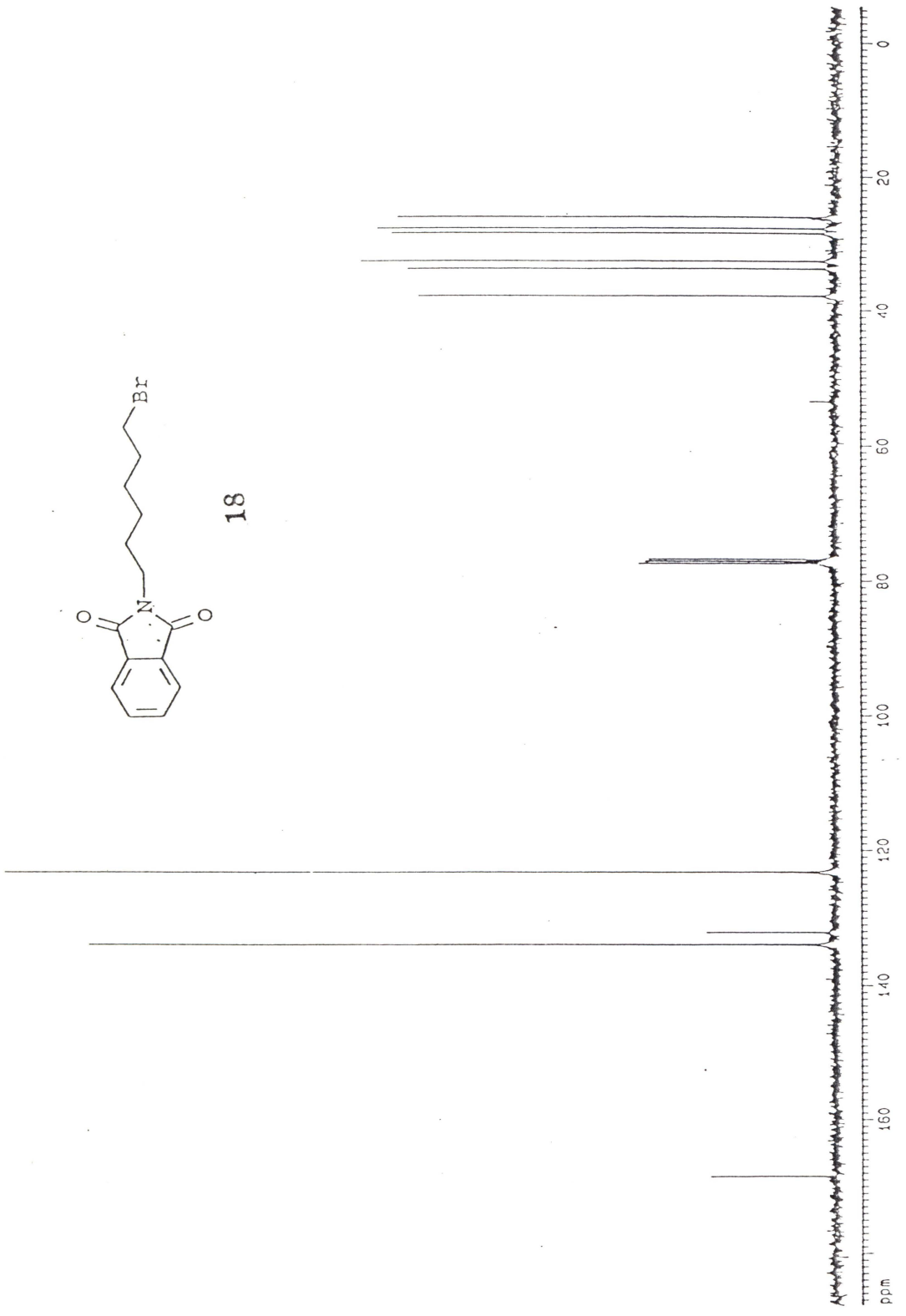


**Fig. A14.** $^{13}C$ NMR spectrum of compound **18**

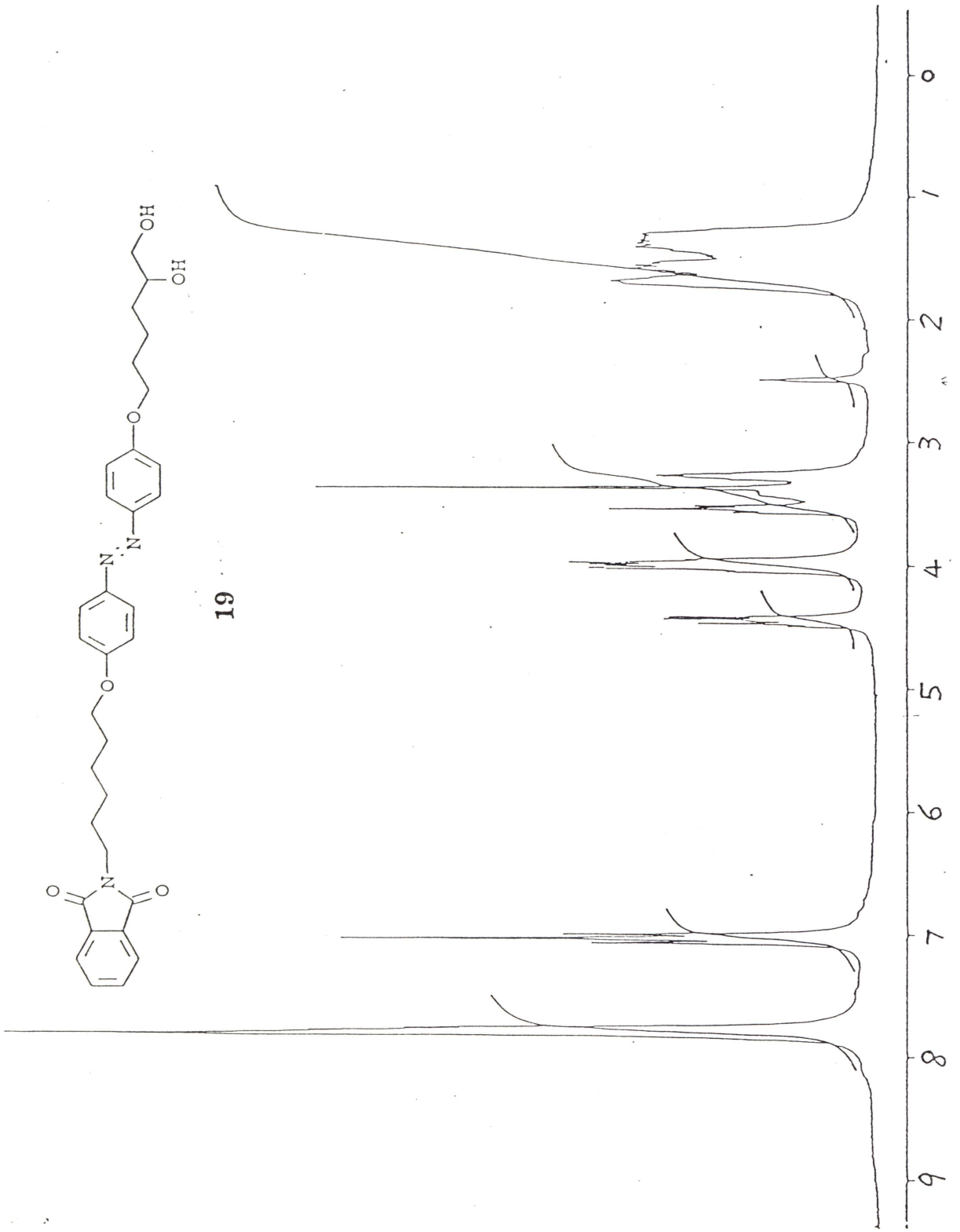


**Fig. A-15.** $^{1}H$ NMR spectrum of compound **19**

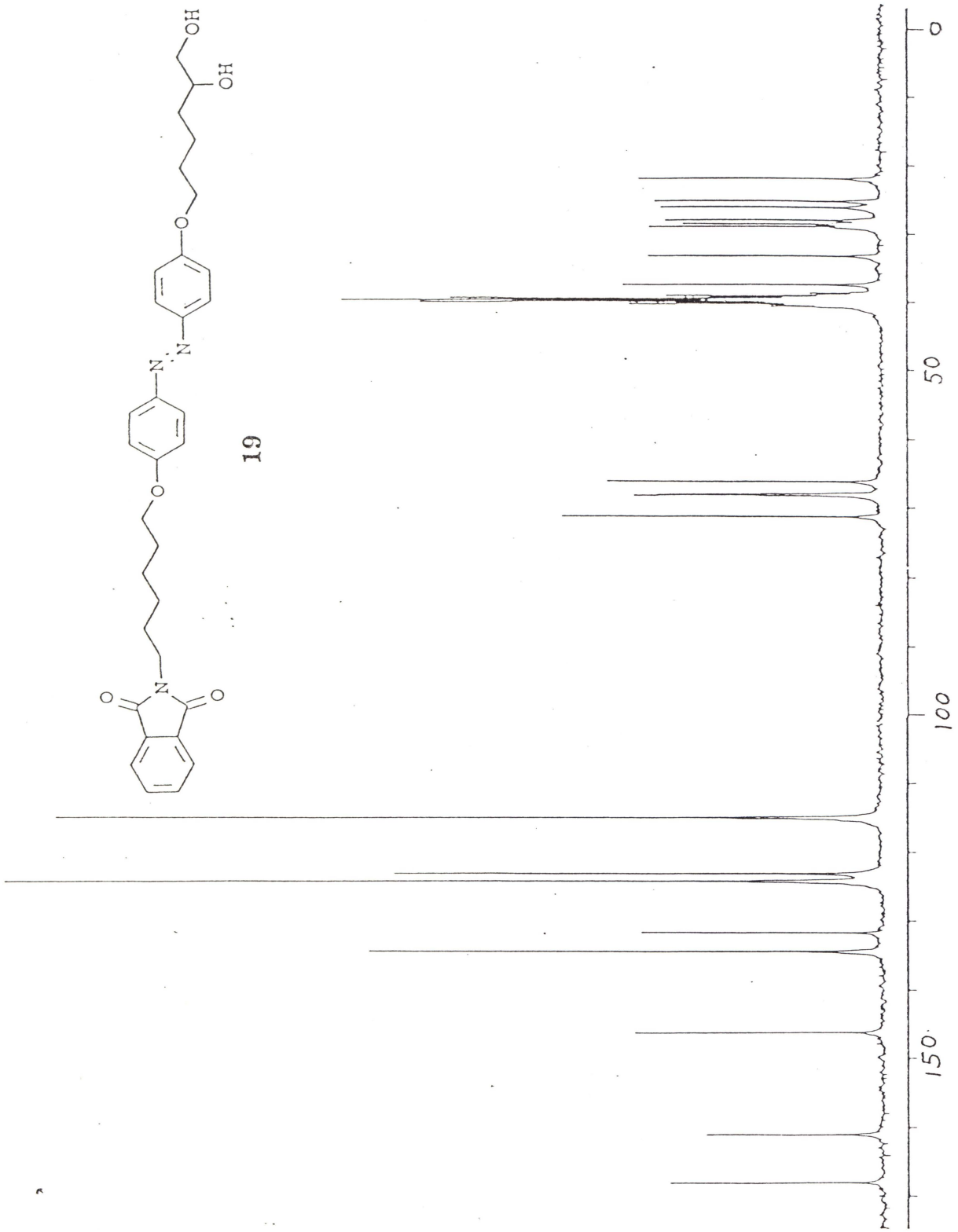


19

**Fig. A-16**. $^{13}C$ NMR spectrum of compound **19**

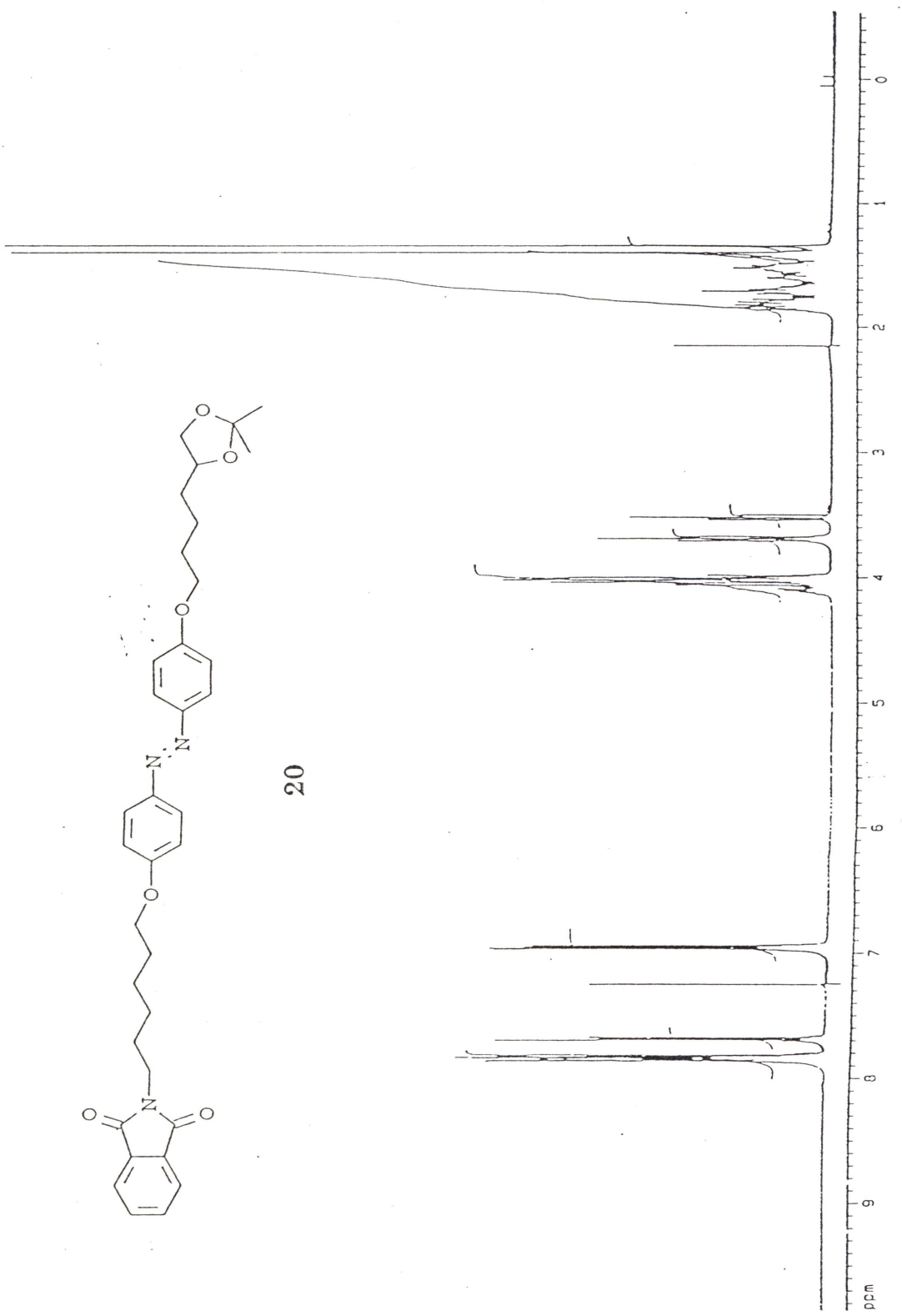


**Fig. A-17.** $^{1}H$ NMR spectrum of compound **20**

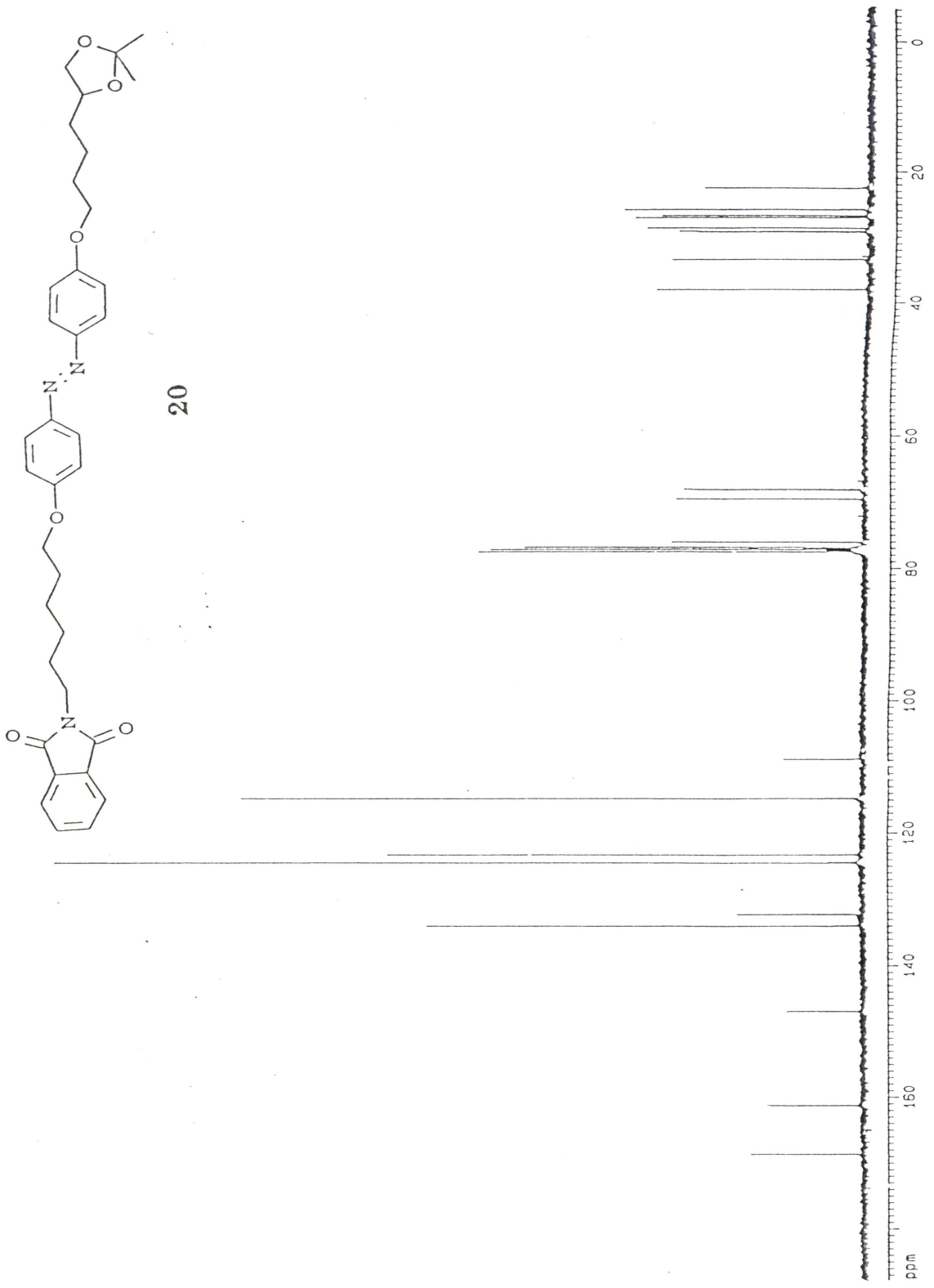


Fig. A-18. $^{13}C$ NMR spectrum of compound **20**


**Fig. A-19**. $^{1}H$ NMR spectrum of compound **21**

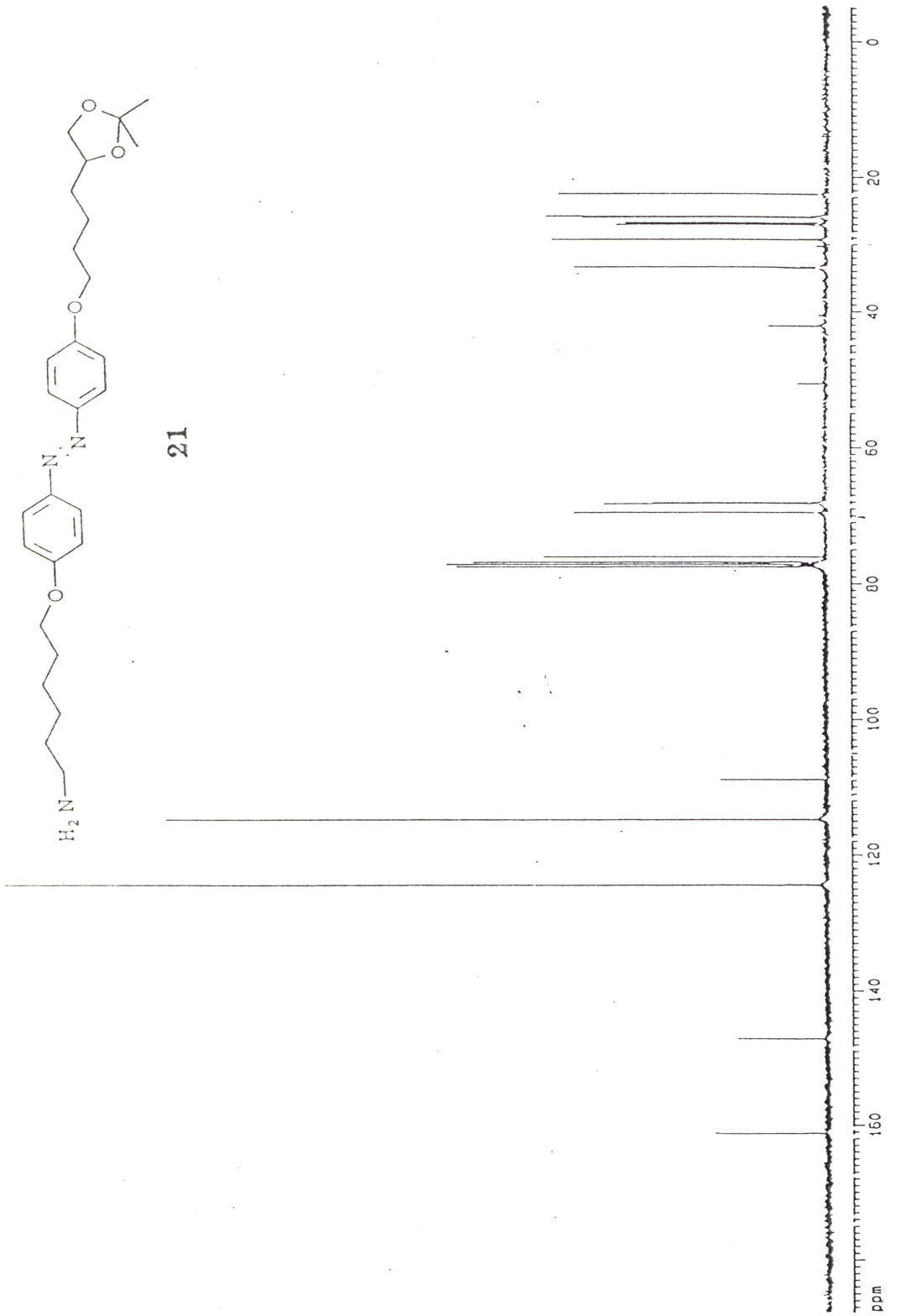


Fig. A-20. $^{13}C$ NMR spectrum of compound **21**

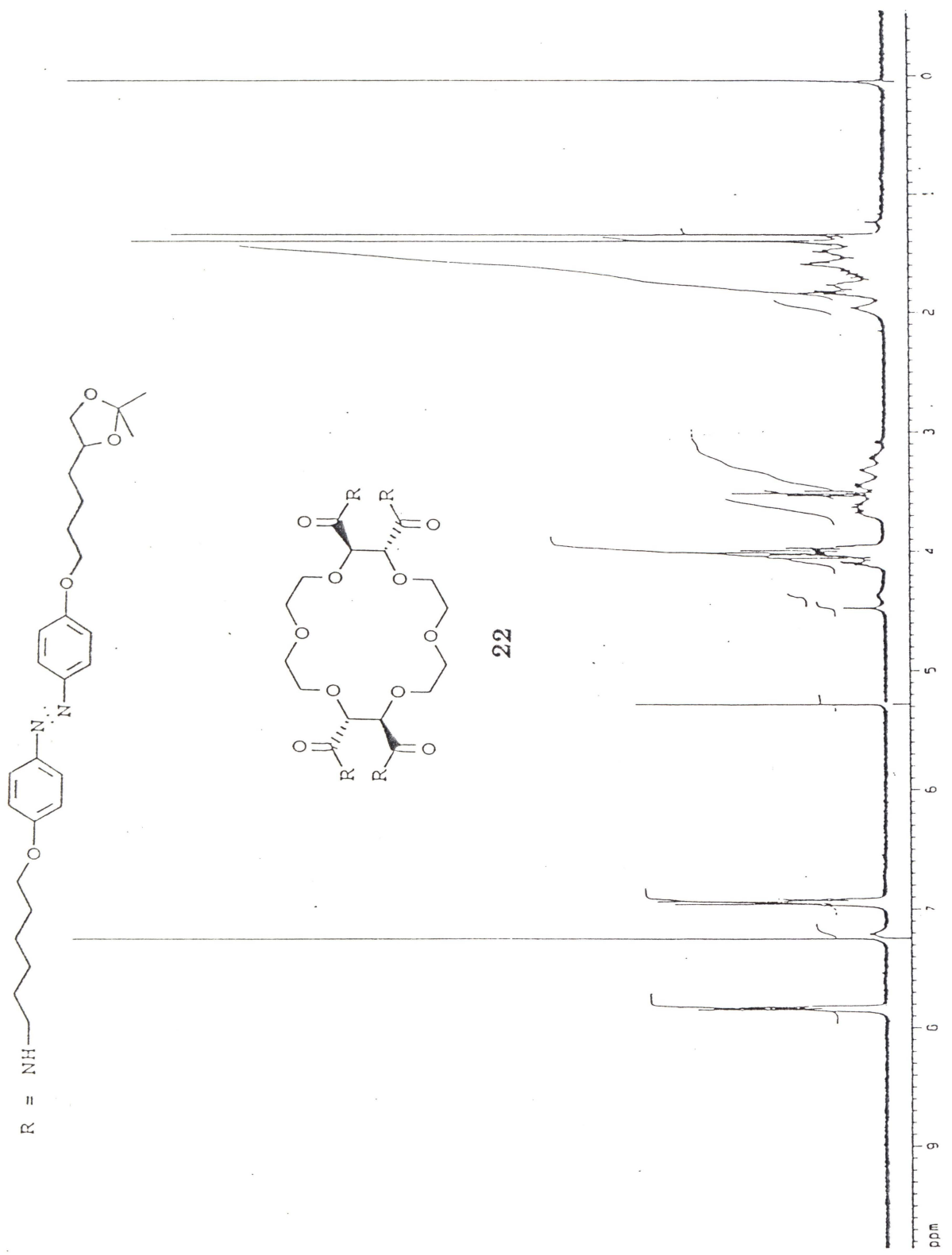


Fig. A-21. $^{1}H$ NMR spectrum of compound **22**


**Fig. A-22.** $^{13}C$ NMR spectrum of compound **22**

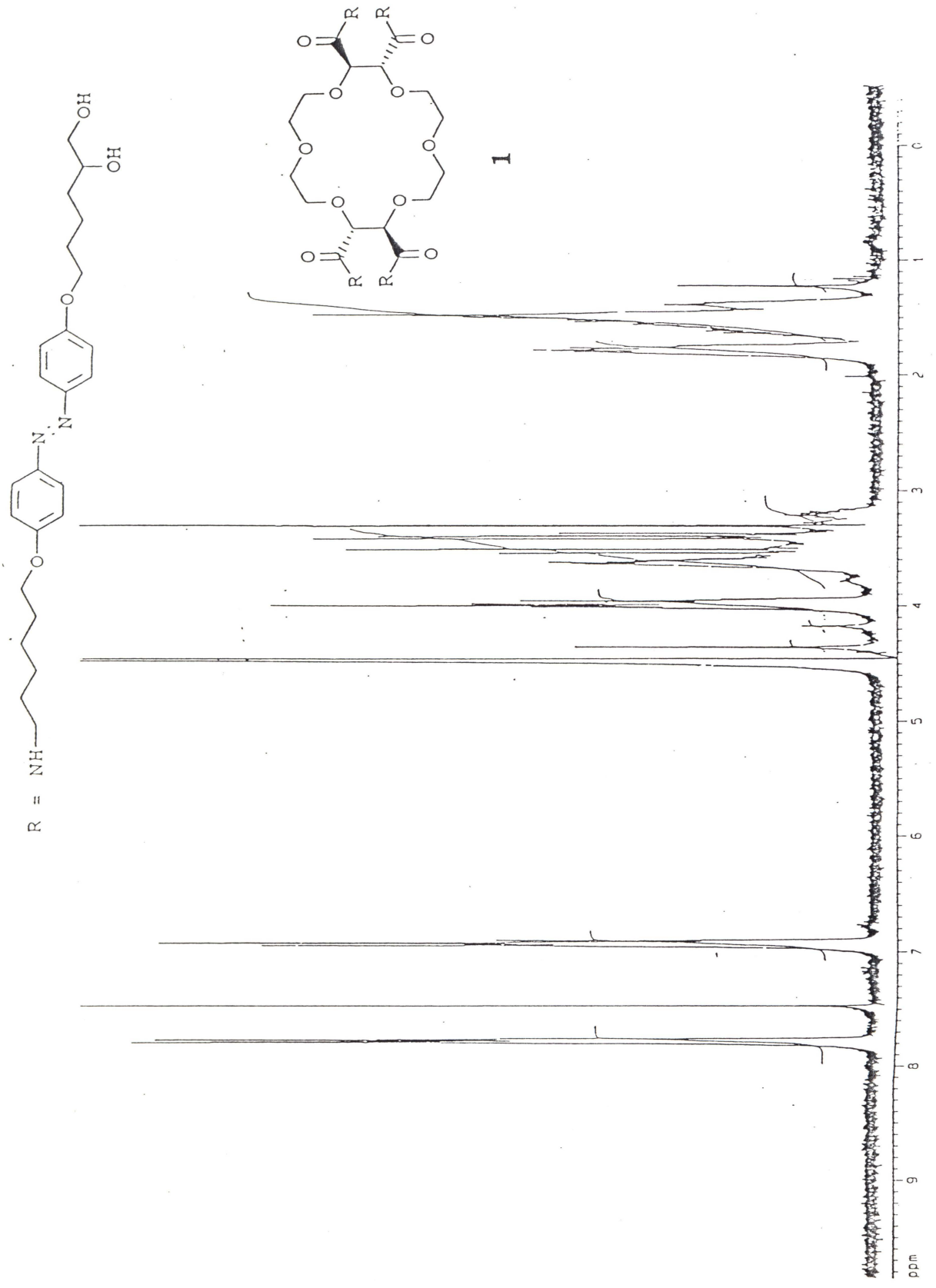


**Fig. A-23**. $^{1}H$ NMR spectrum of compound **1**

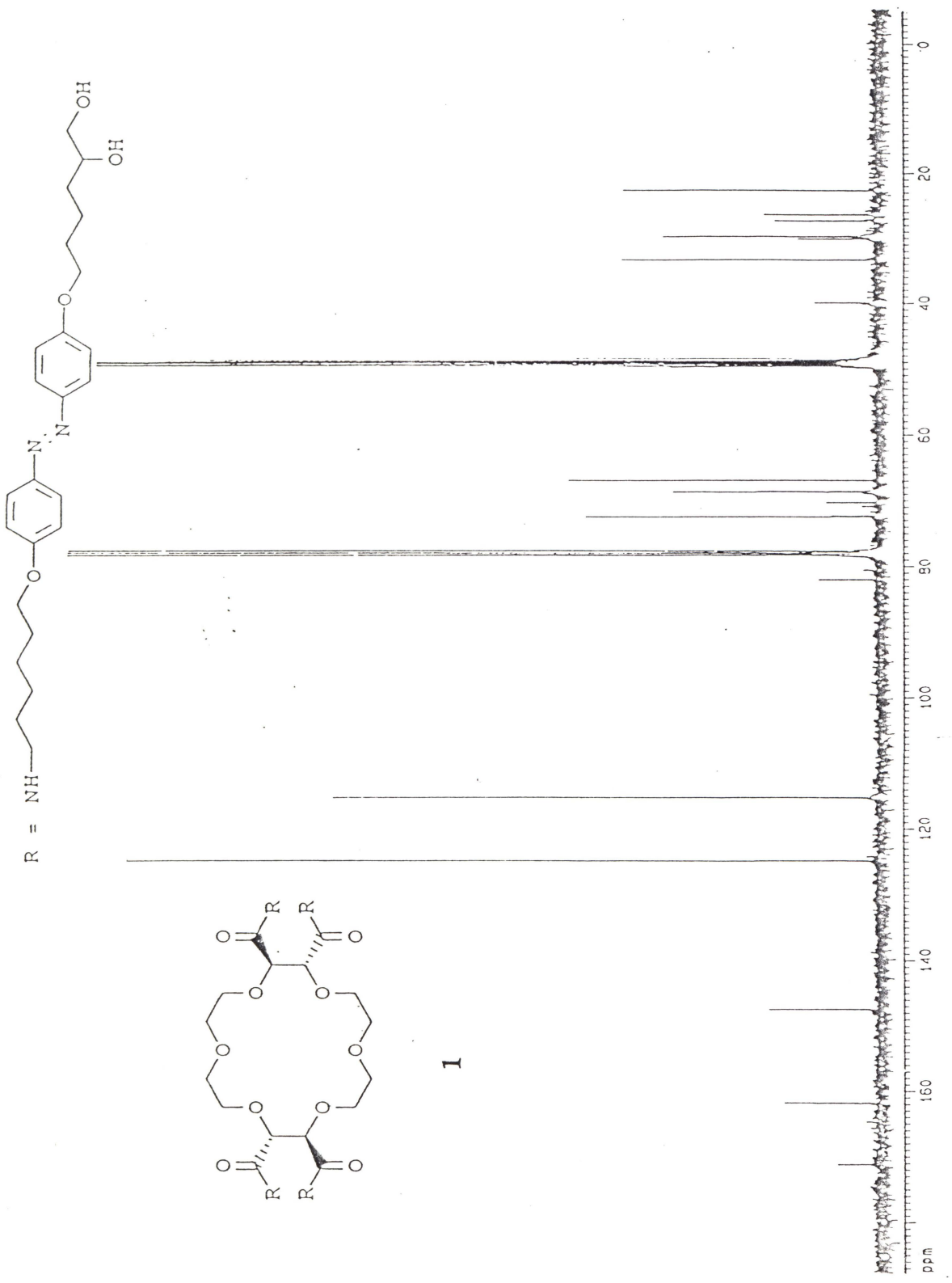


**Fig. A-24.** $^{13}C$ NMR spectrum of compound **1**

# Appendix 2

## Mass spectra of compounds in this thesis (partial)

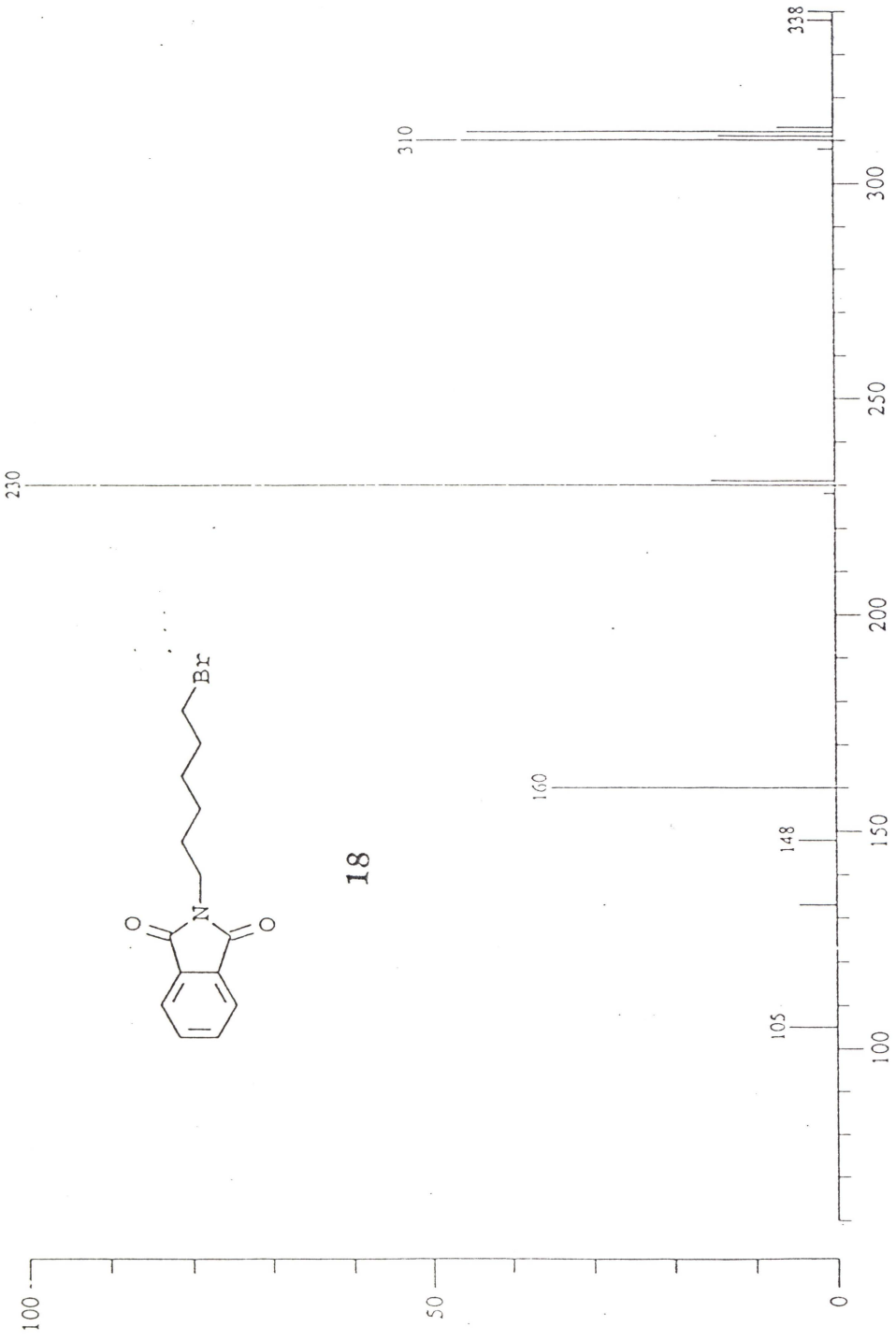


**Fig. A-25**. Mass spectrum (CI) of compound **18**

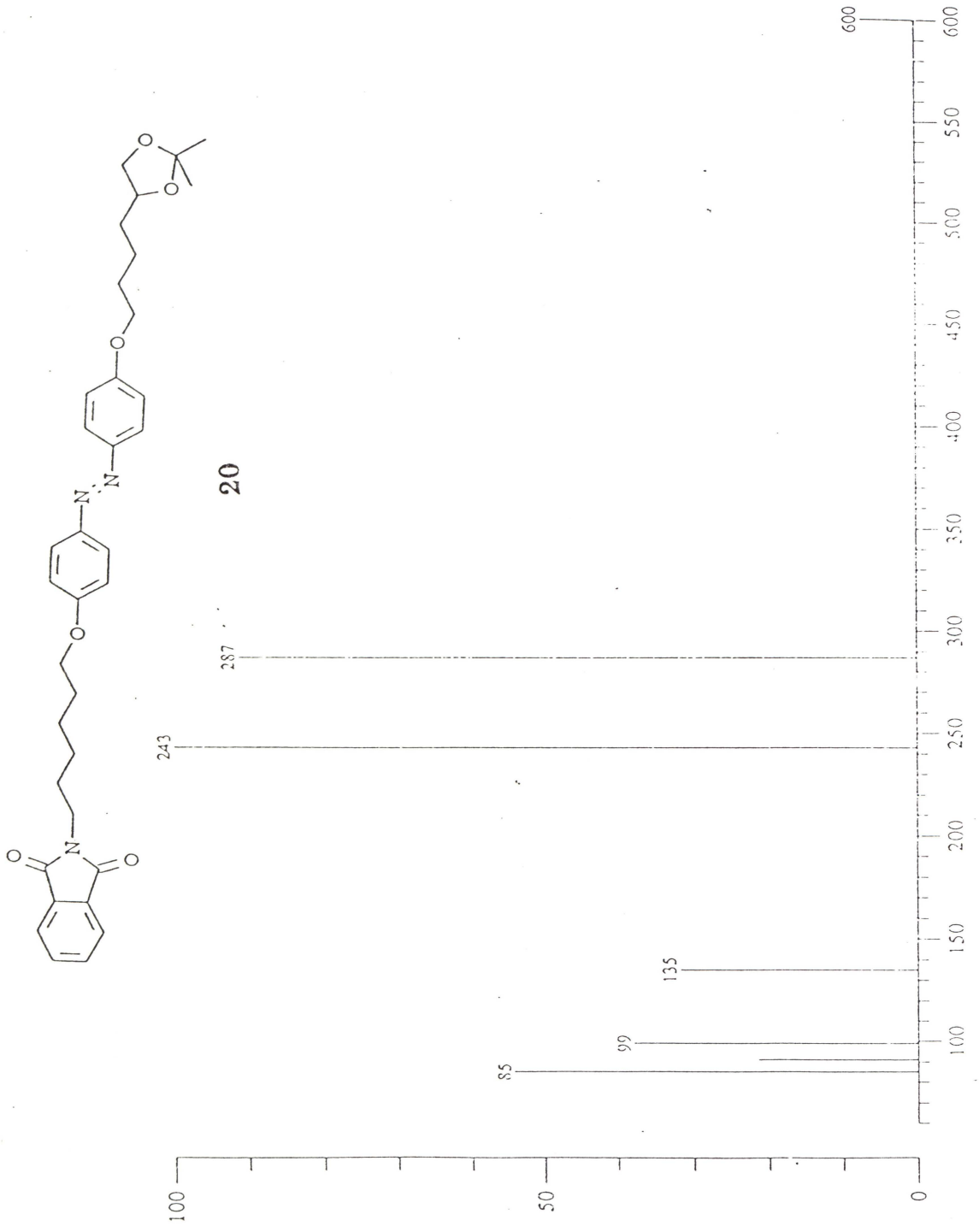


**Fig. A-26**. Mass spectrum (CI) of compound **20**

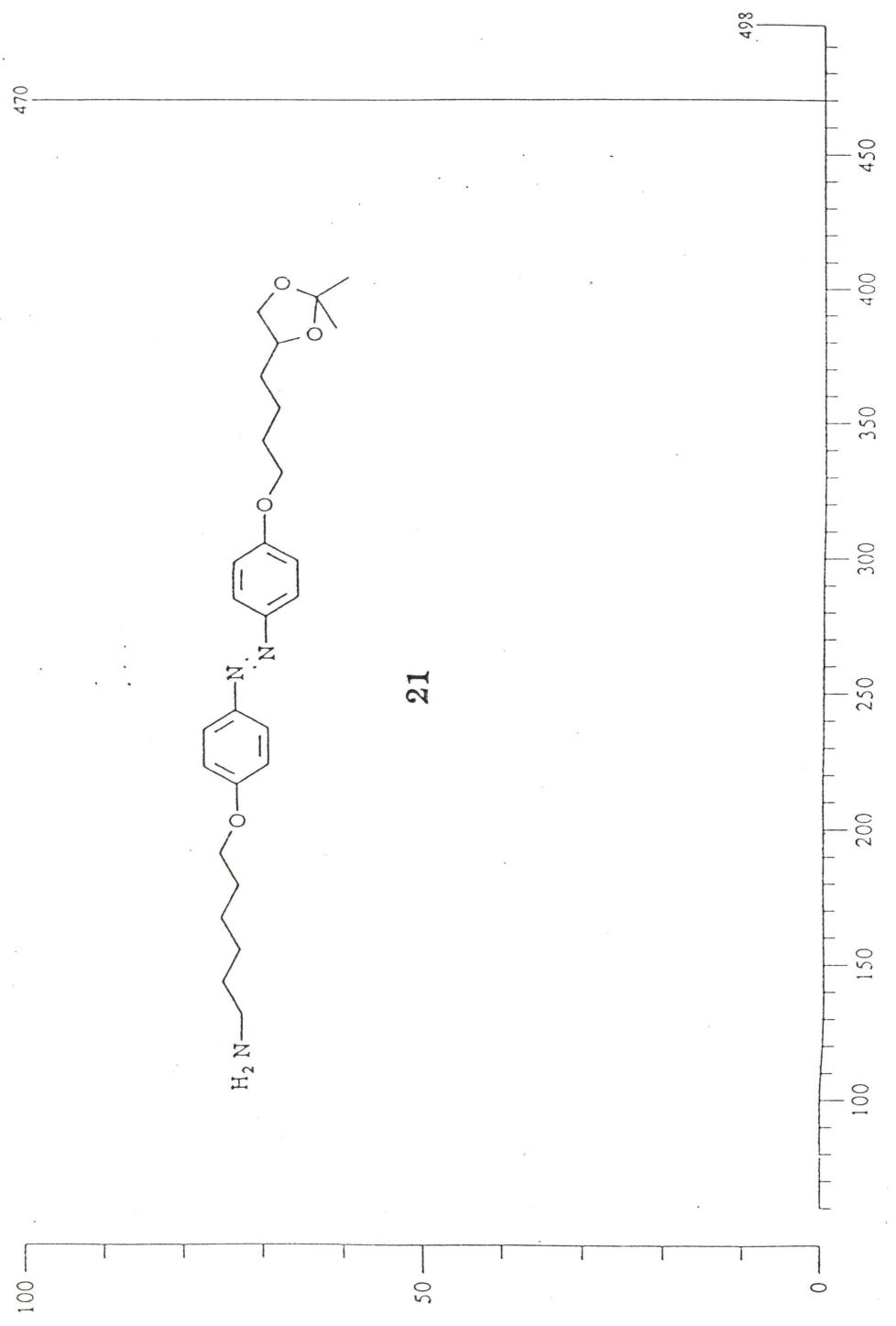


Fig. A-27. Mass spectrum (CI) of compound **21**

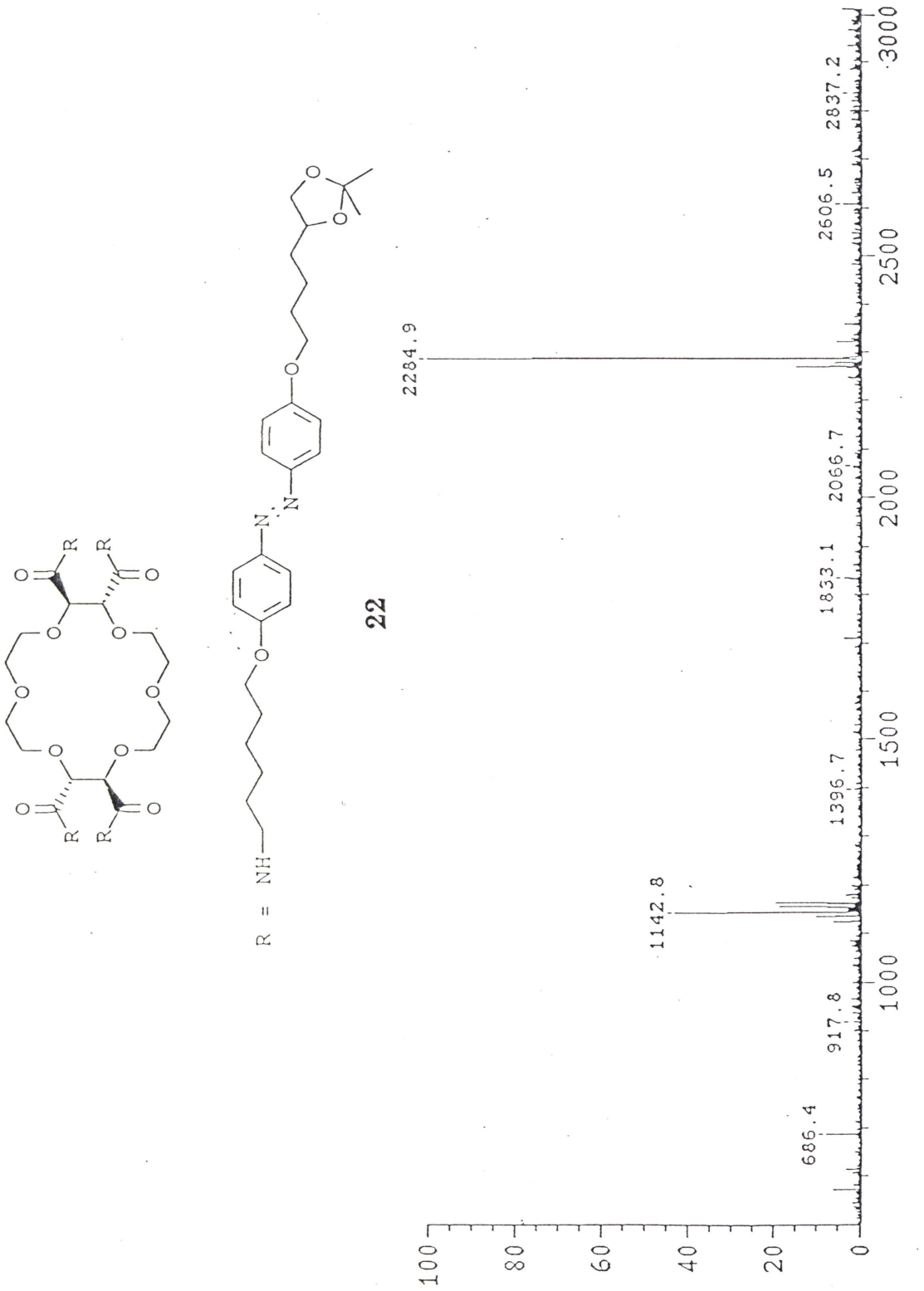


**Fig. A-28**. Mass spectrum (electrospray) of compound **22** (KI, methanol-chloroform 1:1, insulin calibrated)

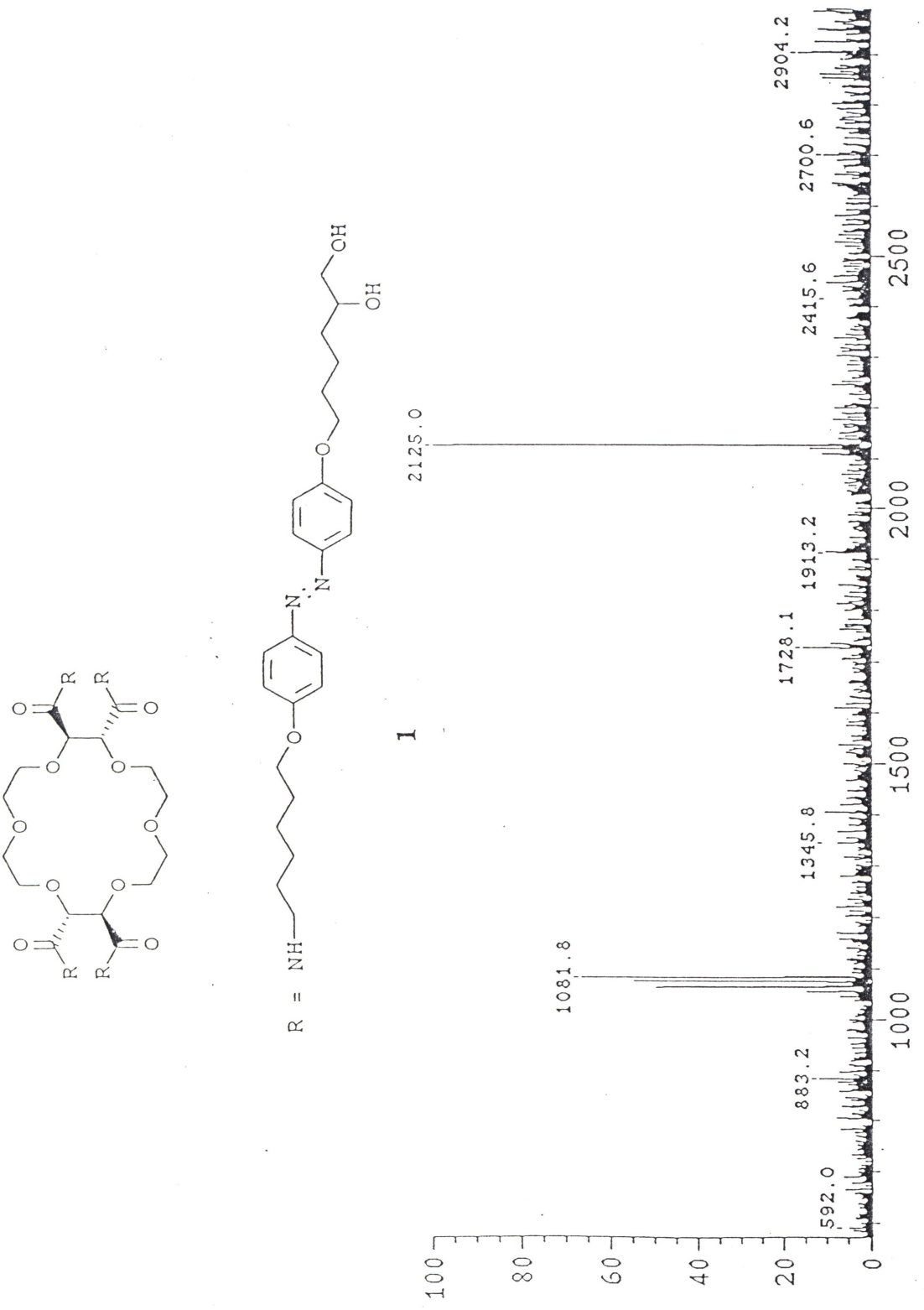


**Fig. A-29**. Mass spectrum (electrospray) of compound **1**
(KI, methanol-chloroform-acetic acid 49.5:49.5:1, insulin calibrated)

## Partial Copyright License

I hereby grant the right to lend my thesis to users of the University of Victoria Library, and to make single copies only for such users or in response to a request from the Library of any other university, or similar institution, on its behalf or for one of its users. I further agree that permission for extensive copying of this thesis for scholarly purposes may be granted by me or a member of the University designated by me. It is understood that copying or publication of this thesis for financial gain shall not be allowed without my written permission.

Title of Thesis: Synthesis, Transport Activity and Selectivity of an Artificial Photogated Ion Channel

Author: [redacted]

CHENGJIN SHAN

July 7, 1995

Date